Distribution Agreement

In presenting this thesis or dissertation as a partial fulfillment of the requirements for an advanced degree from Emory University, I hereby grant to Emory University and its agents the non-exclusive license to archive, make accessible, and display my thesis or dissertation in whole or in part in all forms of media, now or hereafter known, including display on the world wide web. I understand that I may select some access restrictions as part of the online submission of this thesis or dissertation. I retain all ownership rights to the copyright of the thesis or dissertation. I also retain the right to use in future works (such as articles or books) all or part of this thesis or dissertation.

Signature:

_____ _____

Samuel J. Rose Date

A new mouse model of L-DOPA-responsive dystonia

By

Samuel J. Rose

Doctor of Philosophy

Graduate Division of Biological and Biomedical Science

Neuroscience

_____
Ellen J. Hess, PhD
Advisor

_____
H.A. Jinnah, MD/PhD
Committee Member

_____
Gary W. Miller, PhD
Committee Member

_____
Yoland Smith, PhD
Committee Member

_____
David Weinshenker, PhD
Committee Member

Accepted:

_____
Lisa A. Tedesco, Ph.D. Dean of the James T. Laney School of Graduate Studies

_____ Date

A new mouse model of L-DOPA-responsive dystonia

By

Samuel J. Rose

B.S., University of Georgia, 2008

Advisor: Ellen J. Hess, PhD

An abstract of a dissertation submitted to the Faculty of the

James T. Laney School of Graduate Studies of Emory University

In partial fulfillment of the requirements for the degree of

Doctor of Philosophy in Neuroscience

2015

Abstract

A new mouse model of L-DOPA-responsive dystonia

By

Samuel J. Rose

Dystonia is a neurological movement disorder characterized by sustained or intermittent muscle contractions causing abnormal, often repetitive, movements or postures. Abnormal dopamine neurotransmission is associated with many different dystonic disorders. For instance, mutations in genes critical for the synthesis of dopamine, including GTP cyclohydrolase 1 and tyrosine hydroxylase cause L-DOPA-responsive dystonia. Despite evidence that implicates abnormal dopamine neurotransmission in dystonia, the precise nature of the dopaminergic defects that result in dystonia is not known. To better understand these defects, we generated a knockin mouse model of L-DOPA-responsive dystonia that recapitulates the human p.381Q>K TH mutation (c.1141C>A). Mice homozygous for this mutation (DRD mice) had reduced TH activity throughout the brain and striatal dopamine concentration that were ~1% of normal. Although the gross anatomy of the nigrostriatal dopaminergic neurons was normal in DRD mice, the microstructural target of corticostriatal synapses was affected; corticostriatal input in DRD mice showed a shift away from synapses on dendritic spines towards dendrites themselves. DRD mice displayed the core behavioral features of the human disorder, including dystonia that worsened throughout the course of the active phase, and improvement in the dystonia in response to both L-DOPA and trihexyphenidyl. Administration of D1- or D2-type dopamine receptor agonists reduced the dystonic movements while administration of D1- or D2-type dopamine receptor antagonists worsened the dystonia, suggesting that both receptors mediate the dystonic movements. Further, D1-dopamine receptors were supersensitive; adenylate cyclase activity, locomotor activity and stereotypy were exaggerated in DRD mice in response to the D1-dopamine receptor agonist SKF 81297. D2-dopamine receptors responses were blunted or altered in DRD mice with an increase in adenylate cyclase activity and blunted behavioral responses after challenge with the D2-dopamine receptor agonist quinpirole. Together, the findings here implicate developmental dopamine loss within a specific range in the development of dystonia. Further, they implicate maladaptive changes to dopamine receptor responses as important factors for this disorder.

A new mouse model of L-DOPA-responsive dystonia

By

Samuel J. Rose

B.S., University of Georgia, 2008

Advisor: Ellen J. Hess, PhD

A dissertation submitted to the Faculty of the

James T. Laney School of Graduate Studies of Emory University

In partial fulfillment of the requirements for the degree of

Doctor of Philosophy in Neuroscience

2015

Table of Contents

Chapter 1: Introduction

Chapter 4: DA receptor-mediated responses in DRD mice

Chapter 5: General Discussion

List of Figures

List of Abbreviations

L-DOPA = 3,4- L-dihydroxyphenylalanine

DRD = L-DOPA-responsive dystonia

DA = dopamine

NE = norepinephrine

DOPAC = 3,4-dihydroxypheynlacetic acid

5-HT = serotonin

5-HIAA = 5-hydroxyindoleacetic acid

L-DOPS = 3,4-L-dihydroxyphenylserine

BH_4 = tetrahydrobiopterin

cAMP = cyclic adenosine monophosphate

GCH1 = guanosine triphosphate cyclohydrolase 1

TH = tyrosine hydroxylase

DAT = dopamine transporter

VMAT2 = vesicular monoamine transporter 2

AADC = aromatic acid decarboxylase

D1DAR = D1-type DA receptor

D2DAR = D2-type DA receptor

AC = adenylate cyclase

vGluT1 = vesicular glutamate transporter 1

vGluT2 = vesicular glutamate transporter 2

SNc = substantia nigra pars compacta

SNr = substantia nigra pars reticulata

VTA = ventral tegmental area

GPi = internal globus pallidus

GPe = external globus pallidus

STN = subthalamic nucleus

MSN = medium spiny neuron

Ctx = cerebral cortex

Hipp = hippocampus

Cbm = cerebellum

MAO = monamine oxidase

COMT = catechol-o-methyltransferase

PKA = cAMP-dependent protein kinase A

ERK = extracellular signal-regulated kinase

CaMKII = CaM-phospokinase 2

DARPP-32 = 32-kD DA and cAMP-regulated phosphoprotein

DBS = deep brain stimulation

LTD = long term depression

6-OHDA = 6-hydroxydopamine

MPTP = 1-methyl-4-phenyl-1,2,3,6- tetrahydropyridine

PD = Parkinson’s disease

LID = L-DOPA-induced dyskinesia

HPLC = high performance liquid chromatography

FDG-PET = [^{18}F]-fluorodeoxyglucose positron-emission tomography

fMRI = functional magnetic resonance imaging

Neo = Neomycin resistance cassette

PCR = polymerase chain reaction

qRT-PCR = quantitative reverse transcriptase PCR

TBS = Tris-buffered saline

NGS = normal goat serum

s.c. = subcutaneous

Chapter 1: Introduction

Dystonia

The term dystonia originated in 1911, when Oppenheim reported on 4 young patients with "dystonia musculorum deformans" (Oppenheim, 1911). Oppenheim noted that "muscle tone was hypotonic at one occasion and in tonic muscle spasm at another." Oppenheim regarded dystonia as a disorder of muscular origin, though it is now appreciated that central dysfunction causes dystonia. The characterization of dystonia has been updated and refined throughout the last century, culminating in a 2013 consensus definition and classification schema authored by a committee of experts (Albanese et al., 2013). The committee defined dystonia as "a movement disorder characterized by sustained or intermittent muscle contractions causing abnormal, often repetitive, movements, postures, or both." The definition goes on to state that "dystonic movements are typically patterned, twisting, and may be tremulous." Further, "dystonia is often initiated or worsened by voluntary action and associated with overflow muscle activation." This definition distinguishes dystonia from other hyperkinetic movement disorders such as chorea and myoclonus. Further, it defines dystonia based on phenomenology, as opposed to specific biological dysfunction, which distinguishes it from inherited and degenerative disorders.

Current estimates place the number of patients with dystonia at 3 million worldwide (Cloud and Jinnah, 2010), making dystonia the third most prevalent movement disorder behind essential tremor and PD. The actual number of people with dystonia is likely much higher, however, as proper diagnosis requires access to a highly trained neurologist. Current treatment options for dystonia are either palliative or inadequate. The most common treatment for dystonia is *botulinum* toxin injection into the affected muscles (Jankovic, 2006), which chemically silences the neuromuscular junction. Oral medications are only effective in some patients and side effects are common. They include anti-

muscarinics like trihexyphenidyl (THP) and benztropine, as well as muscle relaxers like benzodiazepines (Greene et al., 1988). 3,4-L-dihydroxyphenylalanine (L-DOPA), the biochemical precursor to dopamine (DA), and other dopaminergic compounds are effective in a small subset of dystonia patients (Cloud and Jinnah, 2010). Surgical lesion or deep brain stimulation (DBS) of specific basal ganglia or thalamic nuclei are effective in certain patients, but are primarily used as a treatment of last resort (Ostrem and Starr, 2008).

A distinguishing feature of dystonia is the heterogeneity in its presentation. Dystonia can affect nearly all voluntary muscles, thus the body regions affected are widely varied (Jinnah and Factor, 2015). Dystonia can be generalized, affecting the whole body, focal, affecting one region, segmental, affecting two or more contiguous regions, or multifocal, affecting two or more noncontiguous regions. Further, dystonia can be task-specific, as in writer's cramp, where dystonia only arises when the patient engages in a specific task. Age of onset is also heterogeneous; the initial presentation can occur in early-childhood or in adulthood (Jinnah and Factor, 2015). Lastly, patients with dystonia may present with other types of abnormal movement. For instance, patients with dystonia may also have tremor (Defazio et al., 2015), myoclonus (Nardocci, 2011), and parkinsonism (de Carvalho Aguiar et al., 2004).

Like the heterogeneity in presentation, the causes of dystonia are also diverse. Known etiologies of dystonia fall into two broad categories, inherited and acquired (Albanese et al., 2013). Genes associated with inherited forms of dystonia continue to be discovered (Klein, 2014), including dominant, recessive, X-linked, and mitochondrial modes of inheritance. Some of these inherited disorders may present as a pure dystonia, as is the case for DYT1 dystonia, which is caused by a single codon deletion in the *TOR1A* gene (Ozelius et al., 1997). In contrast, dystonia may be just one feature of a more

complex inherited disorder, as in Lesch-Nyhan disease (Jinnah et al., 2006). These genes implicate varied biochemical processes including DA signaling, transcriptional regulation, the cell stress response, mitochondrial function, and calcium handling (Bragg et al., 2011, Thompson et al., 2011).

Acquired etiologies refer to cases of dystonia caused by a non-genetic nervous system insult. These etiologies are also diverse. They include perinatal and adult brain injury, from stroke or trauma (Krauss et al., 1992, Bhatia and Marsden, 1994, Sanger et al., 2003). Exposure to toxins or infections are also known etiologies (He et al., 1995). Dystonia can also be an outcome of certain drug therapies (Marsden and Jenner, 1980) or the symptom of a degenerative disorders like Parkinson's disease (PD) (Bravi et al., 1993). Lastly, the cause of many dystonia cases are not yet understood. Many adult-onset, focal dystonia cases, for instance, are idiopathic in origin.

Because of this etiological heterogeneity, the dystonia field focuses on different types of research questions than other fields. For instance, in contrast to Huntington's disease research, where research questions focus on the specific effects of mutant *huntingtin,* dystonia research has to consider more than one etiology. Therefore, translational dystonia research has largely focused on two different efforts; (1) understanding the contribution of different neuroanatomical substrates to dystonia through human neuroimaging and animal model studies, and (2) defining commonly disrupted molecular pathways in many forms of dystonia. Discovering new genes associated with dystonia guides the second effort. Biochemical and physiological experimentation on molecular pathways and circuits affected by multiple etiologies are also important. These research efforts have the ultimate goal of developing new surgical and pharmacological treatment strategies to stop involuntary dystonic movement and thus improve patients' quality of life.

Neuroanatomical substrates of dystonia

Since dystonia is not associated with consistent neuropathology, delineating the contribution of different brain regions to dystonic movement has been challenging. Currently, the most accepted neuroanatomical model of dystonia is a network model that incorporates several brain regions necessary for coordinating normal movement. Those include the motor cortex, basal ganglia, cerebellum, thalamus, and brainstem (Neychev et al., 2011, Hendrix and Vitek, 2012, Chen et al., 2014, Prudente et al., 2014). Further, the motor network model posits that dystonia can be caused by different types of dysfunction within this network. First, dysfunction from just one of these brain regions may cause dystonia. Lesion studies and animal model work support a singular role for basal ganglia or cerebellar dysfunction in certain dystonias (Bhatia and Marsden, 1994, Pizoli et al., 2002). Second, the network model suggests that abnormal communication between motor regions can cause dystonia. This idea is supported by diffusion tensor imaging studies demonstrating abnormal connectivity between motor regions in patients with dystonia (Carbon et al., 2004a, Ulug et al., 2011). Lastly, dystonia may require two "hits" to the motor network, or dysfunction co-occurring in different brain regions, an idea supported by some animal model studies (Schicatano et al., 1997). Because of dystonia's heterogeneity in etiology and appearance, it is possible that all three of these mechanisms may cause dystonia in different cases. Thus, these three mechanisms of dysfunction are not considered to be in competition, but rather complementary to one another by the motor network model (Prudente et al., 2014).

Because a major goal of translational and clinical neuroscience is to ascribe dysfunction from one brain region or nuclei to a disorder, much effort has been made to localize the source of dysfunction in specific types of dystonia. Evidence for basal ganglia and cerebellar dysfunction has been the strongest. Below is a summary of the functions

of basal ganglia and cerebellum in the coordination of normal movements, and a discussion of the potential implication of the network dysfunction of these brain regions in dystonia.

Basal ganglia function and dysfunction in dystonia

The basal ganglia are a collection of nuclei located in the basal forebrain that participate in the processing of motor, cognitive, and limbic functions (Fig. 1) (DeLong and Wichmann, 2007). The basal ganglia nuclei are components of cortico-subcortical circuit loops through which cortical information is filtered in the basal ganglia and thalamus networks before it is sent back to the cerebral cortex (Alexander et al., 1986, Kelly and Strick, 2004). In terms of motor function, this filtering of cortical information is essential for the proper selection of movements (Alexander et al., 1986, Graybiel et al., 1994, Mink, 2003).

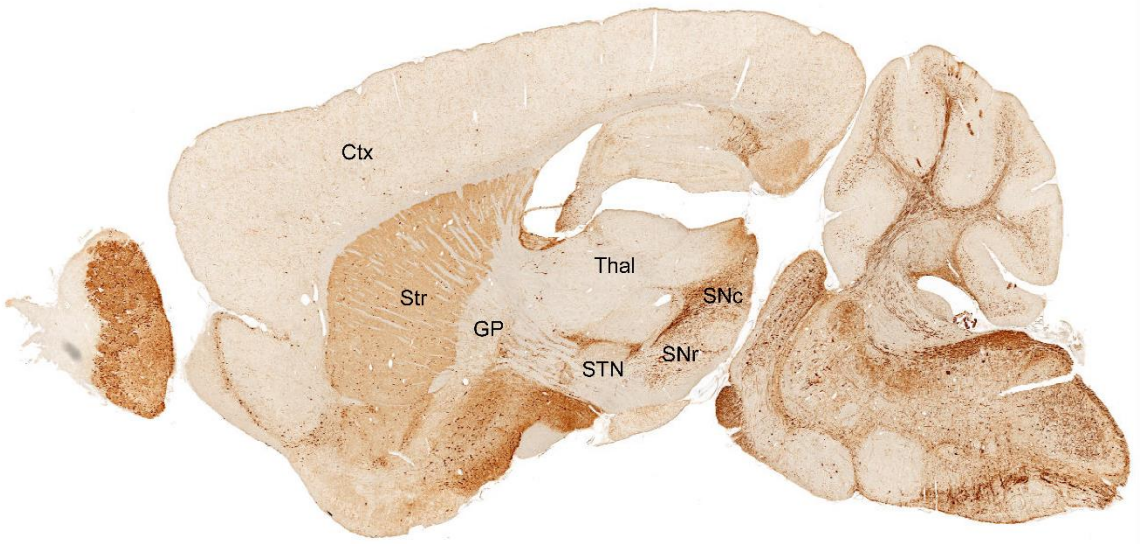

Figure 1: Structures of the basal ganglia and related circuitry in mouse. Sagittal view of the mouse brain, immunostained for TH, courtesy of The Gene Expression Nervous System Atlas Project (GENSAT). Approximate locations of Cortex (Ctx), striatum (Str), globus pallidus (GP), subthalamic nucleus (STN), thalamus (Thal), substantia nigra pars compacta (SNc), and substantia nigra pars reticulata (SNr) are noted.

Anatomical organization dictates how information is processed through the motor striatum (putamen in primates). The information processed in the basal ganglia flows through two parallel pathways, each starting within the striatum (DeLong and Wichmann, 2007). There, two types of γ-aminobutyric acid producing (GABAergic) striatal medium spiny neurons (MSNs) exist, giving rise to so-called direct and indirect pathways. Direct pathway MSNs express D1-type DA receptors (D1DARs), whereas indirect pathway MSNs express D2-type DA receptors (D2DARs) (Gerfen et al., 1990, Surmeier et al., 1996). In primates, direct pathway MSNs project to GABAergic internal globus pallidus (GPi) (or entopeduncular nucleus in rodents) and substantia nigra pars reticulata (SNr). Indirect pathway MSNs project to the GABAergic external globus pallidus (GPe) (or globus pallidus in rodents), which sends projections to the glutamatergic subthalamic nucleus (STN). STN output converges with striatal afferents from the direct pathway in the GPi and SNr, which project to the ventroanterior, ventrolateral and caudal intralaminar nuclei of the thalamus and various upper brainstem nuclei (lateral habenula, pedunculopontine nucleus, superior colliculus, reticular formation). Further, a glutamatergic projection from the cerebral cortex to the STN, termed the hyperdirect pathway, also has influence on basal ganglia output and behavior (Nambu et al., 2002, Chu et al., 2015). Lastly, cholinergic and GABAergic interneurons within the striatum as well as nigrostriatal dopaminergic inputs also play key roles in basal ganglia function (Bolam et al., 2000, Calabresi et al., 2000).

Activation of glutamatergic cortical inputs to striatal direct pathway projection neurons is thought to have a net movement-inducing effect, whereas stimulation of cortical inputs to indirect pathway neurons is thought to have a net movement-inhibiting effect (DeLong and Wichmann, 2009). This classical model of the basal ganglia circuitry, originally introduced in the late 1980s (Albin et al., 1989, DeLong, 1990), was recently

supported by a study where selective optogenetic stimulation of direct pathway MSNs, indeed, caused movements, while stimulation of indirect pathway MSNs inhibited movements in mice (Kravitz et al., 2010). Therefore, an imbalance in activity between these two pathways that favors an increased activity of the direct pathway provides a theoretical model by which basal ganglia dysfunction may cause dystonia. Other data and theoretical models cloud this simplistic explanation. For one, a recent study presents data illustrating that both direct and indirect pathway MSNs are activated during movement initiation (Cui et al., 2013). Further, two competing models of basal ganglia function exist and offer their own explanations for dystonic movement. One argues that an imbalance between striosomal and matrix compartments of the striatum, an organizational structure based on differential expression of certain peptides transmitters and receptors, underlies dystonia (Crittenden and Graybiel, 2011). Another model posits that dystonia arises from a deficiency in center-surround inhibition in the basal ganglia (Mink, 2003). Thus, despite detailed understanding of the anatomical organization of the basal ganglia, the precise role of this circuit in normal movement is not clearly defined as of yet. This gap in the knowledge prevents the acceptance of a universal model of basal ganglia dysfunction in dystonia. Nevertheless, several lines of evidence implicate some type of basal ganglia dysfunction in dystonia.

The most direct, and perhaps most influential, evidence for basal ganglia dysfunction in dystonia comes from a series of studies in the 1980s showing that dystonia is the most common movement disorder caused by basal ganglia lesion, as detected by CT scan (Marsden et al., 1985, Pettigrew and Jankovic, 1985, Obeso and Gimenez-Roldan, 1988). Further, a summary of these findings and other similar studies concludes that dystonia occurs in 36% of basal ganglia lesion cases including focal lesions to caudate nucleus, putamen, or globus pallidus, or large lesions that affected multiple nuclei

(Bhatia and Marsden, 1994). Similarly, dystonia can be a symptom of Huntington's disease, where degeneration of the dorsal striatum occurs (Louis et al., 1999). Providing evidence for causation, basal ganglia lesion in animal models can also cause dystonia (Fernagut et al., 2002, Cuny et al., 2008). Functional imaging studies in patients without structural lesion, using [^{18}F]-fluorodeoxyglucose positron-emission tomography (FDG-PET) and functional magnetic resonance imaging (fMRI), also implicate basal ganglia dysfunction in dystonia (Niethammer et al., 2011, Lehericy et al., 2013). Though these studies show altered basal ganglia nuclei signaling in different types of dystonia, the specific nature of dysfunction differs between studies. For instance, FDG-PET studies of cervical dystonia patients reported increased glucose metabolism in putamen (Galardi et al., 1996, Magyar-Lehmann et al., 1997), while patients with DYT6, an inherited form of dystonia caused by mutations in the *THAP1* gene, show decreased glucose metabolism in putamen (Carbon et al., 2004b). Despite some differences in the specificity of the findings, these studies provide strong evidence for involvement of the basal ganglia in many types of dystonia.

Neurosurgical procedures to the basal ganglia are effective in ameliorating several cases of general dystonia. The most common of these neurosurgical procedure is DBS of the GPi (Ostrem and Starr, 2008). Other neurosurgical procedures for dystonia involve STN DBS (Sun et al., 2007) and electrolytic lesion of the GPi (Cooper, 1976). The mechanisms by which GPi DBS alleviates dystonic movement are not clear, though some evidence suggests that DBS alters the firing patterns of GPi neurons (Cleary et al., 2013). GPi DBS is most commonly used in DYT1 dystonia and other childhood-onset generalized dystonias, where the majority of patients show some improvement (Ostrem and Starr, 2008). Other types of dystonia, including adult-onset cervical dystonia (Hung et al., 2007) and neuroleptic-induced (tardive) dystonia (Damier et al., 2007) also often benefit from

GPi DBS. Together, these clinical findings provide strong evidence that basal ganglia pathophysiology plays a primary role in several forms of dystonia.

Animal models mimicking the genetic basis of certain forms of dystonia also provide evidence for basal ganglia dysfunction. The most commonly studied genetic animal models of dystonia are mice that mimic DYT1 dystonia (Goodchild and Dauer, 2004, Dang et al., 2005, Grundmann et al., 2007). These mice do not show an overt dystonic phenotype, but exhibit subtle motor deficits (Dang et al., 2006, Song et al., 2012). Subtle structural (Goodchild and Dauer, 2004, Song et al., 2013) and physiological (Pisani et al., 2006, Sciamanna et al., 2012) changes are observed in the striatum of these mice. Though their relation to the expression of dystonic movement is still not known, these findings illustrate that dystonia-causing etiologies disrupt normal basal ganglia structure and function.

Cerebellar dysfunction in dystonia

Evidence also implicates abnormal cerebellar signaling in dystonia, though the role for the cerebellum has only been taken into consideration recently. For one, many of the same FDG-PET and fMRI studies that illustrate abnormal basal ganglia signaling in dystonia, also show abnormal cerebellar signaling (Galardi et al., 1996, Magyar-Lehmann et al., 1997, Carbon et al., 2004b). Further, postmortem studies from cervical dystonia patients show lesions and anatomical abnormalities in the cerebellum (Prudente et al., 2013, Zoons and Tijssen, 2013). Surface stimulation of the cerebellum and surgical lesion of cerebellar output have been successful in treating a small handful of dystonia cases (Hitchcock, 1973, Davis, 2000). Lastly, animal model studies have provided the strongest evidence for cerebellar involvement in dystonia. A series of studies with *tottering* mice clearly implicate cerebellar output as the driving force behind the dystonic movement in these mice (Campbell and Hess, 1998, Campbell et al., 1999, Raike et al., 2013).

Cerebellar dysfunction also drives the dystonia in the genetically dystonic *dt* rat (LeDoux et al., 1993), a model of rapid-onset dystonia parkinsonism (Calderon et al., 2011), and a pharmacological model where cerebellar circuitry is activated by kainic acid (Pizoli et al., 2002). Taken together, these data illustrate that the basal ganglia is not the sole driver of dystonic movement and further support a network model of dystonia

How the motor network incorporates pathological signals from basal ganglia or cerebellum to generate dystonic movement is poorly understood. Classical views of the neuroanatomy of the motor network posits that cerebellar output is funneled through thalamus to motor cortex (Allen and Tsukahara, 1974). Similarly, basal ganglia output is funneled through thalamus to motor cortex (DeLong and Wichmann, 2009). In this view, motor cortex would integrate pathological signals from either basal ganglia or cerebellum and deliver this perturbed signal to the spinal cord and muscles. More recently, direct, reciprocal connections between basal ganglia and cerebellum have been discovered (Hoshi et al., 2005, Bostan et al., 2010). Those connections appear to be important neuroanatomical conduits for dystonia in certain animal models (Neychev et al., 2008, Chen et al., 2014). Efforts to incorporate these direct connections into treatment strategies for dystonia are still in their infancy.

Dysfunctional DA neurotransmission as a common molecular pathway in dystonia

Similar to the evidence implicating several brain regions, there is evidence implicating several molecular pathways in dystonia. There is no single molecular pathway disrupted in all forms of dystonia. However, certain molecular pathways are disrupted in several forms of dystonia. Studying how these common molecular pathways are disrupted is critical for the development of therapeutics. The molecular pathways implicated in dystonia involve DA signaling, transcriptional regulation, the cell stress response, mitochondrial function, and calcium handling. The evidence implicating these pathways are highlighted

in several recent reviews (Bragg et al., 2011, Thompson et al., 2011, Ledoux et al., 2013, Klein, 2014). Special emphasis here is placed on the evidence implicating dysfunctional DA neurotransmission in dystonia.

DA was identified as a putative neurotransmitter more than fifty years ago. First thought to be an intermediary in NE synthesis, pioneering work by Carlsson and colleagues identified it as a transmitter in its own right, independent of its role in NE synthesis (Carlsson et al., 1957, Carlsson et al., 1958). Later, integral roles for DA in several neurological and psychiatric diseases were found. First, Ehringer and Hornykiewicz observed that DA concentrations were consistently reduced in the caudate and putamen of PD patients (Ehringer and Hornykiewicz, 1960). This observation lead to the first successful treatment of PD with L-DOPA (Cotzias et al., 1967). Later, DA receptors were identified as the principle mediators of antipsychotic efficacy (Snyder et al., 1970, Seeman et al., 1976), placing DA central to theories of schizophrenia and psychosis. Lastly, DA was identified as the principle mediator of the rewarding effects of cocaine and intracranial self-stimulation (Corbett and Wise, 1980, Ritz et al., 1987), placing DA central to theories of drug addiction. These observations made DA neurotransmission one of the most highly published fields of neuroscience in the later part of the 20th century, and led to detailed understanding of the anatomy and physiology of the DA system.

The distribution of DA-producing neurons was first described in a study using histofluorescence techniques in rat brain (Dahlstroem and Fuxe, 1964). Dahlstroem and Fuxe defined twelve distinct catecholamine-containing nuclei that they designated A1-A12. Though more nuclei were added, that nomenclature is still used today. The most widely studied are the A8-A10 nuclei of the ventral midbrain, containing retrorubral field (A8) substantia nigra pars compacta (A9; SNc), and ventral tegmental area (A10; VTA). These midbrain DA neurons send axonal projections to structures throughout the forebrain, though densest projections are to the striatum (Matsuda et al., 2009). In rodents,

these projections are divided into three forebrain-projecting pathways, nigrostriatal, mesolimbic, and mesocortical (Fallon and Moore, 1978, Prensa and Parent, 2001), though work in primates acknowledges that these pathways are not entirely segregated (Williams and Goldman-Rakic, 1998). Nigrostriatal projections originate from SNc and innervate the dorsal striatum. Mesolimbic and mesocortical projections originate from VTA and innervate the ventral striatum, including nucleus accumbens, as well as the cerebral cortex. Other notable DA producing neurons are the A11 spinal cord-projecting hypothalamic neurons, the A12 arcuate nucleus neurons, the A16 olfactory bulb neurons, and the A17 amacrine cells of the retina (Bjorklund and Dunnett, 2007).

DA neurons are identified based on molecular markers, all of which play a role in DA synthesis and signaling. All DA neurons express the rate limiting enzyme of DA synthesis, tyrosine hydroxylase (TH), which converts dietary tyrosine to L-DOPA (Fig. 2) (Nagatsu et al., 1964). Similarly, DA neurons express aromatic acid decarboxylase (AADC), which converts L-DOPA to DA. DA neurons package DA into synaptic vesicles via the vesicular monoamine transporter 2 (VMAT2). Depolarization of the neuron through action potential causes Ca^{2+} influx, vesicular fusion to the extracellular membrane, and the release of DA. Though many types of DA neurons cannot recycle DA once released, midbrain DA neurons express the DA transporter (DAT), which recovers DA from the extracellular space (Giros et al., 1996).

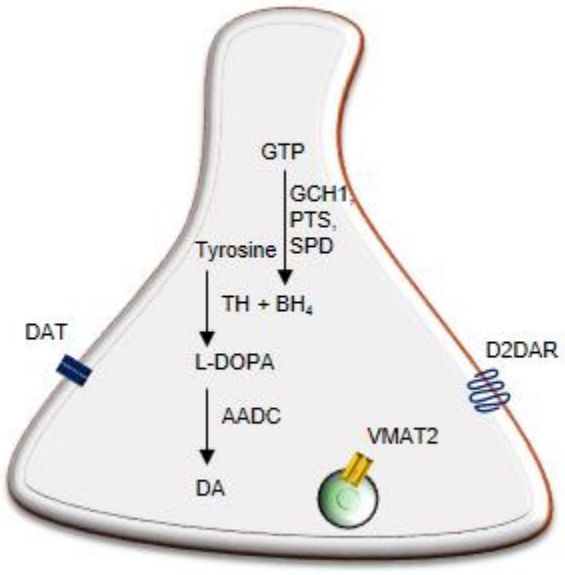

Figure 2: Schematic of a presynaptic DA terminal. Dietary tyrosine is converted to L-DOPA by TH. L-DOPA is then converted to DA by AADC. DA is packaged into synaptic vesicles by VMAT2. Extracellular DA may be subject to reuptake in the presynaptic terminal via DAT. D2DARs exert auto-inhibition on synthesis and release of DA. GTP cyclohydrolase 1 (GCH1), 6-pyruvoyl tetrahydrobiopterin synthase (PTS), and sepiapterin reductase (SPD) are necessary for biosynthesis of the TH cofactor tetrahydrobiopterin (BH_4).

DA is metabolized by monoamine oxidase (MAO) and catechol-O-methyltransferase (COMT). First, MAO-A, expressed intracellularly, oxidizes DA to 3,4-dihydroxyphenylacetic acid (DOPAC) (Westerink, 1985, Wood and Altar, 1988). Extracellular COMTs, expressed on cell-surface membranes, convert DA to 3-methoxytyramine. DOPAC and 3-methoxytyramine can further be broken down by glial COMT and MAO-B, to homovanillic acid. Inhibitors of MAO and COMT alter DA homeostasis and have been used to augment the efficacy of L-DOPA therapy in PD, as well as in the treatment of psychiatric disorders (Shih et al., 1999).

Tyrosine hydroxylase

TH is the rate limiting enzyme in DA biosynthesis (Nagatsu et al., 1964), and thus plays a critical role in DA signaling. Since it discovery, TH has been widely studied. First, within the context of norepinephrine (NE) and epinephrine synthesis in the adrenal glands, and later in DA and NE synthesis in the brain (Kumer and Vrana, 1996). In humans, *TH* mRNA undergoes alternative splicing, whereby 4 different splice-variant protein products, hTH1-4, may be formed (Kobayashi et al., 1988). hTH1 and hTH2 isoforms are the most abundant in brain (Le Bourdelles et al., 1988). Rodents, however, are only known to generate one isoform, with the closest homology to hTH1. TH is divided, broadly, into three functional units. The N-terminal regulatory domain is the site of multiple phosphorylation sites that participate in the regulation of enzyme activity. The internal catalytic domain contains binding sites for iron, BH_4, and tyrosine, and is the site of L-DOPA formation (Fitzpatrick, 2000). The C-terminal domain is necessary for TH to form a functional homotetramer (Vrana et al., 1994).

TH is regulated by multiple mechanisms, all with the potential of altering the rate of catecholamine synthesis. First, catecholamines can regulate TH activity through feedback inhibition (Ramsey and Fitzpatrick, 1998). Catecholamines inhibit TH activity

through competition with BH_4 (Zigmond et al., 1989). While catecholamines acutely inhibit TH activity, they also stabilize the enzyme through interactions with iron (Haavik et al., 1990), structurally preserving the enzyme for reactivation. TH activity is also acutely regulated by phosphorylation. Four serine residue phosphorylation sites, Ser8, Ser19, Ser40, Ser143, are located in the N-terminal regulatory domain and regulate the net activity of the enzyme (Campbell et al., 1986). These sites are phosphorylated by several protein kinases, including cyclic AMP-dependent protein kinase A (PKA), extracellular signal-regulated kinases (ERKs), calcium-calmoduin protein kinase II (CaMKII), to name a few (Kumer and Vrana, 1996), showing that many signaling pathways located at the presynaptic terminal converge on TH to regulate catecholamine synthesis. Notably, D2DARs inhibit TH activity through PKA-dependent phosphorylation of TH (Pothos et al., 1998, Ford, 2014), illustrating a second mechanism by which DA may exert feedback inhibition on TH activity. *TH* transcription and translation are also heavily regulated by feedback inhibition. Direct and indirect DA agonists have been shown to decrease *TH* mRNA levels (Weiss-Wunder and Chesselet, 1992, Vrana et al., 1993), a third mechanism for DA to inhibit its own synthesis. Translation of *TH* mRNA to protein is another site of regulation, shown in a study where human *TH* was transgenically overexpressed in mice. These mice, despite having a 50-fold increase in *TH* mRNA, only show minor increases in levels of TH protein (Kaneda et al., 1991). Taken together, these redundant mechanisms illustrate the importance the DA system places on tuning TH activity to a precise level.

DA receptors

G protein-coupled DA receptors mediate the physiological functions of DA. These receptors have been intensely investigated because most antipsychotic drugs have affinity for DA receptors (Snyder et al., 1970, Seeman et al., 1976). Five different DA receptor

genes have been identified, coding D1-D5 DA receptors (Tiberi et al., 1991, Sibley and Monsma, 1992, Vallone et al., 2000). The five receptors are categorized into two types, based on their pharmacological properties. D1 and D5 DA receptors are $G\alpha_{s/olf}$-coupled and stimulate cyclic adenosine monophosphate (cAMP) production by adenylate cyclase (AC). D2, D3, and D4 DA receptors are $G\alpha_{i}$-coupled and inhibit AC activity (Kebabian and Calne, 1979). Thus, D1 and D5 are grouped with the designation D1-type DA receptors (D1DARs) and D2, D3, and D4 are designated D2-type DA receptors (D2DARs). DA receptors are expressed in pituitary, kidney, adrenal glands, gastrointestinal tract, as well as many other structures outside the brain (Missale et al., 1998, Aperia, 2000, Li et al., 2006). In brain, D1DARs and D2DARs are expressed in most forebrain structures, with the greatest abundance in striatum, cortex and hippocampus (Lein et al., 2007). One distinguishing aspect of DA receptor expression is that D2DARs are expressed by midbrain DA neurons, whereas D1DARs are not. There, D2DARs act as autoreceptors, inhibiting DA synthesis and release (Pothos et al., 1998). MSNs in the striatum primarily express either the D1 or D2 DA receptor (Gerfen et al., 1990, Surmeier et al., 1996), though henceforth the D1DAR and D2DAR designation will be used when referring to striatal DA receptors.

Consisting of α, β, and γ-subunits, all G proteins are activated by a similar mechanism. Without agonist bound to the receptor, the α-subunit is bound to GDP and the βγ-complex in an inactive, trimeric complex. Upon agonist binding, conformational changes in the receptor-G protein complex result in GDP release, GTP binding to the α-subunit, and the dissociation of the α-subunit from the βγ-complex. Once dissociated, the α-subunit can affect second messengers (Casey and Gilman, 1988, Tang and Gilman, 1991). D1DAR-coupled $G\alpha_{s/olf}$ proteins interact with AC to stimulate cAMP production which, in turn, stimulates cAMP-dependent protein kinase A (PKA) activity (Kebabian and Calne, 1979). PKA can affect multiple downstream targets. One of these is the 32-kD DA

and cAMP-regulated phosphoprotein (DARPP-32), which amplifies D1DAR signaling and affects multiple downstream processes (Svenningsson et al., 2004). Downstream of DARPP-32, D1DARs affect the activity of ERK1/2 (Chen et al., 2004). ERK1/2 activity is coregulated by glutamate receptors, thus ERK1/2 integrates signaling from DA and glutamate systems to induce long-term changes to synaptic plasticity and gene transcription (Valjent et al., 2005, Valjent et al., 2006, Girault et al., 2007). Lastly, D1DARs affect ion channels and ionotropic receptors, and thus membrane excitability, through direct association with ion channels (Kisilevsky et al., 2008), or through downstream signaling cascades (Greengard, 2001).

In normal animals, D1DAR activation is correlated with increased behavioral activation, consistent with a model where direct pathway activation increases movement. Indeed, D1DAR-specific agonist administration induces locomotion, while D1DAR-specific antagonists decrease locomotion in rodents (Arnt et al., 1992). Dysregulation of these signaling cascades is seen in animal models of L-DOPA-induced dyskinesias (LIDs) and attention deficit-hyperactivity disorder (ADHD), as well as patients with mutations in *GNAL*, the gene coding $G\alpha_{s/olf}$. Thus, D1DAR signaling plays an important role in motor behavior.

Classical D2DAR signaling occurs through $G\alpha_i$-mediated inhibition of AC and PKA. Thus, activation of D2DARs opposes many of the cellular actions of D1DARs, including the inhibition of DARPP-32 and ERK1/2 (Svenningsson et al., 2004), albeit in different cell-types in striatum D2DARs activation, therefore, has a net inhibitory effect on the membrane excitability of indirect pathway MSNs. A second, β-arrestin2-dependent, mode of D2DAR signaling has also been described. After prolonged activation, D2DARs become phosphorylated by G protein-coupled receptor kinases (GRKs) and recruit β-arrestin2, which ceases $G\alpha_i$ signaling and promotes receptor internalization (Claing et al., 2002). Along with this role, β-arrestin2 signals through a glycogen synthase kinase 3 dependent

cascade to mediate the effects of many dopaminergic drugs (Bohn et al., 2003, Bohn et al., 2004, Masri et al., 2008).

The role of D2DARs activation in the induction and control of movements is more complex than that D1DARs activation. Where D1DAR activation is almost always associated with movement induction, D2DARs activation only induces movements in specific scenarios. For one, selective D2DAR agonists have antiparkinsonian effects in PD patients (Biglan and Holloway, 2002). Likewise, D2DAR knockout mice exhibit parkinsonian-like movement impairment (Baik et al., 1995). Further, D2DAR antagonists inhibit spontaneous and amphetamine-induced locomotion in rodents (Pijnenburg et al., 1975, Sanberg, 1980). The selective D2DAR agonist quinpirole, however, also inhibits locomotion in rodents (Van Hartesveldt et al., 1994, Li et al., 2010). Part of this inhibitory effect may be due to activation of D2DAR autoreceptors. D2DARs expressed on striatal interneurons are also likely involved because quinpirole also inhibits locomotion in mice lacking D2DAR autoreceptors (Anzalone et al., 2012). To complicate matters more, D2DARs appear to mediate the hyperactivity phenotype of an attention deficit hyperactivity disorder model (Fan et al., 2010). Thus, depending on the context or experimental approach, D2DAR activation may facilitate or inhibit movement.

DA and the development of the basal ganglia

Along with DA's role as an important neuromodulator in adult animals, it is becoming increasingly clear that DA plays a role in the development of the basal ganglia. In rodents, midbrain DA neurons begin to send axons to what will become the striatum starting at embryonic day 14 (Verney et al., 1982). DA receptor expression also begins around this time (Schambra et al., 1994). During the first two postnatal weeks, a dramatic increase in striatal DA concentration occurs and DA receptors tune their sensitivity to DA (Roffler-Tarlov and Graybiel, 1987, Kim et al., 2002). By postnatal day 14, DA is necessary for

feeding and movement, as mice deficient in DA exhibit aphagia and akinesia at this age (Zhou and Palmiter, 1995).

DA is not necessary for the development of gross structures in the brain; humans and mice with genetic deficiency in DA synthesis show normal gross anatomy of the brain (Snow et al., 1993, Rajput et al., 1994, Zhou and Palmiter, 1995). While cortical neurons exhibit robust changes in morphology as a result of developmental perturbations to the DA system (Money and Stanwood, 2013), structural changes to the striatum are more subtle. DA is, however, critical for the proliferation and a maintenance of dendritic spines on MSNs. In an MSN cell culture model, DA receptor blockade reduces spine formation (Fasano et al., 2013). Similarly, rats lesioned with the dopaminergic neurotoxin 6-hydroxydopamine (6-OHDA) as neonates show a reduction in MSN spine density (Ingham et al., 1989). Interestingly, the same reduction in MSN spine density is observed in hyper-dopaminergic DAT knockout mice (Berlanga et al., 2011), indicating that proper MSN spine formation requires DA transmission to be tuned to a suitable range. How MSN spine density changes relate to circuit function and dysfunction is not yet known. Further, the importance of spine density changes to developmental disorders where DA signaling is perturbed is not yet clear. These observations do, however, illustrate the importance of DA in the proper anatomical development of the striatum.

Evidence for DA dysfunction in dystonia

Many acquired and inherited dystonias are associated with dysfunction of the DA system. Dystonia is sometimes observed in patients with PD. In fact, a dystonic foot is often the first symptom of PD (Tolosa and Compta, 2006). In early-onset PD cases, blepharospasm and cervical dystonia are also sometimes seen. More commonly, dystonia is an aspect of the motor fluctuations that occur from long-term L-DOPA therapy in PD. Motor fluctuations consist of peak-dose dyskinesia, commonly referred to as LIDs, and off-dystonia. Peak-

dose dyskinesias typically consist of stereotypic, choreaform movements and occur directly following L-DOPA dosage (Voon et al., 2009). Off-dystonia occurs after the L-DOPA dose wanes and consists of debilitating segmental or generalized dystonia (Marconi et al., 1994, Fahn, 2000, Ha and Jankovic, 2011). Animal models have provided some clues to the mechanisms of peak-dose dyskinesia (Andersson et al., 1999, Santini et al., 2007, Westin et al., 2007), but the neural mechanisms involved in off-dystonia are less understood. GPi DBS is an effective treatment for off-dystonia, implicating abnormal basal ganglia output (Ostrem and Starr, 2008).

A second acquired dystonia associated with dysfunctional DA neurotransmission is tardive dystonia, caused by a reaction to DA receptor antagonists. The first family DA receptor antagonists, termed typical antipsychotics, were introduced in the 1950s to treat psychosis in schizophrenia patients. Later, a second generation of atypical antipsychotics like clozapine, were introduced with lower incidence of motor side effects (Correll and Schenk, 2008). Both classes of drugs block D2DARs (Snyder et al., 1970). Typical antipsychotics can cause an acute dystonic reaction in rare cases (Mehta et al., 2015), but tardive symptoms are more common, developing after several months of antipsychotic administration. Roughly 10-20% of patients taking typical antipsychotics for more than a few months develop tardive symptoms, which may include dystonia (Sethi et al., 1990, van Harten et al., 1996). The dystonic movements are typically focal or segmental and involve the trunk and neck (Mehta et al., 2015). The mechanisms of tardive dystonia are poorly understood. It is unclear why tardive dystonia develops rather than other tardive syndromes. Hypotheses currently focus on D2DAR supersensitivity (van Harten and Tenback, 2011, Mehta et al., 2015), with the idea that chronic antagonism of D2DARs produces functional supersensitivity of D2DARs to DA which eventually results in basal ganglia pathophysiology and abnormal movement. Indeed, animal studies illustrate that

chronic antipsychotic administration causes an increase in the expression of functional D2DARs (Prosser et al., 1989, Bernard et al., 1991, Seeman et al., 2005). A cohesive understanding of how these changes to D2DAR sensitivity produces dystonic movement is currently lacking.

Many inherited disorders that disrupt genes necessary for normal DA neurotransmission cause dystonia. The most straightforward and commonly used example of these disorders is L-DOPA-responsive dystonia (DRD), caused by mutations in genes necessary for DA biosynthesis (Gorke and Bartholome, 1990, Ichinose et al., 1994, Ludecke et al., 1995). More recently, other inherited dystonias associated with DA neurotransmission have been described. For one, a mutation in VMAT2 causes a complex, childhood-onset disorder involving dystonic movements as well as mood disturbances and autonomic dysfunction (Rilstone et al., 2013). AADC mutations cause a similar clinical phenotype to VMAT2 deficiency (Brun et al., 2010). Loss-of-function mutations in DAT cause a childhood-onset movement disorder that can involve dystonia and parkinsonism (Ng et al., 2014). Lesch-Nyhan disease causes reduced striatal DA and dystonia (Visser et al., 2000, Jinnah et al., 2006). Patients with VMAT2, AADC, DAT mutations, as well as Lesch-Nyhan disease patients, show poor response to L-DOPA, distinguishing them from patients with DRD (Kurian et al., 2011, Visser et al., 2011).

Recent neuroimaging studies implicate altered DA release in idiopathic dystonia. Using techniques that indirectly assess DA release by measuring the displacement of a radiolabeled DA receptor antagonist, two recent studies found reduced DA release in writer's cramp and spasmodic dysphonia (Berman et al., 2013, Simonyan et al., 2013). Further, deficits in DA receptor binding have been observed in idiopathic blepharospasm and cervical dystonia (Naumann et al., 1998, Horie et al., 2009). These deficits are likely more subtle than those found in the inherited dystonias covered above; however, they

illustrate that some deficiency in DA neurotransmission might be a general feature of a large subgroup of dystonias.

DRD as a disorder prototypical of dystonia arising from DA dysfunction

Despite being relatively rare, DRD is widely cited as a prototypical case where dysfunctional DA neurotransmission causes dystonia (Wichmann, 2008, Tanabe et al., 2009, Bragg et al., 2011, Thompson et al., 2011, Song et al., 2012). One reason DRD is presented in this way is because of its conceptual simplicity, where DA synthesis is disrupted and dystonia results. DRD also serves as prototypical disorder for several other reasons. For one, almost all dystonias arising from DA dysfunction are associated with reduced DA neurotransmission. Tardive dystonia is caused by DA antagonists and off-dystonia by waning of L-DOPA dosage. Most of the inherited dystonias disrupt DA neurotransmission in a way that would predict reduced signaling. One exception may be mutations to DAT, though DAT knockout and knockin mice exhibit complex changes to the DA system including reduced TH protein levels (Jones et al., 1998, Mergy et al., 2014). Thus, some humans with DAT deficiency may also exhibit a net reduction in DA neurotransmission.

Lastly, DRD is a disorder poised to answer several questions about the complex relationship between DA signaling and the disparate presentations of dystonia, parkinsonism, and other movement disorders. As covered earlier, the genetic and acquired etiologies that disrupt DA neurotransmission cause dystonia, but also other movement disorders in several cases. For example, neuroleptic medications may cause tardive dystonia, but tardive dyskinesia or parkinsonism may also occur (Mehta et al., 2015). These varied presentations argues that dystonia is caused by reduced DA neurotransmission along with a very specific set of circumstances. Thus, the reduction in presynaptic DA neurotransmission likely combines with adaptive processes which

together results in dystonia rather than parkinsonism or other outcomes. DRD, particularly an etiological animal model of DRD, provides a means to understand this complex relationship.

DRD: *Clinical features*

The clinical features of DRD were first reported in the 1970s by Segawa and collegues (Segawa et al., 1971). Though genetics have added to our understanding of the disorder and expanded the phenotype to some degree, Segawa's initial description is largely consistent with the current consensus of the clinical presentation of DRD. The classical DRD presentation is characterized by dystonia of the lower limbs, with notable diurnal fluctuations (Kurian et al., 2011). Sometimes, the syndrome progresses to generalized dystonia as patients age. Other movement disorders can co-occur, including tremor, myoclonus, and parkinsonism. Psychiatric symptoms such as anxiety and depression are common in DRD patients, however intellectual disability is rare (Wijemanne and Jankovic, 2015). The typical age of onset is around 6 years old, though adult-onset cases are described (Segawa, 2009). An excellent response to L-DOPA is considered a hallmark feature of DRD. In fact, many patients exhibit a dramatic response to their first dose of L-DOPA (Bandmann and Wood, 2002). Dyskinetic side effects of the L-DOPA therapy are considered rare in DRD patients, though they can occur when doses are too high (de la Fuente-Fernandez, 1999, Hwang et al., 2001). Serum levels of homovanillic acid are low in DRD patients, consistent with impaired catecholamine synthesis (Kurian et al., 2011). Further, reduced brain DA and TH protein, without markers of degeneration, are shown in two postmortem studies (Rajput et al., 1994, Furukawa et al., 1999).

Mutations in tetrahydrobiopterin (BH_4) synthesizing enzymes

DRD is most commonly associated with autosomal dominant GTP cyclohydrolase 1 (GCH1) deficiency. GCH1 is necessary for the initial step in the synthesis of BH_4, a cofactor for TH (Ichinose et al., 1994, Clot et al., 2009). BH_4 is also a cofactor for other important brain enzymes including nitric oxide synthase, phenylalanine hydroxylase, and tryptophan hydroxylase (Longo, 2009). GCH1 deficiency shows partial penetrance, whereby the disorder is more predominant in females by a ratio of roughly 6:1 (Furukawa et al., 1998, Segawa et al., 2003). Molecularly, most GCH1 mutations are missense or deletions (Clot et al., 2009). Mutant GCH1 might interact with the normal protein, encoded by the remaining normal allele, conferring a dominant negative effect on BH_4 synthesis (Thony and Blau, 2006). Alternatively, large deletions in GCH1 may cause haploinsufficiency. Inherited DRDs caused by mutations in other genes necessary for BH_4 synthesis have also been described, including 6-pyruvoyltetrahydrobiopterin reductase (PTS) deficiency and sepiapterin reductase (SPD) deficiency (Kurian et al., 2011). The lack of BH_4 may confer instability in TH. Indeed, reduced staining for TH is observed in the striata of patients with GCH1 mutations (Furukawa et al., 1999).

Mutations in TH

Mutations in TH were first suggested as a cause of DRD based on the observation that the metabolic pathology was different in some DRD patients than others (Gorke and Bartholome, 1990). Gorke and Bartholome observed reduced homovanillic acid but normal 5-hydroxyindolic acid in a DRD patient, and suggested that this may be due to an inherited error in catecholamine synthesis, but normal serotonin (5-HT) synthesis. Later, a missesnse mutation in TH (p.381Q>K) associated with autosomal recessive DRD was discovered in a Dutch family, confirming this assertion (Knappskog et al., 1995, Ludecke et al., 1995). Soon after, a point mutation (p.205P>L) causing infantile parkinsonism was

discovered (Ludecke et al., 1996), illustrating that mutations in TH can cause dystonia or parkinsonism. Recently, a patient carrying two TH mutations was described with myoclonus-dystonia (Stamelou et al., 2012). Because the clinical manifestations of TH mutations do not always overlap with classical DRD, clinicians now use the moniker TH deficiency (THD) to describe these cases (Zafeiriou et al., 2009, Willemsen et al., 2010). In fact, a categorization schema dividing THD into two groups has been proposed (Willemsen et al., 2010). Type A THD denotes the classical DRD presentation, whereas type B denotes a more severe, infantile parkinsonism presentation. Type B THD patients may also exhibit encephalopathy, intellectual disabilities and other complications (Zafeiriou et al., 2009).

To date, 49 causative mutations have been described in 71 different individuals with THD (Willemsen et al., 2010, Fossbakk et al., 2014, Tan et al., 2014). Most of these mutations are unique to the families studied, and only one common variant in *TH* has been found (van den Heuvel et al., 1998). Most THD cases are caused by missense mutations, though five nonsense mutations have been described. All THD patients described in the literature carry two, often different, mutant alleles, though a man carrying one nonsense allele developed PD in his 50s (Bademci et al., 2010). Further, the mutations primarily occur in the catalytic or C-terminal tetramerization domains, though three promotor region mutations haven been described (Willemsen et al., 2010).

The biophysical effects of these mutations have been described in several studies (Knappskog et al., 1995, Ludecke et al., 1996, Royo et al., 2005, Fossbakk et al., 2014). Several THD mutations are positioned at amino acid residues at the predicted active site of the enzyme (Andersen et al., 2002, Calvo et al., 2010). These mutations may affect interactions with BH_4, iron, or the tyrosine substrate at the active site. Alternatively, they may affect substrate selectivity for tyrosine, conferring reduced enzymatic activity. Several

mutations in the C-terminal domain cause reduced protein stability and solubility (Royo et al., 2005, Fossbakk et al., 2014). Stability defects also result from interruption of BH_4 interacting residues, as BH_4 acts as a stability-promoting chaperone (Calvo et al., 2010). Likely, decreased stability and solubility converge to reduce activity, as they often do *in vitro*; though how that may occur in DA neurons is not known. *In vitro* enzymatic activity, however, is a good predictor of disease phenotype in humans, as mutations associated with 15-30% residual activity are associated with type A THD, whereas those associated with 1-10% residual activity are associated with the more severe, type B THD phenotype (Fossbakk et al., 2014).

Animal models closely resembling DRD

To date, no animal models have been developed with the precise genetic etiology of DRD. Several animal models, however, exist on the basis of disrupting DA synthesis early in development, which may be considered the core etiology of DRD. These include developmental dopaminergic lesion models and mice where catecholamine synthesis proteins are knocked out. The phenotypes of these models, as well as mechanistic insights gained from them are presented below.

Neonatal 6-OHDA-lesioned rats

Rats lesioned as neonates with the dopaminergic neurotoxin 6-OHDA have been extensively studied for several decades. Though these rats do not exhibit dystonic movements, they exhibit disrupted DA neurotransmission early in development, similar to what occurs in DRD. Thus, adaptive changes that occur in this model may be similar to those seen in DRD. To produce this model, rats are typically given an intracisternal injection of 6-OHDA between postnatal day 3 and 5. The typical lesion produces over a 90% loss of TH immunostaining and DA content in the striatum by lesioning the axonal

fibers from midbrain DA neurons (Breese and Traylor, 1972). Initial behavioral studies of these rats in adulthood garnered much attention due to their striking difference from rats lesioned with 6-OHDA as adults (Shaywitz et al., 1976, Breese et al., 1984b). Most notably, these rats exhibit a paradoxical hyperactive phenotype, contrasting the notable akinesia seen in rats lesioned as adults (Ungerstedt, 1971a). Feeding behavior is also spared in the neonatal-lesioned animals, whereas adult-lesioned animals exhibit adipsia and aphagia. Thus, the disparity between these two phenotypes illustrates the marked difference in the behavioral effect of adult DA depletion versus DA depletion early in development.

The neural mechanisms of this behavioral disparity have been examined with pharmacological and anatomical techniques. For one, neonatal-lesioned rats exhibit much greater sensitivity to D1DAR activation than adult-lesioned animals (Breese et al., 1984a). Further, these rats show increased sensitization to D1DAR activation, where repeated doses of a D1DAR agonist cause a greater and greater locomotor response (Criswell et al., 1989). Sensitization to D1DAR agonism in neonatal 6-OHDA-lesioned rats requires NMDA receptor activation and coordinated ERK1/2 signaling (Criswell et al., 1990, Papadeas et al., 2004), reflective of long lasting plastic changes to D1DAR signaling. Changes to D1DAR signaling likely are a compensatory mechanism responsible for preserving locomotor behavior in these rats, though they are not without consequence. Neonatal 6-OHDA-lesioned rats also exhibit self-injurious behavior and enhanced aggression through a D1DAR-dependent mechanism (Breese et al., 1984b). Additionally, increased serotonergic innervation of striatum is seen in neonatal 6-OHDA-lesioned rats (Berger et al., 1985), where serotonergic signaling plays a compensatory role in movement induction (Bishop et al., 2004). Taken together, the neonatal 6-OHDA-lesion model illustrates a general principle that may apply to DRD, where plastic changes in the

brain compensate for DA depletion occurring early in development. Those plastic changes, though, may cause a different, maladaptive, phenotype like dystonia.

MPTP-treated primates

Certain non-human primates treated with 1-methyl-4-phenyl-1,2,3,6- tetrahydropyridine (MPTP) exhibit dystonia for a period of weeks following the lesion, then exhibit permanent parkinsonian symptoms (Perlmutter et al., 1997, Tabbal et al., 2006). The transient period of dystonia is associated with moderate reduction in striatal dopaminergic innervations and a transient reduction in D2DAR binding. Though this phenomenon is only described in two studies, these findings argue that dystonia may occur from moderate striatal DA depletion and parkinsonism from a more severe lesion. Alternatively, other factors, like changes to D2DARs, may be more essential in determining the outcome of dystonia versus parkinsonism.

Mice modeling impaired BH_4 synthesis

There are several lines that in some way recapitulate the genetic etiology of DRD, though none carry a mutation homologous to those found in DRD patients, *per se*. Three mouse lines have been characterized as having a deficiency in BH_4 synthesis, thus in some way modeling the more common, dominant form of DRD. First, *hph-1* mice, a line generated by sperm mutagenesis with ethylnitrosourea, exhibit a significant reduction in GTP-cyclohydrolase activity (McDonald et al., 1988). Though these mice exhibit no overt phenotype, some differences in gene expression are observed in basal ganglia (Zeng et al., 2004).

Two different mouse lines where PTS is knocked out via homologous recombination (*pts -/-* mice) have been developed (Sumi-Ichinose et al., 2001, Elzaouk et al., 2003). PTS is necessary for BH_4 synthesis and patients with PTS deficiency exhibit a

DRD-like phenotype (Hanihara et al., 1997); thus, *pts -/-* mice exhibit construct validity for DRD. Without intervention, *pts -/-* mice die soon after birth. The *pts -/-* neonates show weak striatal TH immunostaining and DA content, like the postmortem studies of DRD patients (Rajput et al., 1994, Furukawa et al., 1999). This phenotype is reversible upon oral administration of BH_4, illustrating BH_4's important role as a stability and transport-supporting chaperone of TH in DA neurons. Strikingly, the effect of BH_4 depletion is more pronounced on catecholamine systems than nitric oxide, phenylalanine, and 5-HT synthesis, despite the role for BH_4 in those processes (Sumi-Ichinose et al., 2001, Elzaouk et al., 2003). These findings may provide an explanation for the relative specificity of the DRD phenotype to motor dysfunction.

Later, the *pts-/-* model was refined by the addition of a transgene that expresses human PTS driven by the *Dbh* promoter. In these mice, termed *pts-/-; DPS* mice, BH_4 synthesis is spared in noradrenergic neurons (Sumi-Ichinose et al., 2005). These mice do not require neonatal intervention for survival and develop mild motor impairments, but not overt dystonia (Sumi-Ichinose et al., 2005, Sato et al., 2008). TH immunostaining in these mice is selectively lost in the striosomal compartment of the striatum. The authors interpret from this result that the phenotype of DRD may result from an imbalance between striosomal and matrix components of the striatum (Crittenden and Graybiel, 2011).

Along with the *pts-/-* models, a model of SPR deficiency (*spr -/-*) has been characterized (Homma et al., 2011). SPR deficiency also causes BH_4 deficiency and a DRD-like phenotype in humans (Kurian et al., 2011). *Spr -/-* mice show a similar biochemical and behavioral phenotype to *pts-/-; DPS* mice, with robust DA depletion and mild motor impairments. Taken together, these lines of mice have revealed the specificity of interactions between BH_4 and the enzymes for which it serves as a cofactor, thus illustrating some of the biochemical basis of the dominant form of DRD.

Mutant TH lines

Several TH knockout mice were generated and characterized in the 1990s, with Palmiter and colleagues being the first to publish their findings (Zhou et al., 1995). These mice die i*n utero* due to cardiac failure caused by NE deficiency (Thomas et al., 1995). Two other groups generated their own TH knockout allele and showed similar results (Kobayashi et al., 1995, Rios et al., 1999, Portbury et al., 2003). Palmiter's group refined their model by targeting *Th* to one allele of the *Dbh* promoter, producing mice deficient in TH specifically in dopaminergic cell-types (Zhou and Palmiter, 1995). These mice, termed *DA deficient* mice, are born at Mendellian frequency, but are adipsic, aphagic, and akinetic and die without intervention around 2 weeks of age. Notably, feeding and locomotion are rescued in *DA deficient* are rescued by 50 mg/kg L-DOPA, and the mice survive into adulthood with daily L-DOPA treatment (Szczypka et al., 1999). Dystonic movements are not described in *DA deficient* mice. Like neonatal 6-OHDA-lesioned rats, *DA deficient* mice exhibit D1DAR supersensitivity, illustrating that this developmental response generalizes to multiple models (Kim et al., 2000).

Summary and guiding questions for thesis work

Neuroscience research has provided a detailed understanding of the gross and molecular anatomy of the DA system. Further, DA's physiological effects on basal ganglia circuitry and its general role in movement induction have been well described. However, despite evidence from many sources that dysfunctional DA neurotransmission is a critical player in dystonic movement, its precise role in this type of abnormal movement remains elusive. Mechanistic understanding of DA's role in dystonic movement could guide the development of treatments applicable to several types of dystonia. Work with animal models plays a key role in gaining mechanistic insights like these. For the work presented here, a novel knockin mouse model of DRD was used. These mice were designed to carry

a point mutation homologous to the p.381Q>K (c.1146C>A) in TH that causes autosomal recessive DRD in a Dutch family (Knappskog et al., 1995). Modeling this rare etiology was not done to better understand these few specific cases, but rather to gain insights into DA's role in dystonia in general. With that focus in mind, three general questions guided this thesis:

1. What are the *in vivo* effects of the p.381Q>K mutation in TH in mice?
2. What are the neurochemical, anatomical, and receptor substrates of the dystonic movements observed in this mouse model?
3. What kinds of adaptive changes, downstream of presynaptic DA transmission, occur in the mouse model?

Chapter 2: In vivo molecular, neurochemical, and anatomical effects of the p.382Q>K mutation in TH

Abstract

The work in this chapter provides the initial molecular, neurochemical, and anatomical characterization of the DRD mice. We verified proper insertion and expression of the knockin construct with PCRs. Pre and perinatal lethality of homozygous DRD mice were overcome by outcrossing the allele and supplementing the mice with noradrenergic agonists *in utero* and L-DOPA, postnataly. DRD mice had reduced TH activity throughout the brain, though striatal TH activity was particularly affected, reduced to ~1% of normal. DA concentrations were similarly reduced throughout the brain. Contrasting models of Parkinson's disease, the gross anatomy of nigrostriatal dopaminergic neurons was normal in DRD mice, though immunostaining for TH was weak. Corticostriatal input in DRD mice showed a shift away from synapses on dendritic spines towards dendrites themselves. The studies in this chapter provide construct validity of the DRD mouse model and insights into the *in vivo* anatomical effects of developmentally reduced DA synthesis.

Introduction

The work presented here makes use of a new knockin mouse model of DRD (Jackson Labs allele descriptor: *Th*^{tm1Ehess}, abbreviated here as DRD mice). The mutation selected for modeling, the strategy for creating the mice, and many initial steps in their development were completed prior to my joining the lab. Dr. Hess and colleagues selected the p.381Q>K mutation in TH as the mutation to recapitulate in mice for several reasons. First, a mutation in TH was selected, as opposed to a GCH1 mutation, because BH_4 is involved in many biochemical processes besides catecholamine synthesis, including nitric oxide, 5-HT, and phenylalanine synthesis (Longo, 2009). Though much of the clinical literature implicates DA deficiency as central to the pathogenesis of human GCH1 deficiency (Furukawa et al., 1999, Thony and Blau, 2006), deficiencies in these other processes could not be ruled out as contributors to phenotype in a GCH1 mouse mutant. Thus, selection of a TH mutation confines the genetic insult to catecholamine systems, focusing the characterization of the DRD mice. The p.381Q>K mutation in TH was selected over other TH mutations, first, because the biochemical phenotype was characterized in a 1995 study (Knappskog et al., 1995). Second, while most patients with THD carry two different mutant alleles, the p.381Q>K mutation is carried homozygously by six related Dutch patients with DRD (Ludecke et al., 1995). Thus, homozygous DRD mice are a true genotypic model and there is no need to generate a second mutant allele to create compound heterozygous mice.

To characterize the DRD mice, first, molecular techniques were used to validate the insertion of the targeting construct in the mouse genome, and validate mRNA expression of the mutant allele. Next, TH activity, brain neurochemistry, and nigrostriatal anatomy were examined, establishing construct validity of the DRD mouse model. This characterization, however, is also useful for better understanding the pathomechanisms

associated with THD. Mutations in TH cause a range of biochemical phenotypes, including reductions in protein stability, solubility, substrate selectivity, and enzymatic activity (Royo et al., 2005, Fossbakk et al., 2014), with the p.381Q>K mutation causing reduced protein stability and an ~85% reduction in enzymatic activity (Knappskog et al., 1995, Fossbakk et al., 2014). These previous studies, however, were all carried out in heterologous expression systems. Mice carrying the homologous p.382Q>K (c.1160C>A) mutation provide the unprecedented opportunity to investigate these biochemical phenotypes in DA neurons, *in vivo*. This molecular, biochemical, and anatomical work, plus initial effort in overcoming the pre and perinatal death that the homozygous DRD mice exhibit are covered in this chapter.

Methods

Animals

All studies make use of mice carrying the *Th*^{tm1Ehess} (DRD) allele. DRD mice were originally generated on a C57BL6/J background. For outcrossing the allele, DBA2/J mice were obtained from The Jackson Laboratories (Bar Harbor, ME). Mice group housed in the vivaria at Emory University. The light period was 7am to 7pm. For all studies, 2-4 month-old male and female mice were used. Littermates heterozygous for the DRD allele (Het) and littermates carrying two wild-type alleles (normal) were used as controls. Specialized procedures for generating DRD mice are covered in the results. For those procedures, the date of conception was noted by the presence of copulation plug. For drug treatments in dams' drinking water, isoproterenol, phenylephrine, L-DOPA, benserazide, and ascorbic acid (all from Sigma-Aldrich, St. Louis, MO) were dissolved in dH_2O. Peripheral drug treatments included L-DOPA, benserazide and ascorbic acid, injected subcutaneously (s.c.) in saline vehicle. All procedures were in accordance with Emory University's IACUC and Division of Animal Resources guidelines.

Polymerase chain reaction (PCR) conformation of knockin

Four long PCRs from genomic DNA of mice carrying the DRD allele with a neomycin resistance cassette (DRD +Neo) were used to confirm proper insertion of the targeting construct. Long PCRs were performed in 25 µL reactions containing DNA, specific primers (see below), and a long template PCR kit (Roche, Manheim, Germany) with 40 cycles of 10 sec at 95˚C, 30 sec at 60˚C, and 4 min at 68˚C. The following primers sequences were used, with approximate locations noted in Figure 3A: P1, 5'-GACGTCAGCCTGGCCTTTAAGA-3'; P2, 5'-AGATGGAATGGGAAGGCTCT-3'; P3, 5'-AGGCCAGAGGCCACTTGTGTAG-3'; P4, 5'-GACGAGTTCTTCTGAGGGGATCAA-3'; P5, 5'-ACAGCCTTACCTGTTGTGGG -3'; P6, 5'-AGTCATGGTAGGCTCTGAAAGTGG-3'.

Additionally, two short PCRs were used to confirm the removal of the Neo from the DRD allele. PCRs were performed in 25 µL reactions containing DNA, specific primers (see below), GoTaq polymerase (Promega, Madison, WI), with 40 cycles of 15 sec at 95˚C, 30 sec at 60˚C, and 2 min 72˚C. The following primer sequences were used, with approximate locations noted in Figure 3C: P7, 5'-ACACCGAAGCAGAGACTGT-3'; P8, 5'-CTGATGCTACTTCTCCAGG-3'. P3, as above.

The PCR product of a short sequence (300 bp) encompassing the c.1160C>A mutation was also sequenced to verify that DRD mice carried the point mutation. PCR was performed as above with the P7 and P8 primers. Samples were sequenced by Genewiz, Inc (South Plainfield, NJ). The same PCR conditions were used for typical genotyping.

Quantitative reverse transcriptase PCR (qRT-PCR)

Mice were sacrificed by cervical dislocation and midbrain was rapidly dissected, frozen on dry ice, and stored at -80˚C. Total RNA was isolated using a PureLink RNA kit (Invitrogen, Carlsbad, CA) and cDNA was reverse transcribed using a QuantiTect reverse transcription kit (Qiagen, Venlo, The Netherlands). qPCR was performed using an Applied Biosystems Fast 7500 Real-Time PCR system (Life Technologies, Carlsbad, CA). Gene-specific primers (5'-GGAACGGTACTGTGGCTACC-3' and 5'-AACCAGTACACCGTGGAGAG-3') were designed to amplify a 342 bp region of *Th* mRNA containing the p.382Q>K mutation. All samples were assayed in triplicate in 25 µL reactions containing cDNA, gene-specific primers, and SYBR Green Select Mastermix (Life Technologies) with 40 cycles of 15 sec at 95˚C and 1 min at 60˚C. Data were obtained with Applied Biosystems software and analyzed by the ΔCt method (Schmittgen and Livak, 2008), using amplification of a housekeeping gene (18s rRNA; 5'-TTGACGGAAGGGCACCACCAG-3' and 5'-GCACCACCACCCACGGAAATCG-3') as reference. Reverse transcriptase PCR products were also sequenced, as above, to verify the presence of the p.382Q>K mutation in the mRNA of DRD mice.

Monoamine measurements

Mice were sacrificed at 8pm by cervical dislocation and the brain was rapidly removed and chilled in ice-cold saline for 1 min. Dorsal striatum, midbrain, hippocampus, cortex, brainstem, and cerebellum were dissected on a chilled platform, rapidly frozen on dry ice, and stored at -80˚C. Samples were homogenized by sonication in 10 volumes of chilled 0.1 M perchloric acid. Homogenates were centrifuged at 10,000g for 10 min at 4˚C. The supernatant was filtered through a 0.45 µm PVDF spin filter (Micro-Spin Centrifuge Filter Tubes, Grace Discovery Sciences, Deerfield, IL). The pellet was dissolved in 2% SDS and

protein concentrations were determined by Pierce protein assay (Thermo Fischer Scientific, Waltham, MA), per manufacturer's instructions.

DA, DOPAC, NE, L-DOPA, 5-HT, and 5-hydroxyindoleacetic acid (5-HIAA) were examined by high performance liquid chromatography (HPLC) with electrochemical detection. Monoamines were separated with an ESA MD-150 x 3.2 mm column and detected with an ESA5600A Coularray detector with an ESA 6210 detector cell (ESA, Bedford, MA). Analytical cell potentials were set at -175, 100, 350, and 425 mV. Mobile phase was 1.7 mM 1-octanesulfonic acid, 75 mM NaH_2PO_4, 0.25% triethylamine, and 8% acetonitrile, pH 2.9 at a flow rate of 0.4 mL/min. Monoamines were identified and quantified by comparing the peak retention time and height to that of standards using ESA Coularray software.

In vivo TH activity assay

TH activity was determined *in vivo* by the method of Carlsson et al. (Carlsson et al., 1972). Mice were injected (s.c.) with 150 mg/kg NSD-1015, an AADC inhibitor and sacrificed 45 min later, at 8pm. Brain regions were dissected and L-DOPA was assessed by HPLC.

Western Blotting

Mice were sacrificed at 8pm by cervical dislocation and midbrain was sonicated in 20 mM Tris, and protease inhibitor cocktail (Roche). Homogenates were centrifuged at 18,000 rcf for 20 min at 4˚C. Protein concentration was adjusted and samples were incubated in Laemmli buffer (Bio-Rad, Hercules, CA) and boiled at 95˚C for 10 min. Proteins were separated on a 12% acrylamide gel, transferred to a nitrocellulose membrane, blocked with 2% milk for 1 hr, and probed for 72 hrs with Rabbit anti-TH antibody (1:1000, Pel-Freez, Rogers, AR), at 4˚C. Rabbit anti-actin (1:1000, Abcam, Cambridge, MA) was used a loading control. Blots were then incubated with HRP conjugated anti-rabbit secondary

antibody (1:1000, Jackson ImmunoResearch, West Grove, PA) for 2 hrs at room temperature, developed with a chemiluminescence kit (Bio-Rad) and imaged with a Fuji LAS-3000 digital imager (Fujifilm, Tokyo, Japan).

Immunohistochemistry

Mice were anesthetized with 2,2,2-tribromoethanol, and perfused with a solution of 137 mM NaCl, 22.2 mM dextrose, 23.4 mM sucrose, 2 mM $CaCl_2$, and 1.6 mM sodium cacodylate at pH 7.2, followed by perfusion with 4% paraformaldehyde, 117 mM sucrose, and 67 mM sodium cacodylate at pH 7.2. Brains were removed, post-fixed in the perfusion solution for 16 hrs, and then stored in 67 mM sodium cacodylate at pH 7.2. Before processing, brains were equilibrated in 30% sucrose for 72 hrs and then the entire brain was sectioned (30 µm) using a freezing microtome.

Using every 6th section, parallel series of sections were immunostained for TH or the DA transporter (DAT). For TH, tissue was treated with 0.3% Triton-X in Tris-buffered saline (TBS) for 1 hr, blocked with 5% normal goat serum (NGS) in TBS and 0.1% Triton-X, then reacted for 72 hrs at 4˚C with Rabbit anti-TH antibody (1:1000, Pel-Freez) in TBS, 1% NGS, 0.1% Triton-X, 0.01% NaN. Sections were then incubated for 24 hrs at 4˚C with biotinylated Goat anti-Rabbit antibody (1:500, Jackson ImmunoResearch) in the same solution. Sections were incubated with avidin-biotin complex (Vector Labs, Burlingame, CA) for 2 hrs, and developed in 3,3-diaminobenzadine (Sigma).

For DAT, tissue was treated with Citra antigen retrieval reagent (BioGenex, Freemont, CA) for 1 hr at 70 ˚C blocked with TBS, 10% NGS and 0.15% Triton-X, then reacted with Rat anti-DAT antibody (1:1000, Millipore, Temecula, CA) for 24 hrs at 4˚C. Sections were then incubated with biotinylated Goat anti-Rat antibody (1:200, Jackson

ImmunoResearch) for 24 hrs at room temperature and developed as described for TH immunostaining.

For vesicular glutamate transporters 1 (vGluT1) and vesicular glutamate transporters 2 (vGluT2), tissue was blocked with TBS, 10% NGS, 0.3% Triton-X, and 1% bovine serum albumin, then reacted for 24 hrs with Guinea pig anti-vGluT1 (1:5000, Millipore, Temecula, CA) or Guinea pig anti-vGluT2 (1:5000, Millipore). Sections were then incubated with biotinylated Goat anti-Guinea pig antibody (1:200, Jackson ImmunoResearch) for 90 min at room temperature and developed as described for TH immunostaining.

Densitometry

Digital images of tissue stained for vGluT1 and vGluT2 were acquired with a Leica DC 500 camera (Leica, Wetzlar, Germany). Striatum was divided into four quadrants, dorsolateral, dorsomedial, ventrolateral, and ventromedial. NIH ImageJ software was used to quantify staining intensity of each subregion. Intensity values from anterior commissure were subtracted as a reference for background. Densitometry was performed blind to genotype.

Stereology

For stereological cell counts of TH-positive midbrain neurons, every 6^{th} section, immunostained for TH, was viewed using an Olympus BX51 light microscope (Melville, NY), equipped with a motorized stage (MACC500, Ludl Electronic Products, Hawthorne, NY) and coupled to a computer with StereoInvestigator software (MicroBrightField, Williston, VT). The TH-positive region of the midbrain was outlined using a 4X objective, using a mouse brain atlas (Paxinos and Franklin, 2001) to estimate borders of SNc and

VTA. TH-positive cells were counted at 40X using the optical fractionator probe with a 55,185 μm^2 counting grid and a 10,000 μm^2 frame with 30 µm depth.

The volume of the dorsal striatum was estimated using estimated using the Cavalieri estimator tool, with every 6th section stained for Nissl substance. Stereological counts were performed blind to genotype. The Gundersen coefficient of error was below 0.1 for all measures.

Electron Microscopy

Mice were anesthetized with 2,2,2-tribromoethanol, and perfused with paraformaldehyde (4%) and glutaraldehyde (0.1%) in 0.1 M phosphate-buffered saline. Sections of striatum were cut at 60 µm with a vibrating microtome and immunostained vGluT1 or vGluT2 as above and processed for electron microscopy as previously described (Raju et al., 2008). Briefly, tissue was dehydrated, post-fixed in 1% osmium and embedded in resin on microscope slides. After resin polymerization, blocks of dorsolateral striatal tissue from each animal were cut in ultrathin sections and collected on single slot copper grid and stained with lead citrate.

Sections from the surface of the blocks were scanned at 25,000X with a JEOL electron microscope (Jeol USA, Peabody, MA). To estimate the synaptic density, immunoreactive boutons were counted from 50 randomly collected images in each animal and expressed as the boutons/ area scanned. Images of immunoreactive terminals forming synaptic contacts were randomly collected from each animal. The postsynaptic targets in contact with each labeled terminal were identified based on ultrastructural features (Peters et al., 1991). The ratio of labeled boutons in contact with spines versus dendrites were calculated for each terminal population. Images were analyzed blind to genotype.

Statistics

Monoamine data and weights were analyzed using analysis of variance (ANOVA). Significant effects within groups were tested *post hoc* with the Holm-Sidak test, with normal mice as the control group. Student's *t* test was used for anatomical comparisons between genotypes. SigmaStat (Systat Software, San Jose, CA) was used for all analyses. Detailed statistical results are presented in the Figure Legends.

Results

PCR conformation of DRD knockin allele

My role in the project began after much of the preliminary work on this mouse line had been completed. Dr. Ann Heinzer, in collaboration with my mentor Dr. Ellen Hess, selected p.381Q>K from the literature, generated a targeting vector containing the mouse homologous p.382Q>K mutation, and verified proper insertion of the vector to C57BL6-derived embryonic stem cells with long PCR and Southern blot analyses. Dr. Valerie Thompson and Dr. Robert Raike, two other postdoctoral fellows in Dr. Hess' lab, verified germline transmission of the mutant allele. They also removed the neomycin resistance cassette (Neo) in the mutant allele by breeding the line with a *Cre*-deleter strain. I joined Dr. Ellen Hess' lab and began working with the line as Het carriers of the allele on a C57BL6/J background became available.

First, a series of long PCR reactions were performed to confirm that the DRD knockin construct was correctly inserted into the mouse genome (Fig. 3A and 3B). The 5' insertion site was verified by two reactions (P1-P2 and P1-P3) that used a common forward primer specific to the genomic DNA upstream of and outside of the 5' end of the construct, P1, and a reverse primer upstream of the Neo, P2, and one specific to the Neo, P3. DNA from knockin mice was amplified by both reactions, whereas wild-type DNA was only amplified by the P1-P2, as wild-type mice do not carry the Neo. The 3' insertion site

was confirmed by two reactions (P4-P6 and P5-P6) that used a common reverse primer specific to the genomic DNA downstream and outside of the 3' end of the construct, P6, and one forward primer specific to the Neo, P4, and one downstream of the Neo, P5. Similar to the 5' end verification, both reactions amplified knockin DNA, whereas only the P5-P6 reaction amplified wild-type DNA. These reactions demonstrate that the DRD knockin construct was indeed inserted into the proper position in the genome.

Next, two PCRs were performed to verify proper removal of the Neo from the DRD allele (Fig. 3C and 3D). A reaction with primers flanking the site of the Neo (P7-P8) amplified a 300bp product in DNA from resolved DRD mice but failed to produce a small product in DNA from the DRD allele +Neo. In agreement with these results, a reaction with a reverse primer inside the Neo (P7-P3) amplified DNA from the DRD allele +Neo, but not from resolved DRD allele. Finally, sequences of the DRD allele show the presence of the p.382Q>K mutation in genomic DNA extracted from DRD mice (Fig. 3E). These reactions illustrate that the DRD allele carry the p.382Q>K mutation but do not carry the Neo.

Next, RT-PCR techniques were used to characterize mRNA expression of the p.382Q>K mutation. RNA was extracted from brain and *Th* mRNA was amplified with RT-PCR. Sequences of the RT-PCR product showed the presence of the p.382Q>K in these samples (Fig. 4A). Next, expression of the p.382Q>K mutation was quantified using qRT-PCR. No difference in the abundance of *Th* mRNA between normal and DRD mice was detected (Figure 4B; $p>0.1$). These analyses show that the p.382Q>K mutation is expressed, and in normal abundance in DRD mice.

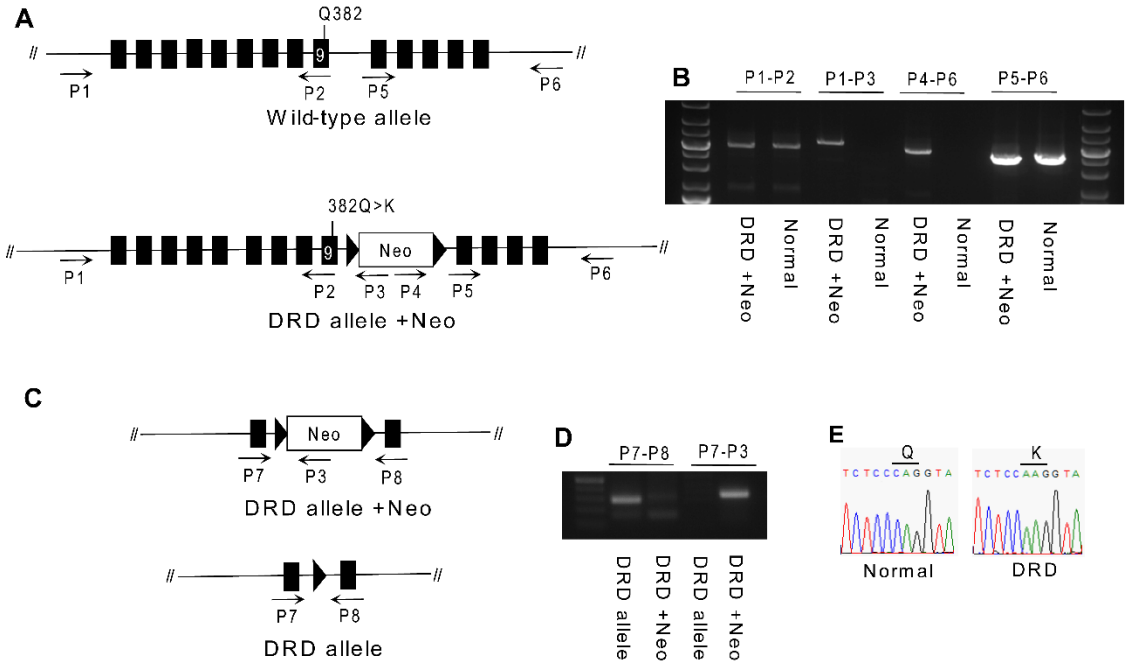

Figure 3: Conformation of knockin and resolution of Neo. (A) Schematic of wild-type *Th* and the DRD allele containing the p.382Q>K mutation in exon 9 of *Th*, and a neomycin resistance cassette (Neo) flanked by two loxP sites. (B) Results of long PCRs confirming the correct genomic insertion of the targeting construct in genomic DNA. Arrows in panel A indicate direction and approximate position of primers used; primers P1 and P6 were to genomic DNA outside of the targeting construct. PCR products (4-6 kb) amplified from knockin (DRD allele +Neo) and normal mouse genomic DNA correspond to the indicated primers. (C and D) Schematic and results of PCRs demonstrating resolution of the Neo. Primers P7 and P8 were to genomic DNA on *Th*, and P3 were to the Neo. (E) Sequences obtained from PCR amplicons from genomic DNA verifying the p.382Q>K mutation

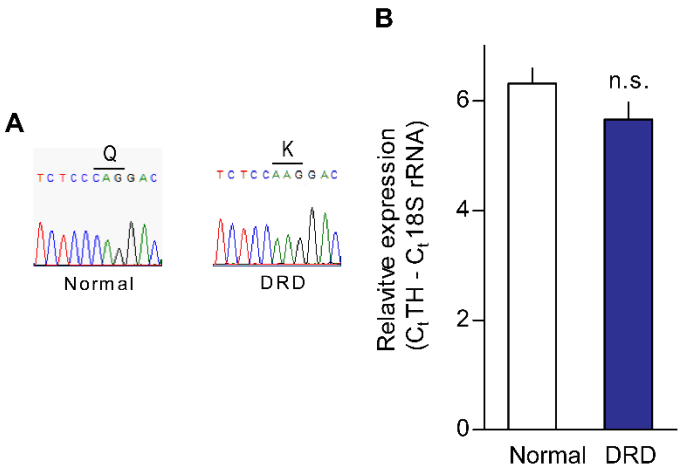

Figure 4: RNA expression of DRD allele. (A) Sequence of the RT-PCR amplicon from brain mRNA illustrating expression of the p.382Q>K mutation in DRD mice. (B) qRT-PCR revealed no difference in the quantity of *Th* mRNA between normal (n=8) and DRD mice (n=8; p>0.1, Student's *t* test). Values represent mean ± SEM.

Generating homozygous DRD mice

Initially, Het mice on a C57BL6/J background were mated to generate homozygous DRD mice. These initial crosses generated zero homozygous DRD pups out of 26 total pups in 4 litters (Fig. 5A). *Th -/-* and *Dbh -/-* mice die between embryonic day 12.5 (E12.5) and E15.5 due to a defect in fetal heart development caused by NE deficiency (Kobayashi et al., 1995, Thomas et al., 1995, Zhou et al., 1995, Rios et al., 1999). We hypothesized that DRD mice were dying *in utero* and could be rescued by similar strategies used to rescue *Th -/-* mice. Supplementation of the dam's drinking water with 2 mg/mL L-DOPA and 2.5 mg/mL ascorbic acid from E8.5 through birth, employed in Zhou et al. 1995 with *Th -/-* mice, was modestly successful at rescuing the DRD mice *in utero*, producing litters with 11% DRD mice (Fig. 5A; 7 DRD mice/61 total, 11 litters). Drinking water supplementation with 100 µg/mL isoproterenol, a β2 adrenergic receptor agonist, and 2.5 mg/mL ascorbic acid from E8.5 to birth, employed in Portbury et al. 2003 with a different *Th -/-* strain, produced litters with 25% DRD mice (Fig. 5A; 7 DRD mice/31 total, 4 litters).

Though these interventions rescued the DRD mice from prenatal death, the DRD pups failed to thrive. Of the 14 DRD pups generated, none survived to postnatal day 21.5 (P21.5) (Fig. 5B). The DRD pups were smaller than their littermates, appeared dehydrated, and did not display typical nursing behavior. Rescue attempts with daily 50 mg/kg L-DOPA, s.c., similar to the rescue strategy for *DA deficient* mice (Zhou and Palmiter, 1995), or with 2 mg/mL L-DOPA in the drinking water were unsuccessful. Hand feeding and sucrose injections, when attempted in parallel with L-DOPA supplementation, were also unsuccessful. *DA deficient* mice also display high postnatal lethality, despite L-DOPA supplementation, on a pure C57BL6/J background (Hnasko et al., 2007). Similarly, certain Type B THD patients are unresponsive to L-DOPA (Zafeiriou et al., 2009). Thus, we concluded that DRD mice were not healthy enough on a pure C57BL6/J background for the types of behavioral analyses necessary for the project.

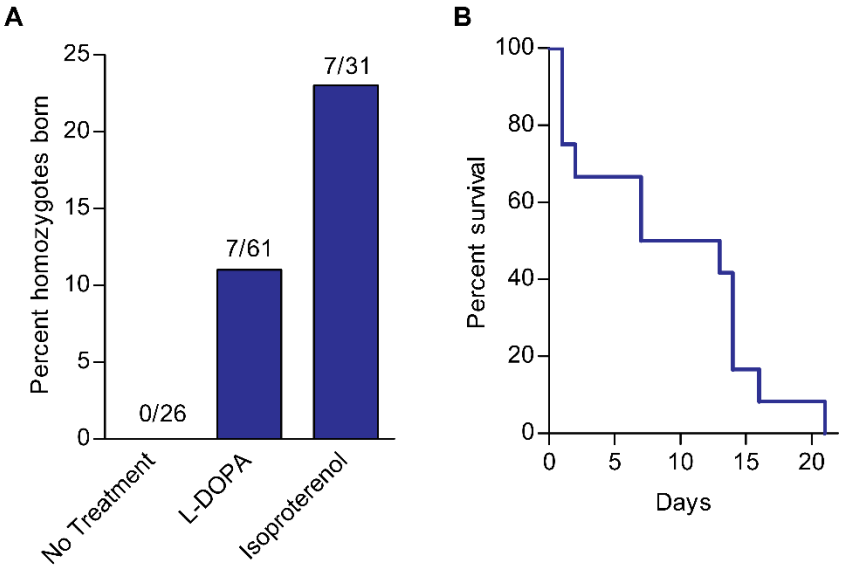

Figure 5: Pre and postnatal death of DRD mice on a C57BL6/J background. (A) Initial attempts to generate homozygous DRD mice on a C57BL6/J background without treatment were unsuccessful (0 DRD pups/ 26 total pups born from Het x Het breeding). Treatment of the dam's drinking water with 2 mg/mL L-DOPA from E8.5-birth produced 7 DRD pups/ 61 total pups. Treatment of the dam's drinking water with 100 µg/mL isoproterenol from E8.5-birth produced 7 DRD pups/ 31 total pups. (B) No DRD pups from these litters survived to P21 (n=14), despite L-DOPA supplementation, hand-feeding and other efforts.

To circumvent the high lethality of the inbred DRD mice, the DRD allele was outcrossed to promote hybrid vigor. Hets on the C57BL6/J background (B6.DRD/+) were crossed with DBA2/J mice, another well characterized inbred mouse (Fig. 6A). Hets from the subsequent F1 generation (D2B6.DRD/+) were intercrossed, generating normal, Het, and DRD mice on a mixed F2D2B6 background. These litters were treated with 100 µg/mL isoproterenol and 2.5 mg/mL ascorbic acid in the dam's drinking water, from E8.5-birth. 20 µg/mL phenylephrine, an α1 adrenergic receptor agonist, was also administered in the dam's drinking water (Schank et al., 2006). DRD mice were born near Mendelian frequency on this background, with these treatments (Figure 6B; 88 DRD/ 419 total mice). Notably, neonatal DRD pups on this background nursed and were indistinguishable from their littermates. By P9.5, deficits in size and became apparent. To facilitate feeding in the DRD mice as they began to seek solid food, a two part L-DOPA supplementation strategy was employed. First, from P9.5 to P16.5, the drinking water was supplemented with 1.5 mg/mL L-DOPA, 0.5 mg/mL benserazide, a brain impenetrable AADC inhibitor used to prevent peripheral metabolism of L-DOPA, and 2.5 mg/mL ascorbic acid. From P16.5 on, mice were injected daily, s.c., with 10 mg/kg L-DOPA, 2.5 mg/kg benserazide and 2.5 mg/mL ascorbic acid in saline. Additionally, litters were culled to 5-6 pups so the smaller DRD mice could compete more successfully during nursing. This strategy produced DRD mice that were ~20% lighter than their normal and Het littermates (Fig. 5C and 5D; $p<0.01$ for males, $p<0.05$ for females), though the DRD mice appeared much more robust than their counterparts on the C57BL6/J background. As described for *DA deficient* mice, DRD mice lose weight rapidly if L-DOPA supplementation is terminated for more than 48 hrs (Szczypka et al., 1999). Thus, DRD mice were maintained with daily L-DOPA supplementation when not involved in experiments. All experiments, unless otherwise stated, were performed after >24 hr L-DOPA washout. To normalize any effects of the treatments, normal and Het controls received all of these treatments in parallel.

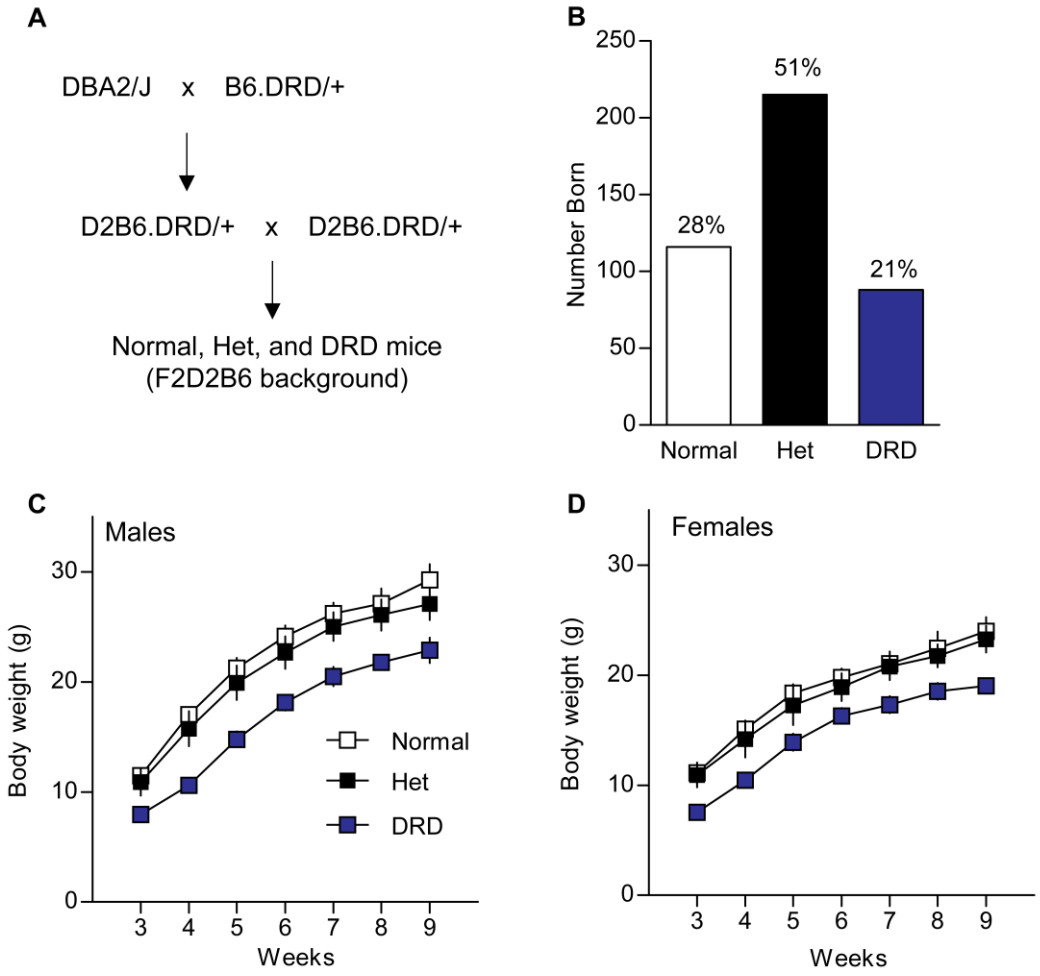

Figure 6: Viability of DRD mice on F2D2B6 background. (A) Breeding strategy to generate outbred DRD mice. Het carriers of the DRD allele on a C57BL6/J background (B6.DRD/+) were crossed with DBA2/J mice, generating D2B6.DRD/+ mice. These mice were intercrossed to create F2D2B6 litters with normal, Het, and homozygous DRD mice. (B) Supplementing the D2B6.DRD/+ dam's drinking water with 100 µg/mL isoproterenol, 20 µg/mL phenylephrine, and 2.5 mg/mL ascorbic acid produced litters near Mendelian frequency (n=116 normal, 215 Het, 88 DRD). Male (C) and female (D) DRD mice were significantly lighter than normal mice throughout postnatal development. Two-way ANOVA revealed a main effect of genotype on weight for males ($F_{2,27}$=5.6, $p<0.01$) and females ($F_{2,19}$=5.7, $p<0.05$). Values represent mean ± SEM.

DRD mice exhibit reduced TH activity and brain catecholamines

The presence of TH protein in DRD mice was verified with immunoblotting. Immunoreactivity for TH was weaker in the midbrain of DRD mice than in littermate controls (Fig. 7, insert). TH activity was assessed *in vivo* by measuring L-DOPA accumulation after inhibition of AADC by NSD-1015 (Carlsson et al., 1972). Preliminary studies indicated that catecholamines were exceptionally low in DRD mice and might be below the level of detection for HPLC. DRD mice, however, exhibited a period of high locomotor activity early in the active period. Therefore, we sacrificed mice for the TH activity assay and neurochemical characterizations at 8pm, during this burst of activity, hypothesizing that catecholamines would be elevated to detectable levels at this time of day in DRD mice. In midbrain, TH activity in DRD mice was significantly reduced by ~85% (Fig. 7; $p<0.001$). This is consistent with the human p.381Q>K mutation, which also shows an ~85% reduction in enzymatic activity (Knappskog et al., 1995). Activity was similarly reduced in cortex ($p<0.001$) and cerebellum ($p<0.001$). A significant reduction in TH activity was also observed in Het mice in midbrain ($p<0.05$) and striatum ($p<0.001$). In the striatum of DRD mice, which receives dense innervation of TH-containing axons from the midbrain, TH activity was reduced by ~99% ($p<0.001$). These results imply that the reductions in TH were more severe in the brain regions containing axon terminal fields than those containing dopaminergic cell somas. Further, they confirm the negative effect of the p.382Q>K mutation on TH activity in mouse brain.

Next, we characterized the neurochemical consequences of the mutation, measuring monoamines and their metabolites in several brain regions. Consistent with the reduction in TH enzyme activity, DA was significantly reduced in striatum ($p<0.001$), midbrain ($p<0.001$) and cortex ($p<0.001$) of DRD mice (Table 1). Surprisingly, the reduction in DA content was as severe in midbrain (~99%) as in striatum (~99%). DOPAC,

the primary metabolite of DA, was also reduced in DRD mice ($p<0.001$). However, the DOPAC/DA ratio in DRD mice was nearly 4-fold higher than normal in midbrain ($p<0.001$) and striatum ($p<0.001$), suggesting that DA turnover occurs at a higher rate in the mutants. This elevated DOPAC/DA ratio may explain the low midbrain DA concentration despite the partial sparing of TH activity in that region. NE concentrations were also significantly reduced throughout brain ($p<0.001$). Sex differences in catecholamine and metabolite concentrations were separately analyzed. Males exhibited a higher DOPAC/DA ratio than females ($p<0.001$; not shown) only in the midbrain; the significance of this finding is not clear. Taken together, these result show that the deficit in TH activity causes severe catecholamine depletion throughout the brain in DRD mice.

With the exception of brainstem, where 5-HT was significantly increased ($p<0.01$), 5-HT concentrations were unaffected (Table 1). However, 5-HIAA, the major metabolite of 5-HT, and the 5-HIAA/5-HT ratio were significantly increased in most brain regions ($p<0.001$). The significance of elevated 5-HT turnover is not clear, though it is similar to the increase in serotonergic innervation of the striatum observed in 6-OHDA-lesioned rats (Berger et al., 1985).

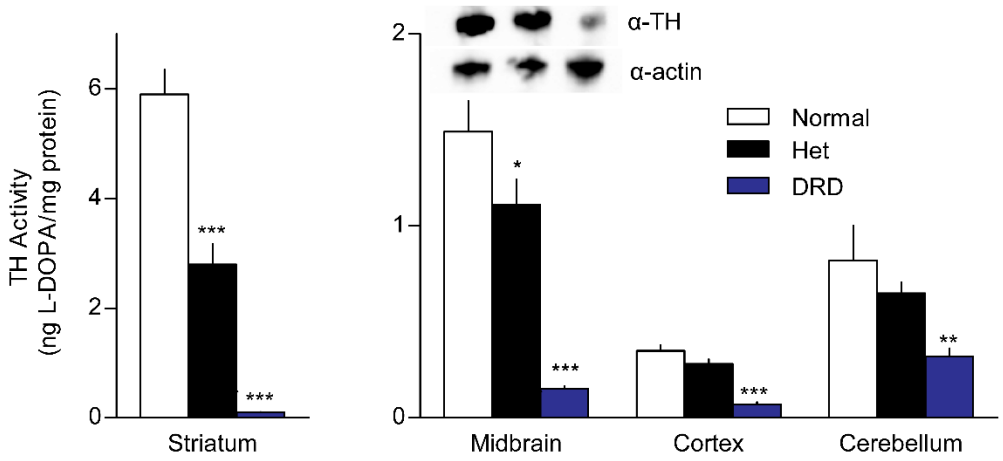

Figure 7: *In vivo* TH activity in DRD mice. TH activity was assessed *in vivo* in normal (n=5), Het (n=7), and DRD mice (n=8). TH activity was significantly reduced in all brain regions tested in DRD mice, including striatum ($F_{2,17}$=96.5, p<0.001), midbrain ($F_{2,17}$=44.1, p<0.001), cortex ($F_{2,17}$=42.3, p<0.001) and cerebellum ($F_{2,17}$=8.3, p<0.01). (Insert) Representative western blot for TH and actin from the midbrain of normal (left), Het (middle), and DRD mice (right). The TH blot was weaker in intensity in DRD mice than controls. Values represent mean ± SEM; statistical analyses for TH activity was performed for each region using a one-way ANOVA with a Holm-Sidak *post hoc* analyses where appropriate. *p<0.05, **p<0.01, ***p<0.001 compared to normal.

Table 1. Regional monoamine concentration (ng/mg protein)

	DA	DOPAC	DOPAC/DA	NE	5-HT	5-HIAA	5-HIAA/5-HT
Striatum							
Normal	72.1 ± 2.7	7.5 ± 0.3	0.1 ± 0.0	0.2 ± 0.0	3.1 ± 0.2	1.7 ± 0.1	0.6 ± 0.0
Het	60.1 ± 5.8***	5.7 ± 0.7**	0.1 ± 0.0	0.1 ± 0.0	3.5 ± 0.5	2.2 ± 0.3	0.6 ± 0.0
DRD	0.3 ± 0.1***	0.1 ± 0.0***	0.5 ± 0.1***	0.0 ± 0.0***	3.2 ± 0.2	3.4 ± 0.3***	1.0 ± 0.1***
Midbrain							
Normal	3.4 ± 0.4	1.0 ± 0.1	0.3 ± 0.0	6.0 ± 0.3	8.8 ± 0.4	2.7 ± 0.3	0.3 ± 0.0
Het	3.5 ± 0.8	0.7 ± 0.1*	0.2 ± 0.0	5.9 ± 0.4	10.0 ± 0.7	3.4 ± 0.3	0.3 ± 0.0
DRD	0.1 ± 0.0***	0.1 ± 0.0***	1.2 ± 0.2***	0.2 ± 0.1***	10.8 ± 0.3	5.4 ± 0.5***	0.5 ± 0.0***
Cortex							
Normal	0.5 ± 0.1	0.1 ± 0.0	0.4 ± 0.1	2.2 ± 0.1	2.6 ± 0.2	1.0 ± 0.1	0.4 ± 0.0
Het	0.4 ± 0.1	0.1 ± 0.0	0.4 ± 0.1	2.1 ± 0.2	2.9 ± 0.5	1.3 ± 0.2*	0.5 ± 0.1*
DRD	0.1 ± 0.0***	0.0 ± 0.0**	0.6 ± 0.1**	0.1 ± 0.0***	2.5 ± 0.3	1.7 ± 0.1***	0.7 ± 0.0***
Brainstem							
Normal	0.4 ± 0.0	0.3 ± 0.0	0.7 ± 0.0	7.0 ± 0.4	8.1 ± 0.7	5.7 ± 0.5	0.7 ± 0.1
Het	0.4 ± 0.0	0.2 ± 0.0*	0.5 ± 0.0*	7.4 ± 1.0	9.1 ± 1.7	7.0 ± 0.9	0.8 ± 0.1
DRD	0.3 ± 0.0	0.0 ± 0.0***	0.1 ± 0.0***	0.9 ± 0.1***	14.1 ± 1.6**	17.2 ± 1.4***	1.2 ± 0.1***
Hipp							
Normal	N.D.	N.D.	—	3.0 ± 0.3	2.8 ± 0.1	2.1 ± 0.1	0.8 ± 0.0
Het	N.D.	N.D.	—	2.7 ± 0.3	2.8 ± 0.3	2.2 ± 0.4	0.8 ± 0.1
DRD	N.D.	N.D.	—	0.3 ± 0.0***	3.5 ± 0.7	2.8 ± 0.2**	0.8 ± 0.1
Cbm							
Normal	N.D.	N.D.	—	3.2 ± 0.3	1.6 ± 0.2	1.0 ± 0.1	0.6 ± 0.1
Het	N.D.	N.D.	—	2.6 ± 0.3*	1.9 ± 0.3	1.1 ± 0.1	0.6 ± 0.1
DRD	N.D.	N.D.	—	0.0 ± 0.0***	1.3 ± 0.1	1.2 ± 0.0	1.0 ± 0.1***

Tissue concentrations of monoamines were measured by HPLC in normal (n=9), Het (n=6), and DRD mice (n=6). Effects of genotype were observed for DA ($F_{2,18}$=151, p<0.001), DOPAC ($F_{2,18}$=144, p<0.001), NE ($F_{2,18}$=170, p<0.001), 5-HT ($F_{2,18}$=7.5, p<0.01), 5-HIAA ($F_{2,18}$=66.9, p<0.001), 5-HT/5-HIAA ($F_{2,18}$=31.2, p<0.001). There was a significant genotype x brain region interaction effect for DOPAC/DA ($F_{2,18}$=24.9, p<0.001). Each analyte was tested with two-way repeated measures ANOVA. Significant main effects were tested within each brain region with one-way ANOVA and Holm-Sidak *post hoc* analyses. Values represent mean ± SEM; *p<0.05, **p<0.01, ***p<0.001. N.D. = not detected.

Normal gross anatomy of midbrain and striatum in DRD mice

To determine if the TH mutation affected the anatomy of midbrain DA neurons, we examined the morphology of TH-positive neurons (Fig. 8A). TH immunostaining of normal mice labeled neuronal soma and dendrites in the midbrain and a dense network of axons in the striatum. . The intensity of TH immunostaining in the DRD mouse brain was weaker. The soma of midbrain DA neurons showed normal staining, but dendrites displayed a much weaker staining than in normal mice. The striatum had particularly weak TH staining, consistent with the TH activity assay (Fig. 7), which showed more severe loss of TH activity in the striatum compared with the midbrain.

The weaker TH staining in DRD mice could be from degeneration of TH-positive neurons. We explored this possibility with stereological counting of TH-positive neurons in the SN and VTA. Despite the relatively weaker TH immunostaining, stereological counts of TH-positive neurons in the midbrain of DRD mice were not significantly different from normal mice (Fig. 8C; $p>0.1$ for SN and VTA). Alternatively, axonal projections to striatum could be selectively lost in DRD mice. To address this possibility, we next conducted immunostains for DAT, another marker of dopaminergic neurons. Despite the loss of TH immunostaining in the DRD mouse striatum, DAT staining was normal in this region (Fig. 8B). Further, stereological measures revealed no difference in striatal volume of DRD mice compared to normal mice (Fig. 8D; $p>0.1$). These results imply that midbrain DA neurons and their axonal projections to the striatum are intact, consistent with anatomical studies of DRD patients (Snow et al., 1993, Rajput et al., 1994).

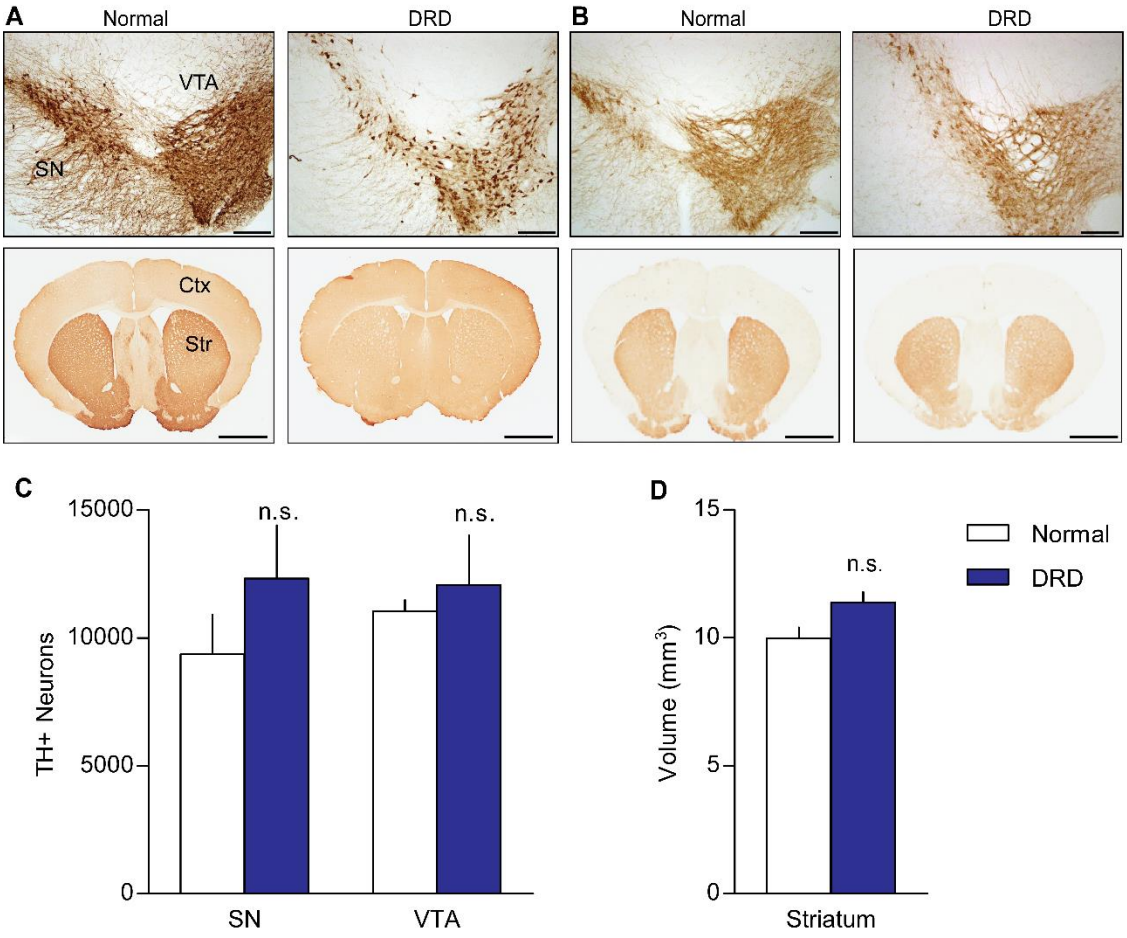

Figure 8: Anatomy of nigrostriatal pathway in DRD mice. Representative sections immunostained for TH (A) or DAT (B) from striatum or midbrain of normal and DRD mice (scale bars = 1.5 mm, striatum; 200 µm, midbrain). (C) Stereological cell counts of TH-positive neurons in the SN ($p>0.1$, Student's *t* test) and VTA ($p>0.1$, Student's *t* test). (D) Stereological assessment of striatal volume ($p>0.1$, Student's *t* test). Values represent mean ± SEM.

Microstructural changes to corticostriatal and thalamostriatal connectivity

We further examined the anatomical consequences of the p.382Q>K mutation to basal ganglia circuitry by examining glutamatergic cortical and thalamic inputs to striatum. These inputs act in concert with DA in the striatum to coordinate normal movement (Bamford et al., 2004, Costa et al., 2006). Further, glutamatergic synapses in the striatum undergo complex changes in other animal models with striatal DA depletion (Ingham et al., 1998, Villalba et al., 2009, Villalba and Smith, 2013). Thus, despite normal DAT-positive innervation and striatal volume (Fig. 8), other changes to striatal circuitry could result from the p.382Q>K mutation.

We first assessed the gross distribution of glutamatergic input to striatum by staining brain sections for vGluT1, a selective marker of corticostriatal terminals, and vGluT2 a selective marker of thalamostriatal terminals. Using densitometry to quantify vGluT1 and vGluT2 staining intensity, no significant differences between genotypes were observed in any of the subregions of striatum examined (Fig. 9; $p>0.1$ for all subregions). Next, we examined the density of corticostriatal and thalamostriatal terminals at the synaptic level in the dorsolateral striatum, counting the number of labeled synaptic boutons in images collected by electron microscopy (Fig. 10A and 10B). In agreement with the light microscopy densitometry data, no significant differences were observed in the density of either population of terminals between normal and DRD mice (Fig. 10C; $p>0.1$). Further, the number of perforated vGluT1-positive ($p>0.1$) or vGluT2-positive ($p>0.1$) synapses did not significantly differ between genotypes (not shown).

However, the ratio of axo-spinous to axo-dendritic synaptic contacts was significantly smaller for vGluT1-positive terminals in DRD mice compared to normal mice (Fig. 10D; $p<0.05$), and there was a similar trend for vGluT2-positive terminals ($p=0.052$). The functional significance of this shift toward more dendritic contacts by corticostriatal

and thalamostriatal terminals has yet to be established. Though, this altered microstructural connectivity might affect the integration of dopaminergic and glutamatergic signals in the DRD mouse striatum. Further, it illustrates that despite normal gross morphology of nigrostriatal structures, DRD mice do show altered neural anatomy at the microstructural level.

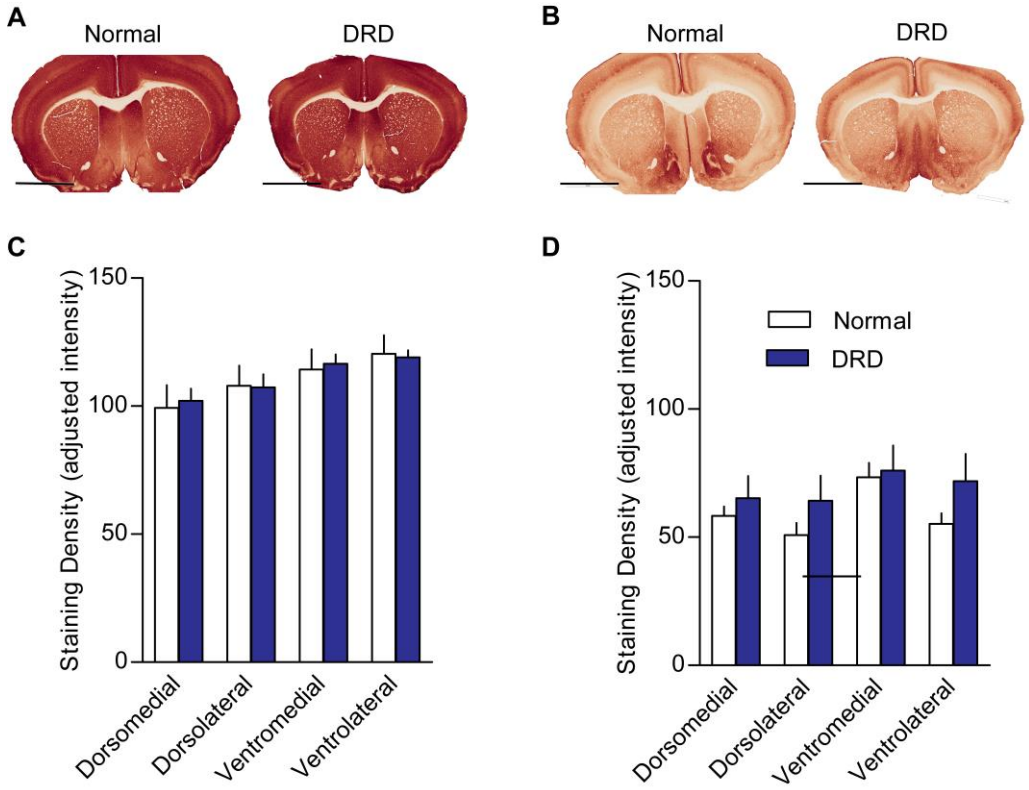

Figure 9: Glutamatergic cortico- and thalamo-striatal immunostraining. (A,B) Examples of vGluT1- (A, corticostriatal) or vGluT2- (B, thalamostriatal) immunoreactivity in the striatum of normal (n=6) and DRD mice (n=6). Scale bar = 2 mm. (C, D) Densitometric analysis of immunoreactivity in all four quadrants of striatum revealed no difference between genotype ($p>0.1$, Student's *t* test for each measure). Values represent mean ± SEM.

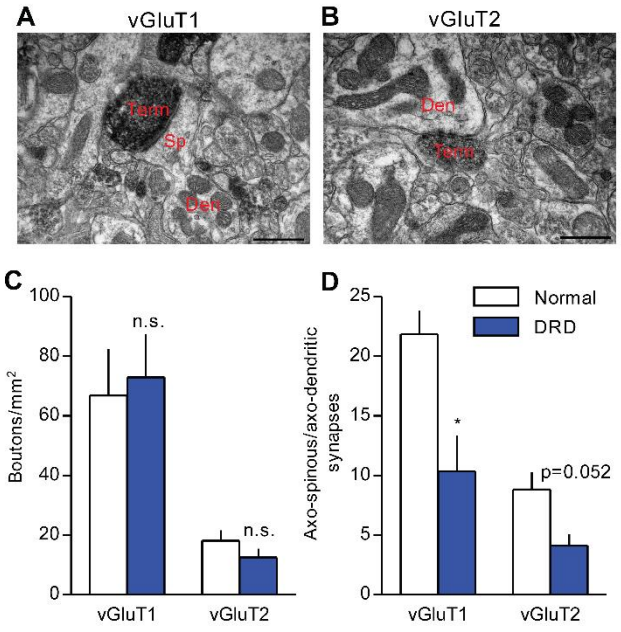

Figure 10: Glutamatergic cortico- and thalamo-striatal terminals in DRD mice. (A,B) Examples of vGluT1- (A, corticostriatal) or vGluT2- (B, thalamostriatal) immunoreactive terminal forming an axo-spinous (A) or an axo-dendritic (B) asymmetric synapse in the mouse dorsolateral striatum. (scale bar = 500 nm in A and B). (C) No significant difference was observed in the density of either vGluT1-positive or vGluT2-positive terminals between the genotypes (n=3/genotype; Student's *t* test). (D) The ratio of vGluT1-positive (n=3 animals/genotype, 177-180 terminals/genotype) or vGluT2-positive (n=3/genotype, 133-155 terminals/genotype) axo-spinous to axo-dendritic synaptic contacts was measured. This ratio was significantly smaller ($p<0.05$, Student's *t* test) for vGluT1-positive terminals, and approached significance for vGluT2-positive terminals ($p=0.052$, Student's *t* test), in the dorsolateral striatum of DRD mice. Values represent mean ± SEM; *$p<0.05$.

Discussion

This chapter describes the initial molecular, neurochemical, and anatomical characterization of a novel knockin mouse model of DRD. Further, we outline the steps necessary for producing healthy DRD mice. Through several PCRs, we demonstrate the proper insertion of the mutant allele in the mouse genome, removal of the Neo, and the presence of the missense mutation in genomic DNA. Further, we demonstrate normal mRNA expression of the missense mutation in brain. The DRD allele causes regionally specific effects to TH function; TH staining and activity are modestly reduced in midbrain, but are drastically reduced in striatum. Despite these neurochemical effects, the gross morphology of the nigrostriatal pathway was normal in DRD mice, though microstructural changes at corticostriatal synapses were observed.

These studies are the first to examine the biochemical effects of a DRD-causing mutation *in vivo*. When assessed *in vitro*, TH mutations affect stability, solubility, substrate selectivity, and enzymatic activity (Royo et al., 2005, Fossbakk et al., 2014). The p.381Q>K mutation, specifically, causes reduced stability and an ~85% reduction in enzymatic activity (Knappskog et al., 1995, Fossbakk et al., 2014). In some ways, the mouse homolog shows a similar phenotype in brain, as DRD mice exhibit a ~85% reduction in midbrain TH activity. In striatum, however, TH activity is reduced to ~99% of normal and immunostaining for TH is very weak. The lack of TH in this region could result from poor stability of the mutant protein. Thus, in DRD mice, expression of new TH may not be sufficient to overcome the rate of TH degradation in striatum. Altered interactions with other factors may also play a role. Studies from the *spr-/-* and *pts-/-; DPS* mice illustrate that BH_4 acts as a molecular chaperone for TH, promoting TH protein expression in the striatum (Sato et al., 2008, Homma et al., 2011). Q382 is located in the catalytic region of TH, though it is not predicted to directly interact with BH_4 (Andersen et al., 2002).

Nevertheless, conformational changes created by the p.382Q>K mutation may affect how TH binds BH_4, as well as the tyrosine substrate, iron, or other interacting factors. Another possibility is that axonal transport of TH may be disrupted by the p.382Q>K mutation. Taken together, the p.382Q>K mutation may cause poor stability of TH, or disrupt interactions between TH, BH_4, or axonal transport machinery to disrupt TH function, *in vivo*.

The extent to which catecholamines were reduced in DRD mice was not predicted by the *in vitro* studies of p.381Q>K TH. In both midbrain and striatum of DRD mice, DA concentrations were reduced by ~99%. NE concentrations were also near the lower limit of detection throughout the brain. This implies that the low amounts of catecholamines synthesized by p.382Q>K TH are rapidly metabolized. Indeed, we show a ~4-fold increase in the DOPAC/DA ratio, a measure of DA turnover, in both midbrain and striatum. One reason for elevated DA turnover could be a lack of D2DAR autoreceptor-mediated inhibition of DA release (Ford, 2014). With less extracellular DA to agonize autoreceptors, DA neurons may be kept in a depolarized state, constantly releasing their limited pool of DA.

The regionally specific reduction in TH protein levels and rapid turnover of DA should be considered as contributing factors for the clinical presentation of THD. Currently, residual TH activity is the only accepted biochemical predictor of disease severity in THD patients (Willemsen et al., 2010, Fossbakk et al., 2014). The protein level and DA turnover findings from DRD mice argue that other genetic, epigenetic, or environmental factors involved in protein degradation, transport, or autoreceptor function, may play important roles in the functional output of midbrain DA neurons in THD patients. Thus, therapies targeting those processes could be beneficial to THD patients, especially to patients with a poor response to L-DOPA (Zafeiriou et al., 2009). Molecular chaperones

that stabilize or promote axonal transport of TH could be beneficial. Further, MAO or COMT inhibitors that slow down DA turnover may also be beneficial. Taken together, the biochemical findings from DRD mice argue that the neuronal environment interacts with the severity of the TH mutation to ultimately confer disease severity.

We also observed elevated concentrations of the 5-HT metabolite 5-HIAA, and the 5-HIAA/5-HT ratio, a measure of 5-HT turnover, throughout most of the brain in DRD mice. Similarly, in neonatal and adult 6-OHDA-lesioned rats, striatal 5-HT fibers “sprout” in the striatum following lesion (Berger et al., 1985, Zhou et al., 1991). 5-HT terminal sprouting is thought to involve changes in trophic signaling brought on by loss of DA neuron terminals (Zhou et al., 1991). This phenomenon causes elevated concentrations of both 5-HT and 5-HIAA in striatum, similar to DRD mice. DRD mice, unlike 6-OHDA lesion models, though, have intact DA terminals in striatum, as evidenced by normal DAT staining. Thus, we demonstrate here an interaction between catecholamine depletion and 5-HT signaling that occurs independent of reduced axonal density. It will be interesting to determine the phenotypic role of the increased 5-HIAA in future studies.

Despite the weak TH staining and low catecholamine concentrations, the gross morphology and number of midbrain DA neurons was normal in DRD mice. This is in general agreement with *Th-/-* and *DA deficient* mouse lines (Kobayashi et al., 1995, Zhou and Palmiter, 1995), though this is the first study to use stereological methods to count DA neurons in this context. Thus, here we confirm for the first time the generally held belief that DRD is not associated with cell loss (Rajput et al., 1994, Furukawa et al., 1999, Bandmann and Wood, 2002, Segawa et al., 2003).

The DRD mice, however, were not without anatomical abnormalities. Despite normal gross anatomy of the striatum and a normal density of glutamatergic inputs to striatum, DRD mice show a shift towards more glutamatergic axo-dendritic synapses than

axo-spinous synapses. Future physiological work will determine the functional significance of this finding, but a reduction in spinous contacts in favor of dendritic contacts by cortical afferents likely alters synaptic plasticity. The molecular machinery for long term depression (LTD), the predominant form of plasticity in the striatum, is mostly expressed on spines (Shindou et al., 2011, Plotkin et al., 2013). Thus, a shift away from spinous synapses towards more dendritic ones, predicts that DRD mice have impaired striatal LTD, thus impaired motor learning, of importance for understanding the pathophysiology of dystonia (Peterson et al., 2010, Quartarone and Pisani, 2011).

The loss of spinous synapses may occur dependently or independently of MSN spine loss in striatum. Loss of MSN spines occurs following neonatal or adult 6-OHDA lesion in rats (Ingham et al., 1989, Ingham et al., 1998) and in primates following MPTP lesion (Villalba et al., 2009). Further, spine loss in 6-OHDA-lesioned mice shows some selectivity for indirect pathway MSNs over direct pathway MSNs (Day et al., 2006). It will be interesting to characterize the dendritic arbor of direct and indirect pathway MSNs in DRD mice, noting similarities and differences with the DA lesion models.

Previously, our lab has shown that a mouse model of DYT1 dystonia (DYT1 mice) also exhibit a shift in the ratio of spinous to dendritic glutamatergic synapses in the striatum (Song et al., 2013). DYT1 mice, similar to DRD mice, show reduced extracellular DA in striatum. Thus, though these forms of dystonia are caused by mutations in different genes, they alter neurochemistry and striatal anatomy in a similar way. Identifying shared abnormalities, such as these, is critical for pinpointing defects central to the induction of dystonia and useful for the identification of novel therapeutic strategies that may be useful in many different forms of dystonia.

Chapter 3: Behavioral phenotype of the DRD mice: special emphasis on diurnal fluctuations and drug responses

Abstract

The work in this chapter outlines the initial behavioral characterization of the DRD mice. We find that the DRD mice show strikingly similar features to patients with DRD. DRD mice exhibit abnormal movements largely composed of dystonic flexion of their limbs and trunk. Abnormal movements, locomotion, cataleptic behavior, and motor performance measures worsen through the active period in DRD mice, with motor output relatively normal at 8pm but impaired at 8am. Diurnal fluctuations in DA turnover, measured by the ratio of DOPAC/DA, correlates with behavioral diurnal fluctuations in DRD mice. DRD mice show a locomotor response to amphetamine, illustrating the behavioral relevance of their residual DA. Notably, L-DOPA and THP reduce abnormal movements in DRD mice, illustrating that the model exhibits predictive validity. Work with L-DOPS and L-DOPA microinjection to specific brain regions illustrate that the L-DOPA response is due to repletion of striatal DA, specifically. This work establishes the DRD mice as a model with face and predictive validity and illustrate the neurochemical and anatomical substrates of dysfunction in the mice.

Introduction

In the previous chapter we established that the DRD mice exhibit reduced brain catecholamines and minimal alterations to nigrostriatal anatomy. Here we expand on the analysis of the DRD mice by examining how those changes affect the behavior of the mice. Focus is placed on examining behavioral phenotypes that have relevance to the typical presentation of DRD in humans to establish face validity of the model. Patients with DRD present with dystonic limb movements that sometimes become generalized dystonia. Dystonic movements worsen through the day, a phenomenon termed diurnal fluctuations. Lastly, the hallmark feature of DRD is the dramatic amelioration of dystonia in response to L-DOPA administration (Hwang et al., 2001, Bandmann and Wood, 2002, Segawa, 2009, Trender-Gerhard et al., 2009). DRD patients also respond to THP, a mixed muscarinic receptor antagonist (Jarman et al., 1997).

For the studies in this chapter, we use observational analyses, standard assessments of rodent motor function, and drug responses to define the motor deficits of the DRD mice. Special emphases is placed on time of day-dependent differences, as patients with DRD exhibit diurnal fluctuations. Further, the response to L-DOPA and several other compounds are examined. Though a model with construct validity allows for specific biochemical questions to be asked, establishing face validity would greatly expand the utility of the DRD mice. The work in this chapter addresses the issue of face validity as well as establishes the neurochemical basis of the behavioral presentation in DRD mice.

Methods

Animals

As described in chapter 2, DRD and normal littermate controls, between 2-4 months old were used. Unless directly stated, experiments occurred following >24 hr L-DOPA withdrawal.

Assessment of abnormal movement

A behavioral inventory was used to define the types of movement including tonic flexion (forelimbs, hindlimbs, trunk, head), tonic extension (forelimbs, hindlimbs, trunk, head), clonus (forelimbs and hindlimbs), twisting (trunk, head), and tremor (forelimbs, hindlimbs, trunk, head), as developed and previously described by our laboratory (Devanagondi et al., 2007, Shirley et al., 2008, Raike et al., 2012). Abnormal movements were observed and scored for 30 sec at 10 min intervals for 60 min. An abnormal movement score was calculated by summing the scores from all scoring bins. All mice had at least 2 exposures to the testing room prior to data collection. For time of day, THP, and microinjection tests, mice were scored in a novel open field. For L-DOPA and 3,4-L-dihydroxyphenylserine (L-DOPS) tests, mice were habituated to test chambers for >24 hr before the test. Trihexhyphenidyl and microinjection tests were performed at 2pm. L-DOPA and L-DOPS tests were performed at 8pm. Behavioral raters were blinded to genotype and treatment. Mice had access to food and water *ad libitum*.

Locomotor Activity

Locomotor activity was tested in automated photocell activity cages (29 x 50 cm), each equipped with 12 infrared beams arranged in a 4 x 8 grid (San Diego Instruments; San Diego, CA) and a computer recorded beam breaks for the duration of the test period. For spontaneous locomotor activity, mice were habituated to photocell activity cages for >24

hr during the L-DOPA washout period; recording started at 1pm and continued for 24 hrs. For amphetamine challenge, mice were injected at 2pm, after mice were habituated to photocell activity cages for >24 hr during the L-DOPA washout period, and locomotor activity was recorded for 1 hr. For time of day, THP, L-DOPA, and L-DOPS effects, locomotor activity was recorded in parallel to abnormal movement assessments, as described above. All mice had at least 2 exposures to the testing room prior to data collection. Mice had access to food and water *ad libitum*.

Systemic drug challenges

Compounds were administered (s.c.) in saline, in a volume of 10 ml/kg. Behavioral experiments started 10 min after drug administration, except L-DOPS, which was administered as described (Thomas et al., 1998). Briefly, L-DOPS was dissolved in 0.2 M HCl and the solution was neutralized with NaOH just prior to injection. 1 g/kg L-DOPS plus 0.25 g/kg benserazide or vehicle was administered 5 hrs prior to testing, because NE levels peak 5 hrs after L-DOPS injection. For dose response experiments, mice were tested in a repeated measures design with a pseudorandom order of drug doses and vehicle; each mouse received every dose only once within an experiment. Mice were given a 4-day drug washout between challenges. Amphetamine, raclopride, L-DOPA, and THP were obtained from Sigma-Aldrich. L-DOPS was generously provided by Dainippon-Sumitomo Inc (Osaka, Japan).

Cling test

Grip strength was tested with the cling test. A 20 × 20 cm square platform with 6-mm grid wire mesh and 5 cm frame was suspended 50 cm above a padded surface. Mice were placed on the platform and allowed to habituate for 1 min. The platform was rotated 90° and held vertical for 1 min, then rotated again 90° and held inverted for 1 min. Each mouse

was timed until falling on 3 different trials and the average latency to fall was recorded. Mice that did not fall were timed at 3 min.

Bar test of catalepsy

Maintenance of unnatural postures, a common result of DA antagonism (Sanberg, 1980, Sotnikova et al., 2006), was tested with the bar test of catalepsy. The mouse's forepaws were gently placed on a horizontal bar (0.5 cm diameter) 4 cm above the cage floor. Time was measured from the placement of the forepaws until both forepaws were removed from the bar. Cutoff time was 1 min for each trial. Each mouse was tested in 3 consecutive trials per session. The average of 3 trials was used to calculate catalepsy.

Rotarod

The rotarod was used to assess motor learning and performance. Mice were placed on a 4 cm diameter rod (Columbus Instruments, Columbus, OH) rotating at 4 rpm. Rotation speed was increased from 4 to 40 rpm over a 6 min period, and latency to fall was recorded. Mice that did not fall during the 6 min period were recorded as 6 min. The average of 3 trials was used to calculate performance. The effect of time of day on rotarod performance was assessed on mice trained on the rotarod for two consecutive days. Mice remained on their usual daily L-DOPA supplementation during the training sessions and DRD mice performed comparably to normal during training. Mice were tested on the third day after >24 hr withdrawal from L-DOPA. The effect of L-DOPA on rotarod performance was assessed over 4 days on mice naïve to the rotarod. Mice were tested following 10 mg/kg L-DOPA or saline at 2pm.

Pole test

The pole test was used as a second method for assessing motor performance. Mice were placed with their head oriented upwards on a 50 cm tall, 1 cm diameter vertical pole placed

inside their home cage. The time for each mouse to descend and have all four limbs on the cage floor was recorded. For time of day and L-DOPA tests, mice were trained on the task for 2 consecutive days with 5 trials/day. Mice remained on their usual daily L-DOPA supplementation during the training sessions. L-DOPA was withdrawn >24 hours prior to the test session in which mice performed 5 trials and the best time for each mouse was used for analysis. The effect of L-DOPA was tested at 2pm.

In vivo TH activity and tissue monoamines

L-DOPA accumulation following NSD-1015 was used to assess *in vivo* TH activity, as in chapter 2. Tissue monoamines were assessed by HPLC, as in chapter 2. The effect of a therapeutic dose of L-DOPA on tissue monoamines was assessed at 8pm. Mice were injected (s.c) with 10 mg/kg L-DOPA and 2.5 mg/kg benserazide and sacrificed for HPLC 45 min later. The effect of L-DOPS on tissue monoamines was also assessed at 8pm. Mice were injected with L-DOPS, as above for behavioral assessments, and sacrificed for HPLC.

Statistics

Monoamine and behavioral data were analyzed using ANOVA. Significant effects within groups were tested *post hoc* with the Holm-Sidak test, with normal mice or saline treatment as the control group. In analyses where there was no obvious control group, as for time of day assessments, Tukey's test was used *post hoc*. For analyses where values spanned several orders of magnitude between genotypes, Student's *t* test was used *post hoc* for comparisons within genotypes. SigmaStat was used for all analyses. Detailed statistical results are presented in the Figure Legends.

Results

Dystonic movements in DRD mice

During our initial observations of the DRD mice, we noted abnormal involuntary movements. Forelimbs were often tucked tightly into the chest while hindlimbs were lifted off the cage floor in a stereotyped paddling motion with toes spread (Fig. 11A). Abnormal movements in DRD mice were sometimes observed at the start of the active (dark) period (8pm) and increased throughout the night with the highest occurrence at the end of the active period (8am) (Fig. 11B; $p<0.001$). This pattern of activity is reminiscent of DRD patients whose symptoms worsen throughout the day. The movements were comprised largely of abnormal flexion of the forelimbs, hindlimbs, and lower trunk (Fig. 11C and D). These movements were dynamic, not fixed postures, and best described as dystonia. No sex bias was observed. Heterozygous mice never exhibited abnormal movements, consistent with the recessive mode of inheritance in humans.

We next investigated whether other DA-dependent motor behaviors displayed deficits based on time of day in DRD mice. First, we examined locomotor activity in normal and DRD mice, after they had been habituated to the testing cages. DRD mice exhibited a normal circadian-dependent burst of locomotor activity at the start of the active period, but this was followed by a rapid decline in locomotor activity to below normal levels throughout the night (Fig. 12A; $p<0.01$). The reduction in locomotor activity was most pronounced during the last 6 hrs of the active period, when dystonic movements were most severe. We also examined locomotor activity in a novel open field at 8pm and 8am. Under these conditions, DRD mice exhibit striking hyperactivity compared to normal mice at 8pm but not 8am (Fig. 12B; $p<0.001$). DRD mice displayed increased catalepsy compared to normal at 8am, but not 8pm (Fig. 12C; $p<0.01$). It is important to note, however, that the ~10-15 s of catalepsy displayed by DRD mice is mild in comparison to

acute models of parkinsonism (Carlsson et al., 1957, Sotnikova et al., 2006). Consistent with the diurnal fluctuation in other motor behaviors, there was no difference in the performance of normal and DRD mice on rotarod or pole test at 8pm. However, at 8am, DRD mice were significantly impaired on both tests (Fig. 12D, $p<0.01$; and 12E, $p<0.001$). Thus, in all the motor behaviors we tested, the DRD mice displayed time of day-dependent dysfunction.

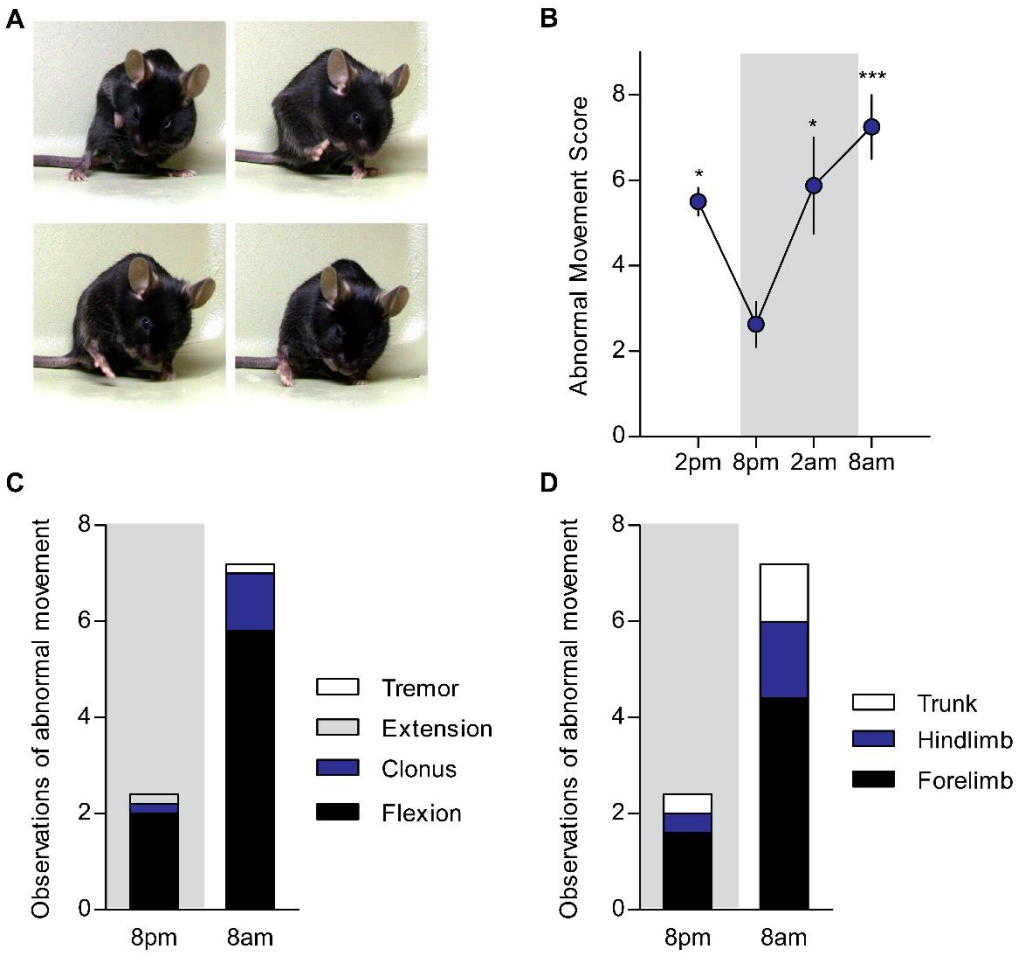

Figure 11: Dystonic movements in DRD mice. (A) DRD mice exhibit abnormal, involuntary movements, resulting in dystonic postures of the limbs and trunk. (B) Dystonic movements were assessed in DRD mice over the course of a day (n=8). DRD mice expressed significantly fewer dystonic movements at 8pm than at other times of day ($F_{3,28}$=6.8, one-way repeated measures ANOVA; p<0.05 8pm vs. 2am and 2pm, p<0.001 8pm vs. 8am, Tukey's *post hoc* analysis). (C) The abnormal movements were largely composed of transiently sustained flexion in both the inactive (light) and active (dark) period. (D) The abnormal movements were most frequent in the forelimb, but also involved hindlimb and trunk in the inactive and active periods. Data collected in the active period is shaded in grey. Values represent mean ± SEM; *p<0.05, ***p<0.001.

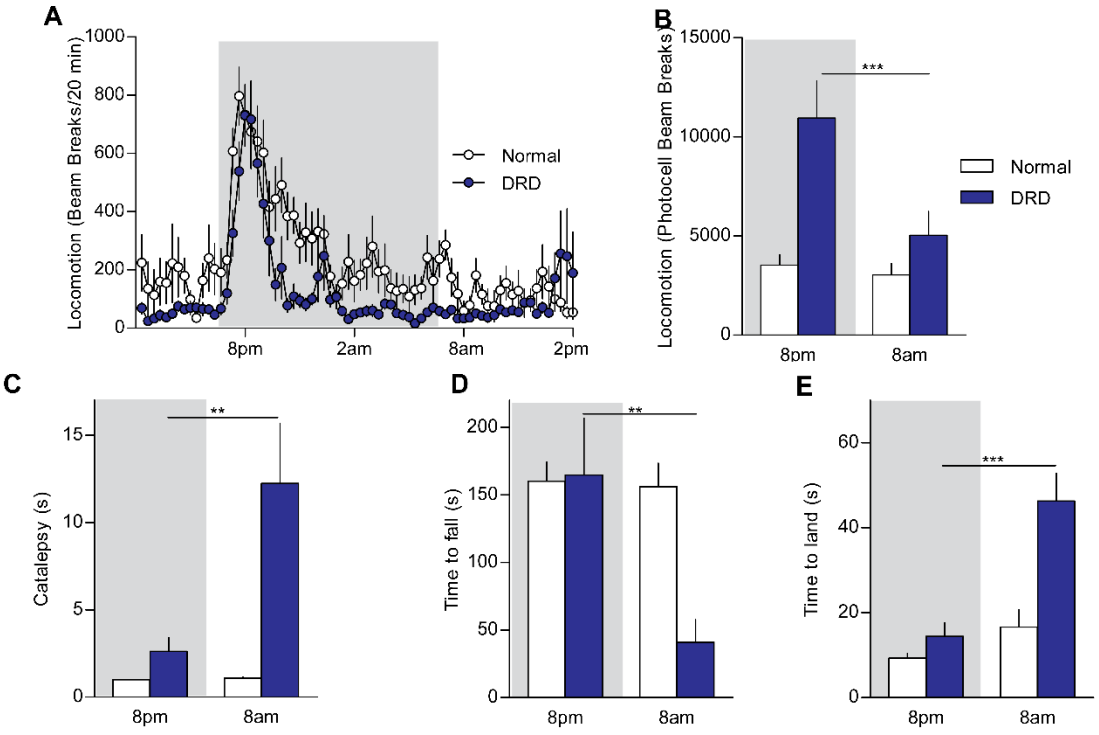
A
Locomotion (Beam Breaks/20 min)
1000
800
600
400
200
0
8pm
2am
8am
2pm
Normal
DRD
B
Locomotion (Photocell Beam Breaks)
15000
10000
5000
0
***
8pm
8am
Normal
DRD
C
Catalepsy (s)
15
10
5
0
**
8pm
8am
D
Time to fall (s)
200
150
100
50
0
**
8pm
8am
E
Time to land (s)
60
40
20
0
***
8pm
8am

Figure 12: Time of day-dependent differences in motor behavior. (A) Spontaneous locomotor activity was assessed over 24 hrs in normal and DRD mice (n=10/genotype). Locomotor activity was significantly reduced in DRD mice compared to normal mice across the entire 24 hr period ($F_{1,18}$=9.6, two-way repeated measures ANOVA; p<0.01, Holm-Sidak *post hoc* analysis). In the active period, there was a significant genotype x time interaction effect ($F_{1,18}$=5.2, two-way repeated measures ANOVA, p<0.05, Holm-Sidak *post hoc* analysis) reflecting the reduction in locomotor activity in DRD mice in the last 6 hrs of the active period. (B) Spontaneous locomotor activity in a novel open field was assessed for 1 hr in normal and DRD mice in the early active period (8pm) and early inactive period (8am) (n=5-7/genotype). There was a significant genotype x time interaction effect, where DRD mice exhibited hyperactivity at 8pm in the novel open field compared to 8am ($F_{1,10}$=25.2, two-way repeated measures ANOVA; p<0.001, Tukey's *post hoc* analysis). (C) Maintenance of unnatural postures, was tested with the bar test of catalepsy in normal and DRD mice at 8pm and 8am (n=7/genotype). There was a significant genotype x time interaction effect, where DRD mice exhibited increased cataleptic behavior at 8am compared to 8pm ($F_{1,12}$=8.1, two-way repeated measures ANOVA; p<0.01, Tukey's *post hoc* analysis). (D) Rotarod performance was assessed at 8pm and 8am (n=7-8/genotype). There was a significant genotype x time interaction effect, where DRD mice exhibited poor performance at 8am but not at 8pm ($F_{1,13}$=15.0, two-way repeated measures ANOVA; p<0.01, Tukey's *post hoc* analysis). (E) Pole test performance was similarly assessed at 8am and 8pm (n=7-8/genotype). There was a significant genotype x time interaction effect, where DRD mice exhibited poor performance at 8am but not 8pm ($F_{1,13}$=9.8, two-way repeated measures ANOVA; p<0.01, Tukey's *post hoc* analysis). Values represent mean ± SEM; *p<0.05, **p<0.01, ***p<0.001.

Diurnal fluctuations in neurochemistry

We hypothesized that changes in DA regulation correlated with the diurnal fluctuations of behavior in DRD mice. To address this possibility, we assessed striatal TH activity, monoamine, and monoamine metabolite concentrations at 8pm, when the frequency of dystonic movements were low, and in a separate cohort of mice at 8am, when the frequency of dystonic movements were high. In normal animals, TH expression and brain DA concentrations have a distinct circadian rhythm, with TH activity and DA concentration peaking in the inactive period (Cahill and Ehret, 1981, Weber et al., 2004, Ferris et al., 2014). In agreement with these studies, we saw a significant increase at 8am, compared to 8pm, in striatal TH activity (Fig. 13A; $p<0.01$), DA (Fig. 13B; $p<0.001$), and DOPAC (Fig. 13C; $p<0.05$) concentrations in normal mice. In DRD mice, we observed a nonsignificant trend towards increased TH activity at 8am. DA concentration showed an opposite trend from normal in DRD mice, with slightly less DA at 8am compared to 8pm. DOPAC concentration supported that trend, with DRD mice showing significantly decreased DOPAC at 8am compared to 8pm (Fig. 13C; $p<0.01$). Since most DOPAC is located in the extracellular space (Wallace and Traeger, 2012), this result suggests that what little DA is synthesized in DRD mice is released at 8pm. The DOPAC/DA turnover ratio further illustrated the time of day-dependent differences in DA regulation in DRD mice. There was a 375% increase in the ratio of striatal DOPAC/DA in DRD mice at 8pm compared to normal mice ($p<0.001$), and compared to both DRD and normal mice at 8am (Fig. 13D; $p<0.001$).

We also examined striatal 5-HT and 5-HIAA concentrations at 8pm and 8am in normal and DRD mice. While striatal 5-HT concentrations did not differ between 8pm and 8am (Fig. 13E), 5-HIAA showed time of day-dependent effects. 5-HIAA was significantly increased in DRD mice at 8pm (Fig. 13F; $p<0.05$), but not different from normal at 8am.

Further the 5-HIAA/5-HT ratio, a measure of 5-HT turnover, was also elevated at 8pm in DRD mice (Fig. 13G; $p<0.001$), but was similar to normal mice at 8am. Thus, measures of 5-HT signaling also showed differences in diurnal regulation in DRD mice, where periods of elevated 5-HT signaling correlated with periods of few dystonic movements.

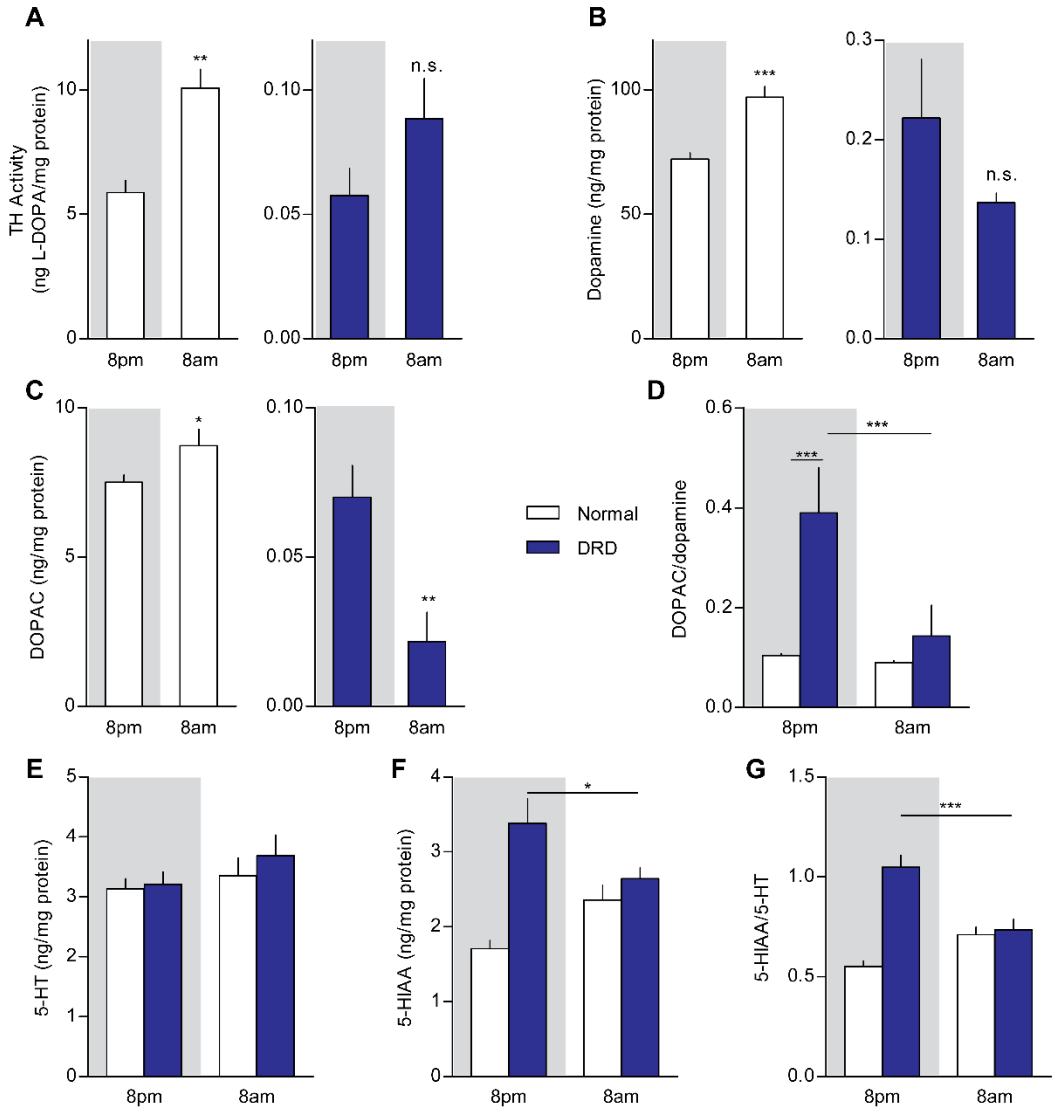
A
TH Activity
(ng L-DOPA/mg protein)
10
5
0
**
8pm
8am
0.10
0.05
0.00
n.s.
8pm
8am
B
Dopamine (ng/mg protein)
100
50
0
***
8pm
8am
0.3
0.2
0.1
0.0
n.s.
8pm
8am
C
DOPAC (ng/mg protein)
10
5
0
*
8pm
8am
0.10
0.05
0.00
**
8pm
8am
Normal
DRD
D
DOPAC/dopamine
0.6
0.4
0.2
0.0
***
***
8pm
8am
E
5-HT (ng/mg protein)
5
4
3
2
1
0
8pm
8am
F
5-HIAA (ng/mg protein)
4
3
2
1
0
*
8pm
8am
G
5-HIAA/5-HT
1.5
1.0
0.5
0.0
***
8pm
8am

Figure 13: Diurnal fluctuations in DA metabolism. (A) Striatal TH activity was assessed in the early active period (8pm) and early inactive period (8am) in normal and DRD mice (n=5-8/condition). There was a significant genotype x time interaction effect ($F_{1,21}$=25.8, p<0.001), with normal mice exhibiting significantly more TH activity at 8am than at 8pm (p<0.01) but no significant difference was observed between times of day in DRD mice (p>0.1). (B) Striatal concentrations of DA, (C) DOPAC, (D) the DOPAC/DA ratio, (E) 5-HT, (F) 5-HIAA, (G) and the 5-HIAA/5-HT ratio were assessed at 8am and 8pm (n=6-9/condition). (B) For DA, there was a significant genotype x time interaction effect ($F_{1,23}$=23.6, p<0.001), with the concentration of DA in normal mice significantly greater at 8am than at 8pm (p<0.01) but no significant difference observed between times of day in DRD mice. (C) For DOPAC, there was a significant genotype x time interaction effect ($F_{1,23}$=4.6, p<0.05), with the concentration of DOPAC in normal mice significantly greater at 8am than at 8pm (p<0.05) but DOPAC was significantly lower at 8am than at 8pm in DRD mice (p<0.01). (D) Similarly, for the DOPAC/DA ratio, there was a significant genotype x time interaction effect ($F_{1,23}$=12.6, p<0.01) with significantly greater DA turnover at 8pm than at 8am in DRD mice (p<0.001), but not normal mice. (E) No significant effect of genotype ($F_{1,23}$=0.6, p>0.1) or time ($F_{1,23}$=1.9, p>0.1) on 5-HT concentrations were observed. (F) For 5-HIAA, there was a significant genotype x time interaction effect ($F_{1,23}$=6.0, p<0.01) with significantly greater 5-HIAA at 8pm than at 8am in DRD mice (p<0.05) and normal mice (p<0.05). (G) Similarly, for the 5-HIAA/5-HT ratio, there was a significant genotype x time interaction effect ($F_{1,23}$=29.1, p<0.001) with significantly greater 5-HIAA at 8pm than at 8am in DRD mice (p<0.001) and normal mice (p<0.05). Statistical analyses were performed using a two-way ANOVA with Student's *t* test *post hoc* analyses for TH activity, DA and DOPAC concentrations, and Holm-Sidak *post hoc* analysis for 5-HT, 5-HIAA, and turnover ratios. Values represent mean ± SEM; *p<0.05, **p<0.01, ***p<0.0

Behavioral responses to indirect catecholamine agonists

To begin to connect neurochemistry to behavior, we used a behavioral pharmacological approach with the DRD mice. We started this work by examining responses to various indirect catecholamine agonists. First, we confirmed that the low levels of catecholamines were in fact behaviorally relevant for the DRD mice by assessing the locomotor response to 5 mg/kg amphetamine in the mice. Amphetamine causes monoamine release from synaptic terminals to cause hyperlocomotion. Indeed, normal mice exhibited a significant increase in locomotor activity with 5 mg/kg amphetamine (Fig. 14A and B; $p<0.001$). DRD mice also exhibited a significant increase in locomotor activity in response to amphetamine ($p<0.01$), albeit less than the increase observed in normal mice. This result suggests that the low concentrations of catecholamines in DRD mice are adequate to mediate behavior.

Alleviation of dystonia upon L-DOPA treatment is the defining feature of DRD. We examined the response to 10 mg/kg L-DOPA in the DRD mice to illustrate that the DRD mice also displayed this feature of the disorder. 10 mg/kg L-DOPA, in mice, is roughly equivalent to a 50 mg dose of L-DOPA for a 60 kg human, accounting for dose translation (Reagan-Shaw et al., 2008), a dose that is effective and well-tolerated in DRD patients (Steinberger et al., 2000). First, we measured the effect on brain monoamine concentrations following this dose in DRD mice. L-DOPA significantly increased DA ($p<0.001$) and NE ($p<0.001$) concentrations throughout the brain (Table 2), specifically restoring striatal DA to 22% of the concentration seen in normal mice. Interestingly, striatal 5-HIAA concentrations ($p<0.01$) and the 5-HIAA/5-HT ratio ($p<0.001$) were reduced by L-DOPA in DRD mice. The significance of this interplay between DA depletion and 5-HT signaling should be addressed in future studies.

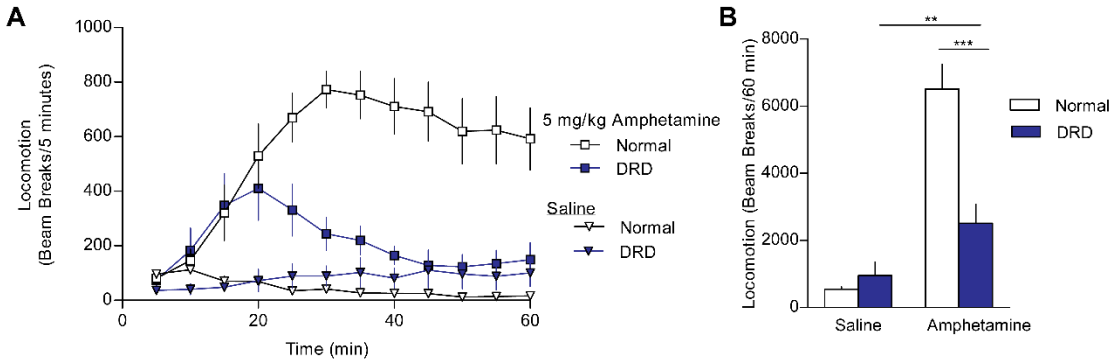

Figure 14: Amphetamine response in DRD mice. (A,B) Effect of 5 mg/kg amphetamine or saline on locomotion in normal (n=8) and DRD mice (n=7) at 2pm. A significant dose x genotype interaction effect was observed ($F_{1,13}$=40.5, two-way repeated measures ANOVA, p<0.001) with amphetamine increasing locomotor activity in DRD mice (p<0.01, Student's *t* test *post hoc*) though less than normal mice (p<0.001, Student's *t* test *post hoc*). Data displayed per 5 min time bin in (A) and as total for 60 min in (B). Values represent mean ± SEM; **p<0.01 ***p<0.001.

This partial restoration of striatal DA by L-DOPA eliminated dystonic movements in DRD mice (Fig. 15A; $p<0.001$). Thus, this important feature of DRD is replicated in the DRD mice. To further examine the behavioral effects of L-DOPA in DRD mice, we measured rotarod and pole test performance after L-DOPA at 2pm. DRD mice showed no deficits in the cling test at 2pm, a test of grip strength, illustrating that the ability to perform these tasks at this time of day ($p>0.1$; not shown). L-DOPA had no effect on rotarod performance in normal mice (Fig. 15B; $p>0.1$); DRD mice, however, showed significant improvement from saline with L-DOPA ($p<0.01$). Similarly, DRD mice showed significant improvement from saline with L-DOPA on the pole test, (Fig. 15C; $p<0.001$), whereas normal mice showed no benefit from L-DOPA ($p>0.1$). DRD mice also showed a hyperlocomotor response to L-DOPA (Fig. 15D; $p<0.001$). Considering this response occurs with tissue striatal DA concentrations that are ~20% of normal, supersensitive DA receptor responses likely occur in DRD mice, which are investigated in Chapter 4. Taken together, these results show that dystonic movements and motor deficits respond to L-DOPA in DRD mice. In agreement with the time of day-dependent neurochemistry differences, these data further illustrate that behavioral deficits occur when presynaptic DA tone is low, and can be reversed with acute repletion of catecho

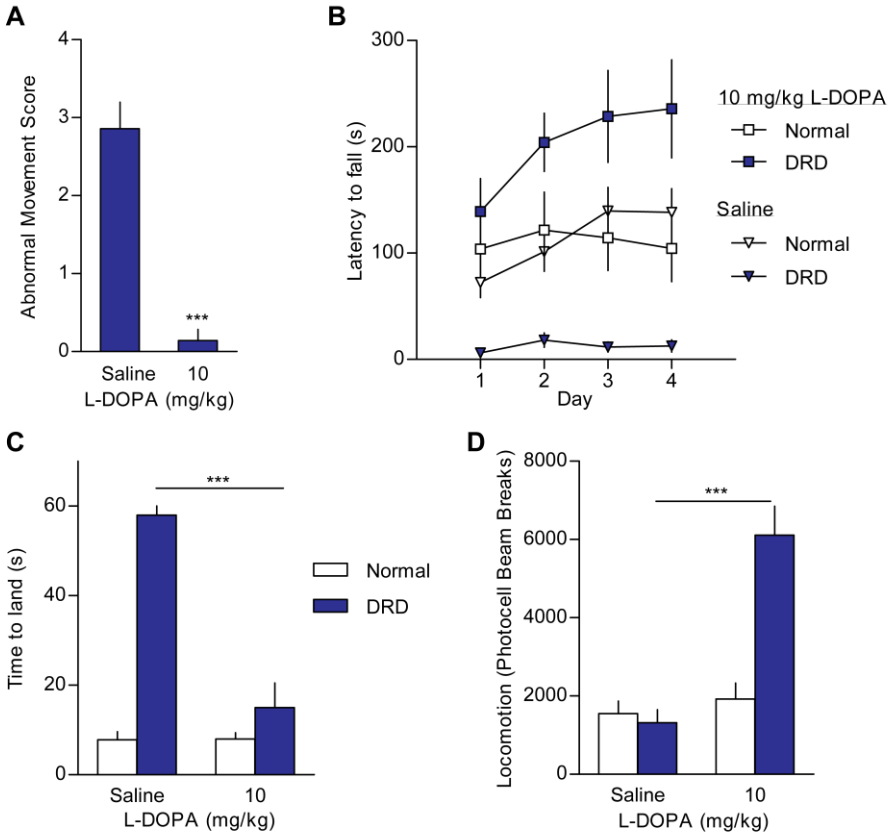

Figure 15: L-DOPA response in DRD mice. (A) Peripheral administration of L-DOPA significantly reduced dystonic movements in DRD mice (n=7/treatment; $p<0.001$, paired Student's *t* test) at 2pm. (B) The effect of L-DOPA on rotarod performance in normal and DRD mice was assessed. Rotarod performance was significantly impaired in DRD mice compared to normal mice after saline treatment, but improved significantly after L-DOPA treatment (n=4/condition; $F_{1,23}=44.1$, two-way ANOVA within day 1, $p<0.01$, Holm-Sidak *post hoc* analysis). (C) DRD mice exhibited a significant deficit in pole test performance compared to normal mice (n=6-7/condition) but L-DOPA treatment significantly improved pole test performance in DRD mice (genotype x treatment interaction effect; $F_{1,23}=44.1$, two-way ANOVA, $p<0.001$, Holm-Sidak *post hoc* analysis). (D) DRD mice (n=7-8/treatment) display a locomotor response to L-DOPA (genotype x treatment interaction effect; $F_{1,13}=42.8$, two-way ANOVA, $p<0.001$, Holm-Sidak *post hoc* analysis), whereas normal mice do not (n=7-8/treatment; $p>0.1$). Values represent mean ± SEM; **$p<0.01$ ***$p<0.001$.

Table 2: Effect of L-DOPA and L-DOPS on monoamines.

	DA	NE	5-HT	5-HIAA	5-HIAA/5-HT
Striatum					
DRD +Saline	0.3 ± 0.1	N.D.	3.2 ± 0.2	3.4 ± 0.3	1.0 ± 0.1
DRD +L-DOPA	15.8 ± 1.1***	0.1 ± 0.1*	2.2 ± 0.2**	1.4 ± 0.1***	0.6 ± 0.1**
DRD +Vehicle	0.1 ± 0.1	0.1 ± 0.0	2.6 ± 0.1	2.1 ± 0.1	0.8 ± 0.0
DRD +L-DOPS	0.8 ± 0.1*	2.4 ± 1.3	2.3 ± 0.4	1.8 ± 0.3	0.8 ± 0.1
Midbrain					
DRD +Saline	0.1 ± 0.0	0.2 ± 0.1	10.8 ± 0.3	5.4 ± 0.5	0.5 ± 0.0
DRD +L-DOPA	5.2 ± 0.9***	2.7 ± 0.4***	12.6 ± 1.0	5.8 ± 0.4	0.5 ± 0.0
DRD +Vehicle	N.D.	0.3 ± 0.0	11.0 ± 0.6	4.5 ± 0.5	0.4 ± 0.0
DRD +L-DOPS	0.3 ± 0.0**	2.4 ± 0.3**	11.6 ± 0.6	4.4 ± 0.4	0.4 ± 0.0
Cortex					
DRD +Saline	0.1 ± 0.0	0.1 ± 0.0	2.5 ± 0.3	1.7 ± 0.1	0.7 ± 0.0
DRD +L-DOPA	2.2 ± 0.6***	2.1 ± 0.5***	2.3 ± 0.5	1.3 ± 0.1*	0.6 ± 0.1
DRD +Vehicle	N.D.	N.D.	7.0 ± 2.0	0.9 ± 0.1	0.9 ± 0.1
DRD +L-DOPS	N.D.	0.7 ± 0.0***	8.5 ± 1.0	0.7 ± 0.0	0.7 ± 0.0
Brainstem					
DRD +Saline	0.3 ± 0.0	0.9 ± 0.1	14.1 ± 1.6	17.2 ± 1.4	1.2 ± 0.1
DRD +L-DOPA	2.4 ± 0.2***	4.7 ± 0.4***	8.1 ± 0.7*	7.3 ± 0.8***	0.9 ± 0.0*
DRD +Vehicle	0.1 ± 0.1	0.4 ± 0.4	5.8 ± 1.0	5.9 ± 0.9	1.1 ± 0.2
DRD +L-DOPS	0.2 ± 0.1	1.0 ± 0.3	6.8 ± 0.5	5.6 ± 1.1	0.8 ± 0.1
Hippocampus					
DRD +Saline	N.D.	0.3 ± 0.0	3.5 ± 0.7	2.8 ± 0.2	0.8 ± 0.1
DRD +L-DOPA	N.D.	1.8 ± 0.2***	3.4 ± 0.1	2.9 ± 0.2	0.8 ± 0.1
DRD +Vehicle	N.D.	0.2 ± 0.1	6.6 ± 0.3	3.0 ± 0.4	0.5 ± 0.1
DRD +L-DOPS	N.D.	0.7 ± 0.1*	7.4 ± 1.6	2.7 ± 0.3	0.4 ± 0.1
Cerebellum					
DRD +Saline	N.D.	N.D.	1.3 ± 0.1	1.2 ± 0.0	0.8 ± 0.1
DRD +L-DOPA	N.D.	2.5 ± 0.7***	1.6 ± 0.4	0.8 ± 0.2*	0.5 ± 0.0**
DRD +Vehicle	N.D.	0.1 ± 0.0	3.9 ± 0.7	0.9 ± 0.2	0.2 ± 0.1
DRD +L-DOPS	N.D.	0.5 ± 0.0***	3.0 ± 0.5	0.4 ± 0.1	0.1 ± 0.0

Tissue concentrations of monoamines were measured by HPLC 45 min after 10 mg/kg L-DOPA (+2.5 mg/kg benserazide) (n=4) or saline (n=6) or 5 hr after 1 g/kg L-DOPS (+0.25 g/kg benserazide) (n=4) or L-DOPS vehicle (HCl/NaOH) (n=3). There was an effect of L-DOPA on DA concentration ($F_{1,8}$=260, p<0.001) and NE concentration ($F_{1,8}$=789, p<0.001) in all regions. There was an effect of L-DOPS treatment on NE concentration ($F_{1,5}$=8.7, p<0.05), and DA concentration in striatum and midbrain ($F_{1,5}$=14.9, p<0.05). Each analyte was tested with two-way repeated measures ANOVA. Significant main effects were tested *post hoc* within each brain region with Student's *t* tests. Values represent mean ± SEM; *p<0.05, **p<0.01, ***p<0.001. N.D. = not detected.

To verify that the elevation in striatal catecholamines was central to the behavioral effect of L-DOPA, we microinjected L-DOPA into the striatum, as well as in cerebellum as a control. Bilateral microinjections of L-DOPA into the dorsal striatum significantly reduced the abnormal movements (Fig. 16; $p<0.01$). By contrast, microinjection of L-DOPA into midline cerebellar vermis had no discernible effect on abnormal movements.

TH is the rate-limiting enzyme in the synthesis of both DA and NE, and both transmitters are reduced in DRD mice. Further, L-DOPA is converted to both DA and NE in the brain. To better understand the role of each catecholamine in the abnormal movements, we challenged DRD mice with L-DOPS, which can be converted to NE by AADC but does not directly increase DA levels (Thomas et al., 1998). Peripheral administration of L-DOPS (1 g/kg) significantly increased NE concentrations throughout the brain (Table 2, $p<0.05$), but had no significant beneficial effect on the abnormal movements (Fig. 17A; $p>0.1$) or locomotor activity (Fig. 17B; $p>0.1$). Thus the acute effect of L-DOPA on both of these behavioral measures likely is a result of specifically repleting DA, not all catecholamines.

To further illustrate the predictive validity of the DRD mouse model, we investigated the behavioral response to THP, a nonselective muscarinic acetylcholine receptor antagonist. THP, like L-DOPA, is effective at reducing dystonia in DRD patients (Jarman et al., 1997). DRD mice exhibited a significant dose-dependent reduction in abnormal movements following THP administration (Fig. 18A, $p<0.05$). Because THP can have sedative effects at high doses, locomotor activity was measured at the same time as the assessment of abnormal movements. Locomotor activity was not affected by any dose of THP tested (Fig. 18B; $p>0.1$), suggesting that the effect on abnormal movements was not attributable to a global reduction in motor behavior.

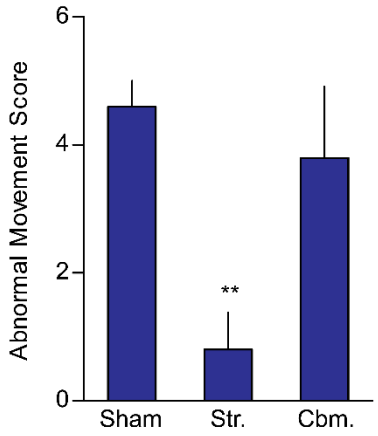

Figure 16: Regional specificity of L-DOPA effects. Microinjection of L-DOPA (200 pg) into the striatum of DRD mice significantly reduced abnormal movements ($F_{2,8}$=6.8, one way repeated measures ANOVA; p<0.01 Holm Sidak *post hoc* analysis), whereas cerebellar microinjections did not (p>0.1, Holm Sidak *post hoc* analysis). Microinjection experiments were performed at 2pm. Values represent mean ± SEM; *p<0.05.

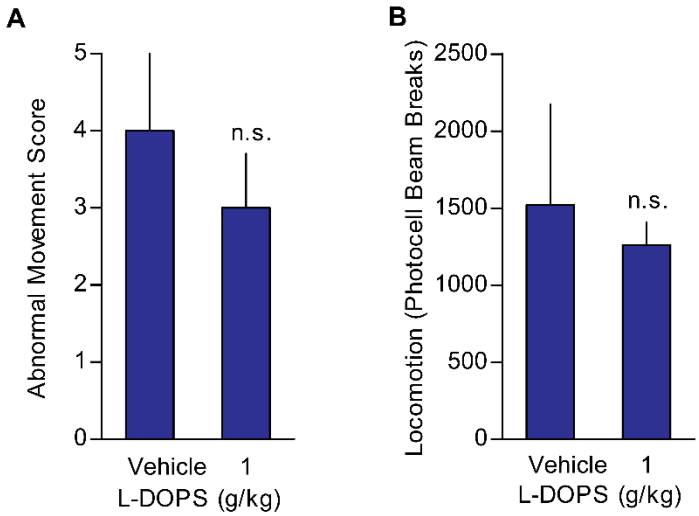

Figure 17: L-DOPS response in DRD mice. (A) Peripheral administration of 1 g/kg L-DOPS did not affect abnormal movements in DRD mice (p>0.1, Student's *t* test). (B) Similarly, 1 g/kg L-DOPS did not affect locomotion (p>0.1, Student's *t* test). L-DOPS experiments were performed at 8pm. Values represent mean ± SEM

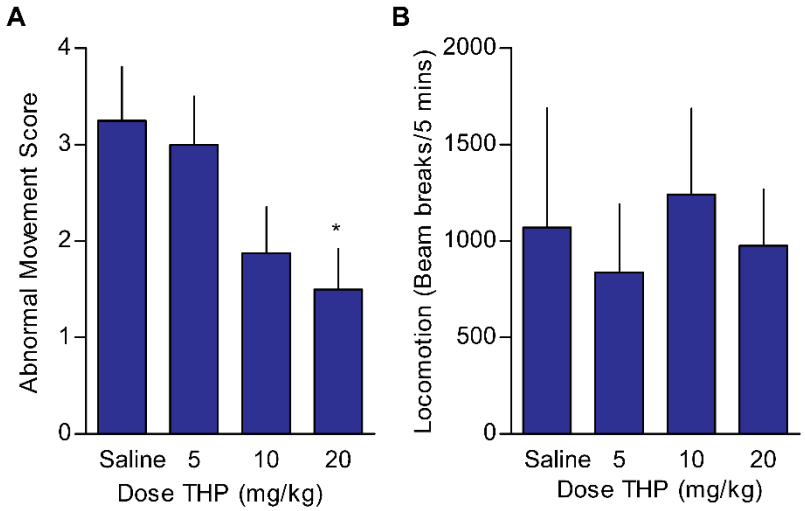

Figure 18: THP response in DRD mice. (A) Administration of THP (n=8/dose), significantly reduced dystonic movements in DRD mice ($F_{3,21}$=3.4, one-way repeated measures ANOVA; p<0.05, Holm-Sidak *post hoc* analysis) at 2pm. (B) THP had no effect on locomotion in DRD mice ($F_{3,21}$=0.3, one-way repeated measures ANOVA, p<0.1). Values represent mean ± SEM; *p<0.05, **p<0.01, ***p<0.001.

Discussion

Here we describe the motor behavioral phenotype of the DRD mice. These mice exhibit abnormal, involuntary movements in their limbs and trunk, which are best described as dystonia, and most closely resemble the milder, type A form of THD. Like patients with DRD, their abnormal movements and overall motor performance worsen through the active period. We show that changes in presynaptic striatal DA regulation correlate with those behavioral changes. We also show that the DRD mice respond to amphetamine, L-DOPA, and THP. Further, the L-DOPA response was due to partial repletion of striatal DA, specifically.

That the DRD mice exhibit dystonic movements could have been predicted. The DRD mice carry the mouse homolog of a mutation that causes a fully penetrant form of dystonia in humans. Further, the anatomy of catecholamine systems are well conserved between the species (Bjorklund and Dunnett, 2007). Thus, it is not surprising that similar phenotypes occur in both humans and mice from this particular genetic insult. Dystonic phenotypes, however, are rare among engineered mouse strains. None of the mouse models that recapitulate the genetics of DYT1 (Song et al., 2012), DYT11 (Zhang et al., 2012), Lesch-Nyhan disease (Jinnah et al., 1994), DAT deficiency (Giros et al., 1996), or VMAT2 deficiency (Caudle et al., 2007) exhibit dystonia. Thus, the DRD mice present a rare opportunity to design experiments that work forwards from genetic etiology, as well as backwards from the behavior to better understand the neural mechanisms of dystonia.

DRD mice have a phenotype that is distinct from other similar strains where TH is genetically disrupted early in development. First, DRD mice display different motor behavioral features than *DA deficient* mice, where TH expression is completely abolished in DA neurons. In those mice, akinesia is the prominent motor behavioral feature (Zhou and Palmiter, 1995, Szczypka et al., 1999). Notably, dystonic movements are not

described in *DA deficient* mice. DRD mice on the other hand, display dystonic movements and only mild deficits in locomotor activity. Further, DRD mice exhibit a burst of activity that is tuned to the start of the active period, and actually display hyperactivity in certain testing paradigms. Thus, the residual catecholamines in DRD mice likely play an important role in determining motor phenotype. One could argue that DRD mice resemble type A THD, whereas *DA deficient* mice resemble type B THD, though both show reductions in striatal TH activity (~99% in DRD mice, 100% in *DA deficient* mice) that would be considered predictive of type B THD.

It is interesting to note, though, that while the motor behavioral phenotypes of DRD and *DA deficient* mice are different, they both show deficits in feeding. Indeed, both strains require daily L-DOPA injections to initiate feeding and maintain a healthy body weight. This argues that maintenance of feeding behavior is more sensitive to DA depletion than the maintenance of locomotor activity. Or more specifically, in DRD mice, the low levels of DA are sufficient to initiate locomotor activity and dystonic movement, but too low to maintain sufficient daily consumption of food and water.

DRD mice also have a phenotype that is distinct from *pts-/-; DPS* mice, where DA neurons lack the capability to synthesize BH_4. In those mice striatal TH activity and DA concentrations are 15%-20% of normal, and neither dystonia nor locomotor deficits are seen (Sumi-Ichinose et al., 2005, Sato et al., 2008). Taken together, the findings from *DA deficient*, *pts-/-; DPS*, and DRD mice argue that dystonia is associated with residual TH activity and DA concentrations within a specific range. First, DA must be below a threshold, lower than that in *pts-/-; DPS* mice, for dystonic movements to emerge in mice. This concept of a threshold of DA depletion for symptom onset is widely accepted for PD (Bernheimer et al., 1973), but is rarely discussed for DRD. Also, some residual TH activity and DA concentration, greater than those in *DA deficient* mice, must be spared for dystonic

movement to be initiated. While other factors, such as genetic background and differences in the noradrenergic system may also play a role, the levels of residual striatal DA are likely central in determining the motor outcomes in these different mouse strains. Thus, in DRD mice, TH activity and DA concentrations are reduced to levels that are in a “sweet spot” for the induction of dystonic movement.

Further illustrating the importance of DA concentrations in determining motor outcomes, we show that changes in DA regulation correlate with time of day differences in dystonic movement and motor performance in DRD mice. At 8pm, when dystonic movements were rare and motor performance was normal, we saw elevated DA turnover. At 8am, when dystonic movements were frequent and motor performance was poor, we saw those DA turnover values reduced to those in normal mice. Thus, even within the DRD mice, acute fluctuations in how the residual DA is handled by the presynaptic terminal affected the symptomatic presentation.

These data provide a possible mechanism for diurnal fluctuations in symptoms, a hallmark feature of DRD (Segawa, 2011). Our data show that DRD mice fail to exhibit the significant increase in TH activity at the end of the active period that normal mice show. In normal animals, that peak in TH activity may be a means by which to replenish DA stores after the active period, when animals exhibit increases in both extracellular DA and exploratory activity (Paulson and Robinson, 1994, Ferris et al., 2014). In DRD mice, mutational effects on TH protein prevents the circadian spike in *Th* mRNA (Weber et al., 2004) from translating into a significant increase in TH activity. Thus, when striatal DA stores deplete during the active period, there is no means to replace it. Further, DA turnover is elevated in the early active period in DRD mice, which as discussed in chapter 2, may be due to minimal autoreceptor-mediated feedback on the presynaptic terminal. Therefore, a large proportion of the limited DA store is subject to increased MAO and

COMT-mediated metabolism at this time. Taken together, these neurochemical data from DRD mice argue that diurnal fluctuations occur from a general rundown in presynaptic DA tone that occurs during the active period. Deficits in circadian upregulation of TH protein levels and poor regulation of the residual DA likely both contribute to this rundown.

In addition to the time of day-dependent differences in DA regulation, we observed time of day-dependent differences in 5-HT regulation as well. 5-HT signaling, like most biological processes, is regulated by circadian rhythm (Quay, 1963). Here, we show that 5-HT turnover, measured as the 5-HIAA/5-HT, is elevated at 8pm in DRD mice, but is similar to normal mice at 8am. Thus, elevated 5-HT signaling correlates to times of day when dystonic movement is infrequent in DRD mice and may play some role in alleviation from symptoms. Similarly, agonism of 5-HT_{1A} receptors is effective in reducing dyskinetic movement in LIDs (Bara-Jimenez et al., 2005, Eskow et al., 2007, Bishop et al., 2009). The role for 5-HT signaling in augmenting the dystonic movements of DRD mice can be elucidated in future studies. This role, while possibly important, is most likely secondary to that of DA signaling, however, as the 5-HIAA/5-HT ratio is significantly reduced by L-DOPA, which also eliminates the dystonic movements in DRD mice.

That the DRD mice show a reduction in dystonic movements after L-DOPA administration further illustrates the acute connection between DA signaling and the dystonic movements in these mice. Like the brief elevation in DA neurotransmission observed at 8pm in the DRD mice, pharmacological repletion of DA stores similarly reduces abnormal movement. We show, through microinjections of L-DOPA, that restoration of catecholamines in striatum, specifically, is sufficient for reducing dystonic movement. Further, we show that repletion of NE, but not DA, with L-DOPS, is insufficient for reducing the dystonic movements. Thus, here we confirm the longstanding, but yet unproven, hypothesis that striatal DA depletion is the primary, instigating factor for

dystonic movement in DRD (Rajput et al., 1994, Furukawa et al., 1996, Bandmann and Wood, 2002, Segawa, 2009).

Though these studies establish striatal DA depletion as central to the instigation of the dystonic movement in DRD mice, acutely, it is important to highlight the role for development in these phenotypes. Rodents models with DA depletion in adulthood are akinetic and cataleptic, rather than dystonic (Carlsson et al., 1957, Ungerstedt, 1971a, Sotnikova et al., 2006). An animal model of akinesia most apt for this comparison between developmental and adult-onset DA depletion is the DA deficient DAT knockout mouse, or DDD mouse. This model is the result of DAT knockout mice given an acute dose of the TH inhibitor alpha-methyl-para-tyrosine as adults. Because these mice have no means of DA reuptake, striatal DA concentrations are reduced to levels comparable to those seen in DRD mice, and DDD mice display profound catalepsy (Sotnikova et al., 2005). The differing motor phenotypes of DDD and DRD mice highlight the importance of developmental adaptation in the induction of dystonic movement. One possible difference between these models that we cannot dismiss is the influence of developmental NE depletion. Though, we show through our L-DOPS experiment that NE depletion has a minimal role in the acute initiation of dystonic movements, the effects of NE depletion on the developing brain may be important. *Dbh -/-* mice display altered motor phenotypes (Rommelfanger et al., 2007), and show deficits in the developmental of other brain regions (Shepard et al., 2015). Thus, the influence of NE depletion on the developing brain could play a role in the development of dystonia and can be addressed in future experiments.

Lastly, we show that THP reduces dystonic movements in DRD mice, as in DRD patients (Jarman et al., 1997). Non-selective antimuscarinics like THP are one of the few effective treatment options for many dystonias, though these drugs are often poorly tolerated by patients (Jinnah and Factor, 2015). Several muscarinic receptors are

expressed in striatum on different cell-types, and perform various functional roles (Calabresi et al., 1998, Pisani et al., 2007). Specific muscarinic receptor antagonists hold promise as potential treatment options for dystonia as side-effects could be limited with more specific pharmacology. Indeed, specific M1 and M2 muscarinic receptor antagonists reverse synaptic abnormalities in DYT1 mice (Sciamanna et al., 2012, Maltese et al., 2014). The role for DRD mice in this effort is in providing an animal model with a therapeutic behavioral response to this class of drug. Thus, new therapeutics may be tested in the mice and mechanistic insight can be gained. Future work with the model can move beyond the acute connection between DA regulation and dystonic movement, described here, and find functional roles for neurotransmitter interactions like this one between acetylcholine and DA, as well as focus on important developmental events that lead to dystonic movement.

Chapter 4: DA receptor-mediated responses in DRD mice

Abstract

The work in this chapter uses behavioral and pharmacological techniques to investigate DA receptor dysfunction in DRD mice. We show that antagonism of either D1DAR or D2DAR worsen the dystonic movements in DRD mice. Agonism of either D1DAR or D2DAR alleviated these symptoms. Classical DA receptor responses were perturbed in DRD mice. By examining locomotor responses, stereotypic behaviors and second messenger responses, we show that D1DARs were functionally supersensitive. Conversely, classical behavioral and second messenger responses to D2DAR agonism were blunted or altered in valence. Further, the cataleptic response to DA receptor antagonism was blunted. These changes were not accompanied by any changes in DA receptor expression, binding, or affinity. Thus, these studies illustrate the involvement of DA receptors in the dystonic movements of DRD mice and that maladaptive changes to DA receptor signal transduction may play some role in generating dystonic movement in DRD mice.

Introduction

In the previous chapter we established that the dystonic movements in DRD mice are associated with low striatal DA concentrations. In this chapter, we further investigate striatal dopaminergic mechanisms of the dystonic movement, focusing on DA receptors. Striatal DA concentrations are low in the striatum of DRD, but not zero. Thus, how that limited residual pool of DA signals through DA receptors is likely important to the phenotype observed in chapter 3. Focusing on DA receptors and their responses will allow us to start characterizing adaptive changes, downstream of presynaptic DA transmission in the DRD mice.

The five DA receptor genes are grouped into two types; D1 and D5 are designated D1-type DA receptors (D1DARs), while D2, D3, and D4 are designated D2-type DA receptors (D2DARs). These subtypes differ in their expression pattern and roles in physiology and behavior (Kebabian and Calne, 1979, Gerfen et al., 1990, Surmeier et al., 1996). D1DARs are expressed on direct pathway MSNs, where they couple to $G\alpha_{s/olf}$ proteins and stimulate cAMP production by AC (Kebabian and Calne, 1979). In normal animals, D1DAR agonism causes increased locomotion and stereotypic behaviors at high doses (Arnt et al., 1992). Dysregulation of D1DAR-dependent signaling is observed in animal models of LIDs, whereby signaling through supersensitive D1DARs causes dyskinetic movement (Westin et al., 2007). Conversely, loss-of-function mutations in *GNAL*, the gene coding $G\alpha_{s/olf}$, cause dystonia (Fuchs et al., 2013, Vemula et al., 2013). Therefore, D1DAR supersensitivity is associated with dyskinetic movement, whereas D1DAR hypofunction is associated with dystonic movement.

D2DARs couple to $G\alpha_i$ to inhibit AC activity, inhibiting membrane excitability of indirect pathway MSNs, among other cellular effects (Missale et al., 1998). D2DARs are also expressed on DA neuron terminals and act as autoreceptors (Pothos et al., 1998), on

glutamatergic terminals where they affect glutamate release (Bamford et al., 2004), as well as on cholinergic interneurons where they augment neuronal firing in those cell-types (Pisani et al., 2006). Because of this promiscuous expression, D2DARs' role in movement are more complex than D1DARs. For one, D2DAR knockout mice exhibit reduced locomotion (Baik et al., 1995). Further, D2DAR antagonists reduce locomotion and cause catalepsy (Sanberg, 1980). Selective D2DAR agonists like quinpirole, however, also reduce locomotion in rodents (Van Hartesveldt et al., 1994, Li et al., 2010), though the mechanisms remain unclear (Anzalone et al., 2012). Hypofunction of D2DARs has been hypothesized as central to the pathogenesis to several dystonias (Todd and Perlmutter, 1998). Reduced striatal D2DAR binding is observed in idiopathic dystonias (Hierholzer et al., 1994, Naumann et al., 1998, Horie et al., 2009) and DYT1 dystonia (Asanuma et al., 2005). Reduced D2DAR binding is also associated with the acute dystonic phase exhibited by certain primate species following MPTP treatment (Perlmutter et al., 1997). Lastly, acute dystonia can occur from neuroleptic D2DAR antagonists (Mehta et al., 2015).

As data suggest the contribution of both D1DAR and D2DARs in dystonia, we integrated both DA receptor subtypes into our analysis of the DRD mice. We used subtype-selective DA receptor pharmacology to address which receptors were involved in the dystonic movement of DRD mice. Further, we examine DA receptor expression and classical DA receptor responses in the DRD mice to better understand what types of adaptive changes to DA receptors, and perhaps signaling within striatum as a whole, underlie the phenotype of the DRD mice.

Methods

Animals

As described in chapter 2, DRD and normal littermate controls, between 2-4 months old were used for these studies. Experiments occurred following >24 hr L-DOPA withdrawal.

Systemic drug challenges

Compounds were administered (s.c.) in saline, in a volume of 10 ml/kg. Behavioral experiments started 10 min after drug administration. For dose response experiments, mice were tested in a repeated measures design with a pseudorandom order of drug doses and vehicle; each mouse received every dose only once within an experiment. Mice were given a 4-day drug washout between challenges. SKF 81297 and quinpirole were obtained from Tocris Biosciences (Bristol, UK). SCH 23390 and raclopride were obtained from Sigma-Aldrich.

Assessment of abnormal movement

Abnormal movements were assessed with a behavioral inventory, as described in chapter 3. For the experiments in this chapter, mice were habituated to test chambers for >24 hr during the L-DOPA washout period. Assessments were performed at 8pm. Behavioral raters were blinded to genotype and treatment. Mice had access to food and water *ad libitum*.

Locomotor Activity

Locomotor activity was tested in automated photocell activity cages, as described in chapter 3. For the experiments in this chapter, mice were habituated to the photocell activity cages for >24 hr during the L-DOPA washout period. For SKF 81297 challenge, mice were injected at 2pm, and locomotor activity was recorded for 1 hr. For quinpirole

challenge, mice were injected at 8pm, and locomotor activity was recorded for 1 hr. All mice had at least 2 exposures to the testing room prior to data collection. Mice had access to food and water *ad libitum*.

Stereotypy

Stereotypic behaviors like vacuous chewing and repetitive grooming occur at high dose DA receptor stimulation (Creese and Iversen, 1972). Mice were rated for stereotypy during the locomotor activity tests every 10 min for 30 sec. A 0-5 behavioral scale was used: 0 = sleeping; 1 = awake, inactive; 2 = active or exploring; 3 = hyperactive; 4 = hyperactive with bursts of stereotypy; and 5 = continuous stereotypy. Behavioral raters were blinded to genotype and treatment.

Bar test of catalepsy

The bar test of catalepsy was performed as described in chapter 3. DRD and normal mice were tested at 8pm. Mice were tested for baseline catalepsy, then tested again, 20 min after injection.

qRT-PCR

qRT-PCR was performed as described in chapter 2 to assess the abundance of DA receptor mRNAs in striatum and midbrain. Gene specific primers were as follows. D1DAR*:* 5'-ATCGTCACTTACACCAGTATCTACAGGA-3' and 5'-GTGGTCTGGCAGTTCTTGGC-3'; D2DAR: 5'-TGGCTGCCCTTCTTCATCACGC -3' and 5'-TGAAGGCCTTGCGGAACTCAATGT -3'; D3DAR: 5'-CCTCTGAGCCAGATAAGCAGC-3' and 5'- AGACCGTTGCCAAAGATGATG -3'. Data were analyzed by the ∆Ct method (Schmittgen and Livak, 2008), using 18s rRNA as reference.

Receptor binding

Mice were sacrificed by cervical dislocation and striata were rapidly dissected, frozen on dry ice, and stored at -80˚C. Samples were homogenized by sonication in 40 volumes of

chilled 50 mM Tris-HCl (pH 7.4). Homogenates were centrifuged at 35,000 g for 10 min, washed, and resupended in 50 mM Tris-HCl. For [^{3}H]SCH23390 (81.9 Ci/mmol, Perkin Elmer, Boston, MA) binding, the assay buffer consisting of 50 mM Tris-HCl (pH 7.4), 5 mM $MgSO_4$, 0.5 mM EDTA, and 40 nM ketanserin (Tocris Biosciences). Incubations were initiated by adding 0.2-0.4 µg protein to duplicates containing 5 concentrations of [^{3}H]SCH23390 (2 nM, 1, 0.5, 0.25, 0.125) in a final volume of 0.6 mL, carried out for 30 min at 37ºC, and terminated over Whatman GF/C glass fiber filters (Brandel, Gaithersberg, MD). Non-specific binding was defined by 500 nM cis-flupentixol (RBI, Frederick, MD). [^{3}H]Spiperone (73.49 Ci/mmol, Perkin Elmer) binding was performed similarly in a buffer of 50 mM Tris-HCl (pH 7.4), 120 mM NaCl, 5 mM KCl, 1 mM $CaCl_2$, 5 mM $MgSO_4$, 0.1% ascorbic acid, and 40 nM ketanserin. Duplicates containing 5 concentrations of [^{3}H]spiperone (1 nM, 0.5, 0.25. 0.125. 0.0625) were incubated for 30 min at 37ºC, and terminated over Whatman GF/C filters. For both [^{3}H]SCH23390 and [^{3}H]spiperone, filters were washed rapidly with 15 mL of ice cold Tris-HCl and counted by scintillation spectroscopy at an efficiency of 15-30%. After normalizing to protein concentration, a one-site model for saturation binding was applied to obtain B_{max} and K_d for each animal using Prism 5 (GraphPad Software, La Jolla, CA).

AC activity

Mice were sacrificed by cervical dislocation and striata were rapidly dissected, frozen on dry ice, and stored at -80˚C. Samples were homogenized by sonication in buffer containing 10 mM imidazole (pH 7.4) and 2 mM EDTA. Homogenates were centrifuged at 500 g for 10 min to remove debris, then centrifuged again at 25,000 g for 15 min, and finally resuspended in buffer containing 10mM imidazole (pH 7.4) and 2 mM EDTA. All reactions were performed at 0.1 mL volume in triplicate. For the SKF 81297 activation assay, reactions were performed in 10 mM imidazole (pH 7.4), 4 mM $MgCl_2$, 0.5 mM 3-isobutyl-

1-methylxanthine (IBMX), 2 mM EDTA, 10 mM pargyline, 5 μM GTP, 2 mM ATP, 20 mM phosphocreatine, 5 U of creatine phosphokinase and 1mg BSA at 37°C for 15 min. For the quinpirole-induced inhibition assay, reactions were performed in 80 mM Tris-HCl (pH 7.4), 150 mM NaCl, 4 mM $MgCl_2$, 2 mM EDTA, 0.5 mM IBMX, 2 mM ATP, 20 mM phosphocreatine, 5 U of creatine phosphokinase, 1 mg BSA, 100 μM GTP and 0.1 μM forskolin at 37°C for 7 min. Forskolin-induced activation was tested as above without quinpirole. About 15 μg protein was added to initiate the reaction. The reaction was terminated by boiling the mixture for 3 min. After centrifuging the reaction mixture at 20,000 g for 10 min, cAMP accumulation was assessed by ELISA (Cell Biolabs, San Diego, CA). Protein concentration was determined as above and AC activity was expressed as pmol cAMP/mg protein/min.

Statistics

Behavioral data and AC activities were analyzed using ANOVA. Significant effects within groups were tested *post hoc* with the Holm-Sidak test. Student's *t* test was used for radioligand binding and qRT-PCR measures. SigmaStat (Systat Software) was used for all analyses. Detailed results of the statistical analyses are presented in the Figure Legends.

Results

DA receptors mediate dystonic movements

We began our examination of DA receptor responses in DRD mice by assessing their contribution to the dystonic movements. In chapter 3, we described enhanced DA turnover that correlated with alleviation from dystonic movements in DRD mice at 8pm. Thus, blunting DA signaling at this time of day should worsen the dystonic movements. We tested this hypothesis by challenging the DRD mice with DA receptor antagonists at 8pm. First, we challenged mice with the D1DAR antagonist SCH 23390. We observed a significant dose-dependent increase in dystonic movements in response to SCH 23390 (Fig. 19A; $p<0.05$). Next, we challenged mice with the D2DAR antagonist raclopride, also at 8pm. Similarly, we observed a significant dose-dependent increase in dystonic movements in response to raclopride (Fig. 19B; $p<0.05$).

We also examined the responsiveness of dystonic movements to DA receptor subtype-selective agonists. Similar to L-DOPA, low doses of either the D1DAR agonist SKF 81297 (Fig. 19C; $p=0.051$) or the D2DAR agonist quinpirole (Fig. 19D; $p<0.001$) reduced dystonic movement. Taken together, these results illustrate that both D1DARs and D2DARs play a role in the dystonic movements of DRD mice. Further, they illustrate that endogenous DA signaling through DA receptors is highly relevant to the expression of dystonic movement in DRD mice, as blockade of this signal worsens the dystonia.

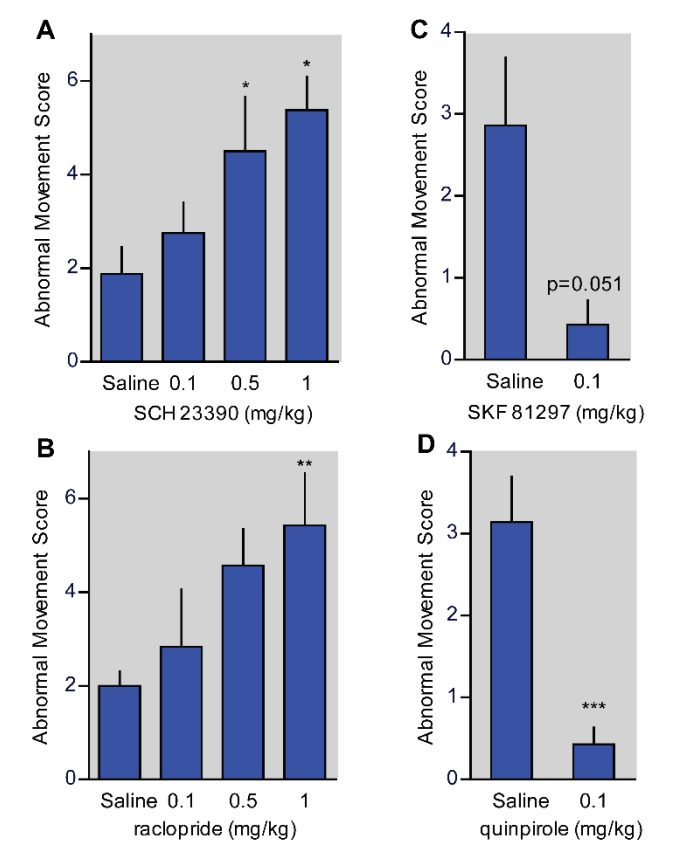

Figure 19: Abnormal movement response to DA receptor-specific agonists and antagonists (n=7-8/dose). (A) The D1DAR antagonist SCH 23390 dose-dependently increased dystonic movements ($F_{3,21}$=4.64, one-way repeated measures ANOVA, p<0.05, Holm-Sidak *post hoc* analysis). (B) The D2DAR antagonist raclopride dose-dependently increased dystonic movements ($F_{3,18}$=3.68, one-way repeated measures ANOVA, p<0.01, Holm-Sidak *post hoc* analysis). (C) The D1DAR agonist SKF 81297 reduced dystonic movements (Student's paired *t* test, p=0.051). (D) The D2DAR agonist quinpirole reduced dystonic movements (Student's paired *t* test, p<0.001). Values represent mean ± SEM; *p<0.05, **p<0.01, ***p<0.001.

Abnormal DA receptor responses in DRD mice

Because DA receptors appear to be important mediators of the dystonic movements in DRD mice, we next assessed DA receptor function. To assess DA receptor function, we first compared the behavioral sensitivity to subtype-selective agonists between DRD and normal mice. For these experiments, we used locomotion and stereotypy, rather than abnormal movement, as outcome measures, because both normal and DRD mice express these behaviors, allowing for direct comparison. The D1DAR agonist SKF 81297 significantly and dose-dependently increased locomotor activity in normal and DRD mice (Fig. 20A; $p<0.001$ for each genotype). However, the dose-response curve for DRD mice was shifted to the left; the ED50 for the SKF 81297-induced increase in locomotor activity in normal mice was 1 mg/kg, but the ED50 in DRD mice was 0.08 mg/kg, an order of magnitude lower than normal. SKF 81297 also dose-dependently increased stereotypic behaviors in both genotypes (Fig. 20B; $p<0.001$ for each genotype), and the dose response curve for DRD mice was again shifted to the left. These parallel results argue for D1DAR supersensitivity in DRD mice.

Next we examined locomotion and stereotypy in response to the D2DAR agonist quinpirole. Unlike SKF 81297, quinpirole reduces locomotion in normal mice (Li et al., 2010, Anzalone et al., 2012). In line with these findings, our data showed a dose-dependent reduction in locomotion in normal mice treated with quinpirole (Fig. 21A; $p<0.01$). In DRD mice, however, quinpirole did not suppress locomotion, but reduced abnormal movements (Fig. 19D), suggesting that the doses being used did exert a central effect in DRD mice. Although quinpirole dose-dependently decreased stereotypic behaviors in normal mice (Fig. 21B; $p<0.01$), it dose-dependently increased stereotypic behaviors in DRD mice ($p<0.05$). Taken together, these results show that DA receptor responses are altered in DRD mice. Further, they are altered in different ways, with

D1DARs showing behavioral supersensitivity and D2DARs showing either blunted or altered responses.

Lastly, we examined the cataleptic response to DA receptor antagonists. Typically, antagonism of both DA receptor subtypes results in catalepsy in rodents (Snyder et al., 1970, Zetler, 1975, Morelli and Di Chiara, 1985). Because preliminary experiments showed that the cataleptic responses to individual DA receptor antagonists were subtle in DRD mice, we maximized our chances of seeing an effect by co-administering both the D1DAR antagonist SCH 23390 and the D2DAR antagonist raclopride. As expected, normal mice responded to these antagonists with profound catalepsy (Fig. 22; $p<0.001$). DRD mice also showed a mild cataleptic response to the antagonist mixture ($p<0.05$), though that response was blunted in comparison to normal mice ($p<0.001$). This blunted response to antagonism occured despite decreased competition from the endogenous ligand, DA, in DRD mice (chapter 2). Thus, these results further illustrate abnormal behavioral responses to DA receptor challenges in DRD mice.

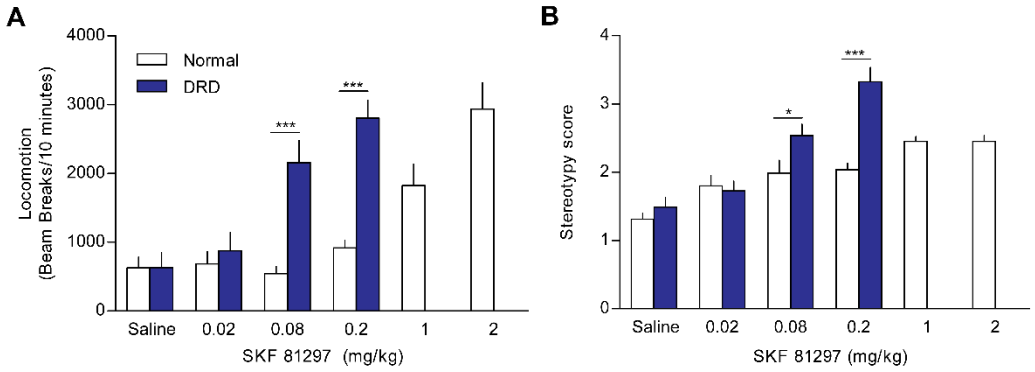

Figure 20: Behavioral sensitivity to D1DAR agonism in DRD mice. Locomotor activity and stereotypic behaviors were assessed after administration (s.c.) of the D1DAR agonist SKF 81297 at 2pm (n=6-8/genotype and condition). (A) For SKF 81297-mediated locomotor activity, there was a significant genotype x dose interaction effect for the lower doses (0.02, 0.08, and 0.2 mg/kg) where both genotypes were tested ($F_{3,42}$=18.7, two-way repeated measures ANOVA; p<0.001) with a significant increase in locomotor activity in DRD mice but not normal littermates (p<0.001). At higher doses, SKF 81297 also induced an increase in locomotor activity in normal mice ($F_{5,35}$=19.5, one-way repeated measures ANOVA; p<0.001, Holm-Sidak *post hoc* analysis). (B) For SKF 81297-mediated stereotypy, there was a significant genotype x dose interaction effect for the lower doses where both genotypes were tested ($F_{3,42}$=8.9, two-way repeated measures ANOVA; p<0.001) with a significant increase in stereotypy in DRD mice but not normal littermates (p<0.01, Holm-Sidak *post hoc* analysis). At higher doses, SKF 81297 also induced an increase in stereotypy in normal mice ($F_{5,35}$=17.0, one-way repeated measures ANOVA; p<0.001, Holm-Sidak *post hoc* analysis). Values represent mean ± SEM; *p<0.05, **p<0.01, ***p<0.001.

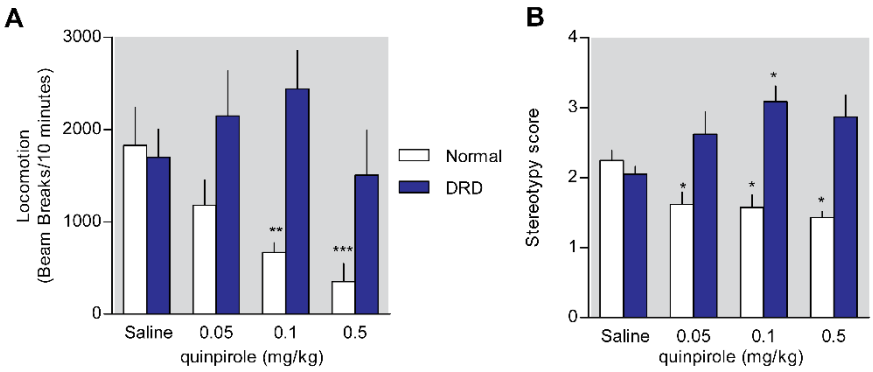

Figure 21: Behavioral responses to D2DAR agonism in DRD mice. Locomotor activity and stereotypic behaviors were assessed after administration (s.c.) of the D2DAR agonist SKF quinpirole at 8pm (n=6-8/genotype and condition). (A) For quinpirole-mediated locomotor activity, there was a significant main effect of genotype ($F_{1,33}$=16.4, two-way repeated measures ANOVA; p<0.01, Holm-Sidak *post hoc* analysis) whereby quinpirole reduced locomotor activity in normal mice ($F_{3,18}$=5.6, one-way repeated measures ANOVA; p<0.01, Holm-Sidak *post hoc* analysis), but not in DRD mice. (B) There was a significant genotype x dose interaction effect on stereotypy after administration of quinpirole ($F_{3,33}$=8.1, two-way repeated measures ANOVA; p<0.001). Quinpirole significantly decreased stereotypy in normal mice ($F_{3,18}$=5.8, one-way repeated measures ANOVA; p<0.01, Holm-Sidak *post hoc* analysis) but significantly increased stereotypy behaviors in DRD mice ($F_{3,18}$=5.8, one-way repeated measures ANOVA; p<0.01, Holm-Sidak *post hoc* analysis). Values represent mean ± SEM; *p<0.05, **p<0.01, ***p<0.001.

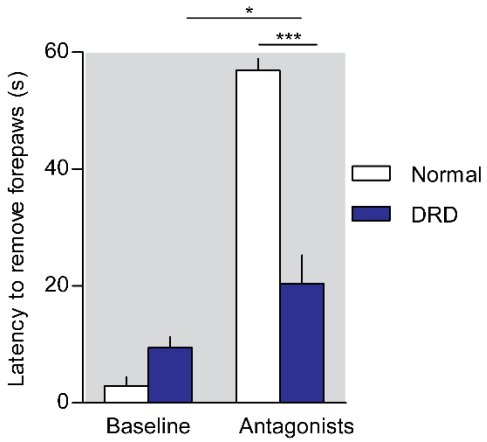

Figure 22: Cataleptic response to DA receptor antagonists in DRD mice. Mice were tested for catalepsy at baseline, and again after injection of 1 mg/kg SCH23390 and 1 mg/kg raclopride (labeled antagonists) in normal (n=8) and DRD mice (n=12) at 8pm. A significant interaction between genotype and drug condition was observed ($F_{1,18}$=54.6, two-way repeated measures ANOVA; p<0.001) whereby the antagonists increased catalepsy in normal (p<0.001, Holm-Sidak *post hoc* analysis) and DRD mice (p<0.05, Holm-Sidak *post hoc* analysis), though DRD mice exhibited less catalepsy than normal upon antagonist administration (p<0.001, Holm-Sidak *post hoc* analysis). Values represent mean ± SEM; *p<0.05, ***p<0.001.

Ex vivo DA receptor expression and second messenger responses

To examine possible mechanisms for the abnormal DA receptor behavioral sensitivity, we first examined the expression of DA receptor mRNAs in striatum with qRT-PCR. No change in the abundance of D1, D2, or D3 DA receptor mRNAs was observed (Table 3). Further, we assessed D2-autoreceptor expression by repeating our analyses on tissue from the midbrain. Similarly, no change in midbrain D2 DA receptor expression was observed (Table 3). Thus, the expression of DA receptors was not changed in DRD mice. Next, we assessed density and affinity of DA receptors in the striatum with *ex vivo* radioligand binding. We used [^{3}H]SCH 23390 as a specific ligand for D1DARs and [^{3}H]spiperone as a specific ligand for D2DARs. Similar to our results from the expression studies, no change in the abundance (B_{max}) or affinity (K_d) of either receptor was observed (Table 4).

To assess functional changes in striatal D1DAR and D2DAR signaling, we measured striatal AC activity. First, we assessed baseline AC activity with the AC activator forskolin, *ex vivo*, in striata from normal and DRD mice. We observed a nonsignificant trend towards increased baseline AC activity in DRD mice (Fig. 23A; $p=0.086$). D1DAR-stimulated activation of AC activity was assessed with SKF 81297. SKF 81297-stimulated AC activity was significantly higher, overall, in DRD mice compared to controls (Fig. 23B; $p<0.001$). Within the lower two doses, AC activity was increased in DRD mice ($p<0.05$ within 0.01 µM and 0.1 µM). D2DAR-mediated inhibition of forskolin stimulated-AC activity was assessed with quinpirole. AC activity in DRD mice was significantly higher, overall, in this experiment (Fig. 23C; $p<0.01$), and there was a significant difference between normal and DRD mice in response to 10 µM quinpirole ($p<0.05$).

Table 3: qRT-PCR for DA receptors.

	D1 DA receptor	D2 DA receptor	D3 DA receptor
Striatum			
Normal	6.1 ± 0.3	5.8 ± 0.3	12.2 ± 0.4
DRD	5.4 ± 0.4	5.1 ± 0.5	12.3 ± 0.7
Midbrain			
Normal	not tested	5.9 ± 0.3	not tested
DRD		5.6 ± 0.2	

Tissue mRNA abundance was determined with qRT-PCR and normalized to 18s rRNA (n=8/genotype). No difference between genotypes was observed for any mRNA ($p>0.1$, Student's *t* tests for each measure). Values represent mean ± SEM.

Table 4: DA receptor binding.

	[^{3}H]SCH 23390		[^{3}H]spiperone	
	B_{max} (fmol/mg)	K_d (nM)	B_{max}	K_d
Normal	62.0 ± 12.0	1.4 ± 0.6	12.9 ± 4.4	0.26 ± 0.1
DRD	62.4 ± 3.3	1.6 ± 0.1	13.1 ± 4.0	0.22 ± 0.1

Striatal densities (B_{max}) and affinities (K_d) of D1DARs and D2DARs were determined using [^{3}H]SCH 23390 and [^{3}H]spiperone, respectively (n=6/genotype). No differences between genotypes were observed in D1DAR or D2DAR density or affinity ($p>0.1$, Student's *t* tests for each measure). Values represent mean ± SEM.

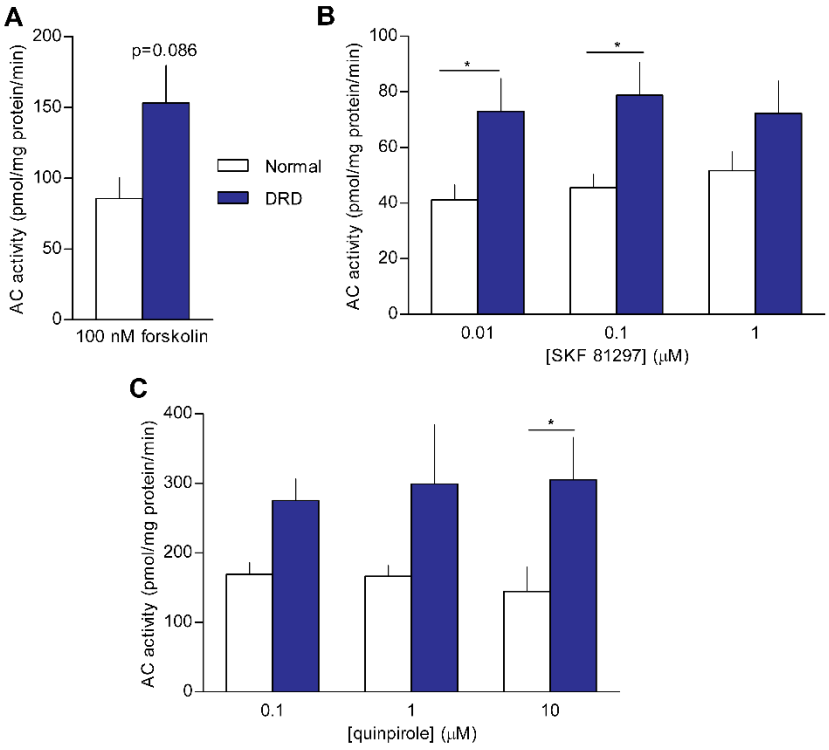

Figure 23: *Ex vivo* striatal AC activity. AC activity in striatal tissue homogenates from DRD and normal mice (n=4-5/genotype and condition). (A) Baseline AC activity was measured with 100 nM forskolin stimulation. There was a trend towards increased baseline AC in DRD mice (Student's *t* test; p=0.086). (B) There was a significant effect of genotype on SKF 81297-induced AC activity ($F_{1,24}$=14.6, two-way ANOVA; p<0.001, Holm Sidak *post hoc* analysis) with increased activity in DRD mice at 0.01 μM (p<0.05; Holm Sidak *post hoc* analysis) and 0.1 μM (p<0.05; Holm Sidak *post hoc* analysis). (F) There was a significant effect of genotype on quinpirole-induced suppression of AC activity ($F_{1,23}$=14.6, two-way ANOVA; p<0.01, Holm Sidak *post hoc* analysis) with a significant difference between normal and DRD mice in response to 10 μM quinpirole (p<0.05; Holm Sidak *post hoc* analysis). Values represent mean ± SEM; *p<0.05.

Discussion

In this chapter, we examined DA receptor responses in the DRD mice. We show that antagonism of either D1DAR or D2DAR worsened the dystonic movements. Conversely, agonism of either D1DAR or D2DAR alleviated these symptoms. Further examination revealed that DA receptor responses were abnormal in DRD mice. D1DARs were functionally supersensitive, whereas D2DAR responses were blunted or altered in valence. Further, the cataleptic response to DA receptor antagonism was blunted. These changes were not accompanied by any changes in DA receptor expression, binding, or affinity, though changes in second messenger responses were observed.

Here we show, through DA receptor subtype-specific challenges, that diminished signaling through DA receptors contributes to the dystonic movements of DRD mice. These results are consistent with our findings in chapter 3 that established the association between reduced DA turnover and dystonic movements in DRD mice. Human neuroimaging and animal model data have previously illustrated associations between diminished DA receptor signaling and dystonia (Perlmutter et al., 1997, Asanuma et al., 2005, Zhang et al., 2012). In those studies, however, DA receptor abundance is lowered, while such is not the case in DRD mice. Further, these data not only illustrate an *association*, but they also show that acute antagonism of DA receptors can *cause* dystonic movement.

That antagonism of *either* D1DAR or D2DAR causes dystonic movements in DRD mice is somewhat surprising. Expression of D1DAR and D2DARs is confined to different subtypes of MSNs, and those subtypes give rise to different, functionally opposing, basal ganglia circuits (Alexander et al., 1986, Gerfen et al., 1990, DeLong and Wichmann, 2009). Thus, one might hypothesize that dystonia arises from the dysregulation of one DA receptor, but not the other. Because activation of D2DARs inhibits movement-suppressing

indirect pathway MSNs, a D2DAR hypofunction hypothesis for dystonia has been posited and is backed by clinical evidence (Todd and Perlmutter, 1998). For one, reduced striatal D2DAR binding is observed in idiopathic dystonias (Hierholzer et al., 1994, Naumann et al., 1998, Horie et al., 2009) and DYT1 dystonia (Asanuma et al., 2005). Reduced D2DAR binding is associated with dystonia in MPTP-treated monkeys (Perlmutter et al., 1997). Further, acute dystonia can occur from neuroleptics, which antagonize D2DARs (Mehta et al., 2015). More recently, however, evidence for D1DAR involvement in dystonia has been found. In certain patients, dystonia is caused by loss-of-function mutations in *GNAL* (Fuchs et al., 2013, Vemula et al., 2013). *GNAL* encodes the $G\alpha_{s/olf}$ subunit that transduces D1DAR signaling in MSNs (Zhuang et al., 2000), therefore these patients are hypothesized to exhibit diminished D1DAR signaling. Thus, in humans, a reduction in *both* D1DAR and D2DAR function is associated with dystonia, consistent with DRD mice.

Not only are both D1DAR and D2DARs involved in the dystonic movements of DRD mice, they appear to serve redundant roles for this behavior. Similarly, in normal rodents, D1DAR or D2DAR antagonism induces catalepsy (Snyder et al., 1970, Zetler, 1975, Sanberg, 1980, Morelli and Di Chiara, 1985). Stated another way, antagonism of only one of the DA receptor subtypes is necessary to induce catalepsy. The same relationship between DA receptor antagonism and dystonic movement appears to exist in DRD mice. It is interesting to note, however, that DA receptor antagonism in DRD mice causes only mild catalepsy, co-expressed with dystonia. Adaptive, functional changes to DA receptors, possibly occurring during development, may ultimately be the mechanism that shifts the response to DA receptor antagonism from catalepsy to dystonia in DRD mice.

Indeed, we show functional changes to DA receptor signaling in the form of altered locomotor and *ex vivo* second messenger responses to DA receptor agonism in DRD

mice. We show D1DAR supersensitivity in DRD mice with a leftward shift in the locomotor dose response to SKF 81297 and an increase in *ex vivo* SKF 81297-induced AC activity in DRD mice. These results are in agreement with findings from other early-life DA depletion models like *DA deficient* mice (Kim et al., 2000) and neonatal 6-OHDA-lesioned rats (Breese et al., 1984a). Since low dose D1DAR agonism reduces dystonic movement and causes hyperlocomotion in DRD mice, D1DAR supersensitivity may actually be adaptive for the DRD mice. D1DAR supersensitivity may help preserve locomotor activity in the DRD mice and prevent a more severe dystonic phenotype, though further experimentation will be needed to determine the precise role for D1DAR supersensitivity in the motor phenotype of DRD mice.

In adult 6-OHDA-lesioned rodents, repeated administration of L-DOPA causes LIDs (Picconi et al., 2003). Interestingly, despite the fact that both the LID model and DRD mice exhibit D1DAR supersensitivity (Corvol et al., 2004), D1DAR agonists *induce* abnormal movements in the LID model (Westin et al., 2007), while they reduce dystonia in DRD mice. It will be interesting to compare changes in the signaling cascades downstream of D1DARs, such as DARPP-32-ERK1/2-ΔFosB signaling, which have been implicated in LIDs (Andersson et al., 1999, Santini et al., 2007). Differences in these downstream processes between DRD mice and the LID model may reveal important differences between LIDs and dystonia.

Along with changes to D1DAR, we also show changes in D2DAR responses in DRD mice. While D2DAR agonism with quinpirole eliminated dystonic movements, it had minimal effect on locomotion or second messenger signaling in the DRD mice. Further, quinpirole actually induced stereotypic behaviors in DRD mice, while reducing them in normal mice. Because of the promiscuous expression of D2DARs in striatum, it is difficult to ascribe a specific neural mechanism to these altered responses, although D2-

autoreceptor-mediated effects in DRD mice likely play some role. Quinpirole-induced activation of D2-autoreceptors, which reduces extracellular DA concentrations in normal animals (Linthorst et al., 1990), likely has a minimal effect on extracellular DA concentration in DRD mice, where extracellular DA concentrations are already very low. Thus, D2-autoreceptor activation by quinpirole has a minimal locomotor-suppressing effect in DRD mice. Still, though, some of the locomotor-suppressing effect of quinpirole in normal mice comes from D2DARs expressed on non-dopaminergic cell-types, as mice that lack D2-autoreceptors also exhibit a reduction in locomotion from quinpirole (Anzalone et al., 2012). Thus, that the DRD mice do not exhibit locomotor suppression from quinpirole is consistent with blunted D2DAR-mediated responses in MSNs and the other non-dopaminergic cell-types in striatum. Specifically, net behavioral and second messenger responses are consistent with a blunting of D2DAR-mediated inhibition of AC. Indeed, we saw a trend for increased baseline AC activity in the DRD mice, which may contribute. Alternatively, changes to $G\alpha_i$ activation, or changes in βarrestin2-mediated desensitization (Ferguson et al., 1996), all could contribute to the D2DAR hypofunction we observed.

Taken together with the D1DAR data, our data argue that the residual pool of DA in DRD mice signals through altered DA receptors. D1DARs are supersensitive, whereas D2DARs are hypofunctional or altered in valence. Imbalanced striatal signaling has long been hypothesized to be a central pathology of dystonia (Todd and Perlmutter, 1998, Mink, 2003, Crittenden and Graybiel, 2011). Though it may be tempting to interpret that the dystonic movement from DRD mice results from imbalanced DA receptor-mediated responses, this explanation may be too simplistic. For one, if dystonic movements were caused by DA receptor subtype imbalance, agonism of one DA receptor subtype should worsen the dystonic movements of DRD mice. In fact, both D1DAR and D2DAR agonism

alleviate the dystonic movements. A more realistic explanation would be that diminished signaling through both DA receptor subtypes mediates the dystonic movements, but distinct changes to D1DAR and D2DAR signaling contribute to striatal circuit dysfunction as a whole. Further work will be needed to understand how striatal circuitry, and the motor network as a whole integrate D1DAR and D2DAR-mediated signals and how that dysfunction generates dystonic movement.

Chapter 5: General Discussion

DRD mice: contribution to the field

Animal models of neurological diseases play an important role in preclinical research. For disorders like dystonia, where neuropathology provides sparse clues, animal models are essential tools for understanding the pathomechanisms that cause the disorder. Animal models of dystonia are typically classified as either etiological or symptomatic (Jinnah et al., 2005, Wilson and Hess, 2013). In the last decade, several mouse lines have been engineered as etiological models of dystonia. Most notably, various mouse strains mimicking DYT1 dystonia have been extensively characterized (Dang et al., 2005, Goodchild et al., 2005, Dang et al., 2006, Zhao et al., 2008). Studies with these mice have largely focused on working forward from genetic etiology towards uncovering cellular abnormalities in relevant cell-types (Pisani et al., 2006, Zhang et al., 2011, Song et al., 2013, Song et al., 2014). For example, DYT1 knockin mice have been instrumental in illustrating that mutant torsinA causes nuclear envelope abnormalities (Goodchild et al., 2005). How these abnormalities relate to the expression of dystonia in humans has been questioned because the DYT1 mutant mice do not exhibit dystonic movements (Dang et al., 2005, Sharma et al., 2005, Dang et al., 2006).

On the other hand, there are several symptomatic animal models of dystonia. These animals exhibit dystonic movements, without precisely mimicking an etiology shown to cause dystonia in humans. Symptomatic models have been studied for longer than engineered mouse lines and include both pharmacological and spontaneous mutant animals (Wahnschaffe et al., 1990, LeDoux et al., 1993, Campbell and Hess, 1998, Pizoli et al., 2002). Studies with these models typically work backward from phenotype to identify the anatomical and physiological substrates of the behavioral presentation. For one, mice injected with a low dose of kainic acid in the cerebellar vermis exhibit dystonia. These

mice have been instrumental in illustrating that the cerebellum is integral in the induction of dystonic movements (Pizoli et al., 2002). Further, this model has been integral in defining dystonia as a motor network disorder that involves important interactions between several brain regions (Neychev et al., 2008). Such models have their limitations as surgical application of kainic acid to cerebellum has little relation to the kinds of etiologies seen in a movement disorders clinic. Taken together, both etiological and symptomatic models of dystonia have utility, but also carry important limitations.

DRD mice are a rare example in the dystonia field of an engineered, etiological model that has a symptomatic presentation resembling that of the human disorder. Stated another way, the DRD mice exhibit construct validity, in that they are designed to mimic a cause of dystonia in humans. They also exhibit face validity, in that they display a motor syndrome similar in appearance to humans with DRD. Lastly, though not directly related to the discussion here, the DRD mice also exhibit predictive therapeutic validity; L-DOPA and THP, two drugs used to treat DRD in humans, show therapeutic efficacy in these mice. Thus, studies may be designed to work forward from etiology and backward from presentation, with the ultimate goal of understanding the neural mechanisms of the disorder. In the work presented here, we applied both approaches to the DRD mice.

Our neurochemical and anatomical characterization is a good example of the "forward" approach. We applied what's known about TH, catecholamines, and nigrostriatal anatomy to characterize the *in vivo* effects of the dystonia-causing mutation on these specific systems. We showed that the p.382Q>K mutation in TH causes regionally selective reductions in TH activity without causing dopaminergic degeneration. We also applied the "backward" approach for several studies. For example, we examined the contribution of DA receptor subtypes to the dystonic movements in DRD mice with pharmacological challenges during behavioral examination. We showed that both DA

receptors display altered responses to agonists and play a role in the dystonic movements of DRD mice. Future studies can apply either approach to other specific questions. Further, investigators can apply both approaches congruently, designing complimentary experiments that work both forward from etiology and backwards from phenotype in the DRD mice. Such studies could present convincing evidence as they would likely illustrate parallel physiological and behavioral outcomes.

Another potential approach with the DRD mice is one that integrates data from several animal models. We show that the DRD mice have altered striatal synaptic circuitry, whereby the ratio of axo-spinous synapses to axo-dendritic synapses is halved. A similar result was shown recently in DYT1 knockin mice (Song et al., 2013). Future studies could integrate the DRD mice with several other animal models where the goal is to find similar pathomechanisms at play. Such studies would be in keeping with recent discussions in the field about etiological heterogeneity and convergent mechanisms in dystonia (Bragg et al., 2011, Thompson et al., 2011, Ledoux et al., 2013). Thus, DRD mice would fill a role where they represent dystonias caused by reduced dopaminergic transmission, whereas other models would represent other etiologies. The ultimate goal of such studies would be to determine how disparate etiologies converge to cause a similar phenotypic presentation. Thus, the DRD mice were not generated to be, nor are they now presented as a “gold standard” dystonia model. Rather, going forward, they should be considered a useful model for the dystonia field, albeit with more utility than many of the other models.

Dystonia vs. parkinsonism

The data presented here are interesting in the context of understanding pathomechanisms that distinguish dystonia from parkinsonism. In terms of outward appearance, dystonia and parkinsonism are markedly different. Dystonia manifests as involuntary overactivity of certain muscle groups, whereas parkinsonism manifests as hypokinesia, bradykinesia,

and rigidity. Nevertheless, several of the same etiologies cause both dystonia and parkinsonism. For one, patients with PD often presents with a dystonic foot as their initial symptom (Tolosa and Compta, 2006). Further, several genetic disorders cause both dystonia and parkinsonism, sometimes co-occurring in the same patient. These include not only monoaminergic disorders like TH and GCH deficiency (Kurian et al., 2011), but also X-linked dystonia-parkinsonism (Rosales, 2010) and rapid onset dystonia-parkinsonism (de Carvalho Aguiar et al., 2004), to name a few. Further, DBS of the GPi is effective for alleviating both parkinsonian and dystonic movements in patients with those disorders (DeLong and Wichmann, 2001, Ostrem and Starr, 2008, Wadia et al., 2010). Thus, basal ganglia pathophysiology causes both types of abnormal movement, though the precise pathophysiologies downstream of DA loss likely differ between dystonia and parkinsonism. The DRD mice may be useful for distinguishing these pathophysiologies because individual DRD mice exhibit both dystonic and parkinsonian symptoms, although the parkinsonian symptoms are milder. For instance, one could examine neuronal activity in specific basal ganglia nuclei during dystonic movement, during a parkinsonian-like behavior such as catalepsy, and during normal movement, and compare the three. Such work would not only shed light on these pathomechanisms, but also provide tremendous insight into the normal functioning of basal ganglia.

Still, though, the work presented here, in conjunction with data from other animal models and dystonic patients, provides clues about the mechanisms through which reduced striatal DA neurotransmission causes a phenotype characterized by prominent dystonia and mild parkinsonism. Specifically, these findings suggest that both the timing and extent of striatal dopaminergic insults are key determining factors for the development of dystonia versus parkinsonism. In DRD mice, the fact that the dopaminergic insult occurs during the development of the motor system appears to be key. Similarly, the age of onset

is an important factor in humans with GCH1 deficiency. The typical age of onset for DRD from GCH1 deficiency is 10 years old, but patients who have an age of onset over 20 years old often present with parkinsonian symptoms (Tadic et al., 2012). In PD, the average age of onset is 62, but in some rare cases symptoms can appear before 45. Sixty percent of those early onset cases present with dystonia (Wickremaratchi et al., 2011). Another relevant comparison can be made between rats undergoing 6-OHDA lesion as adults versus as neonates. Adult rats given severe bilateral 6-OHDA lesion of nigrostriatal projections exhibit a parkinsonian phenotype, whereas neonates lesioned with 6-OHDA intracisternally (but with a similar effect on DA concentration as adults) exhibit hyperactivity (Ungerstedt, 1971a, Shaywitz et al., 1976, Breese et al., 1984a). Taken together, DA depletion likely interacts with plastic processes in the brain, which are more prominent during development and young adulthood, to produce a specific motor phenotype. One explanation is that parkinsonism is the "default" phenotype of striatal DA depletion, whereas dystonia, hyperactivity and other phenotypes result from DA depletion *plus* plastic processes that occur in the young brain. Alternatively, parkinsonism and dystonia may result from different plastic processes, with parkinsonian plasticity more common in the aged brain. This hypothesis is supported by the observation that DRD patients develop more parkinsonian symptoms as they age (Trender-Gerhard et al., 2009).

The extent of DA depletion also appears to be important. The spectrum of phenotypes exhibited by *DA deficient* mice, DRD mice, and *pts-/-; DPS* mice argue that dystonia is associated with a specific level of DA depletion (Zhou and Palmiter, 1995, Sumi-Ichinose et al., 2005). This has been suggested to occur in humans with TH and GCH1 mutations, where subtle GCH1 mutations are associated with no movement disorder (Clot et al., 2009), intermediate GCH1 and TH mutations are associated with DRD, and more severe mutations in both genes are associated with a parkinsonism

(Horvath et al., 2008, Zafeiriou et al., 2009). This has also been shown in MPTP-treated primates, where dystonia correlates with an intermediate phase of dopaminergic degeneration, prior to parkinsonian symptom output (Perlmutter et al., 1997). Further, the dystonic foot in early PD, likely at a moderate stage of dopaminergic degeneration, also supports this idea. Thus, clinical and animal model data indicate that dystonia is associated with DA concentrations intermediate of normal and parkinsonism-associated concentrations. The scale may differ between rodents and primates, however. The data from the DRD mice argue that dystonia in rodents is associated with striatal DA concentrations ~1% of normal, whereas concentrations are reported to be ~15% of normal in GCH1 deficiency patients with a typical DRD presentation (Rajput et al., 1994, Furukawa et al., 1999).

DA receptor mechanisms specific to dystonia

The above data argue that the timing and extent of DA loss interact with downstream plastic, adaptive processes in the induction of dystonic movement. What are those adaptive processes? Our findings show altered DA receptor responses in DRD mice. The D1DAR supersensitivity shown here in DRD mice is also observed in parkinsonian models (Ungerstedt, 1971b), although work in neonatal 6-OHDA-lesioned rats suggests that D1DAR supersensitivity is more profound after developmental DA loss (Breese et al., 1985). We show blunted D2DAR responses in DRD mice in the form of locomotor responses to D2DAR agonism. On the other hand, D2DAR supersensitivity is observed in parkinsonian models in the form of electrophysiological responses to D2DAR agonism (Calabresi et al., 1993, Kostrzewa, 1995, Prieto et al., 2009). Side-by-side comparison of the DRD mice with an appropriate parkinsonian model, similar to the comparisons performed by Breese and colleagues (Breese et al., 1985), will be needed to fully elucidate the specificity of the abnormal D2DAR responses to DRD mice. However, they are

suggestive that different adaptive changes to D2DAR signaling are important for distinguishing dystonia from parkinsonism.

Future directions

Herein lies the value of the DRD mice going forward. They can be used not only for finding pathophysiology that distinguishes dystonia from parkinsonism, but also in finding treatment strategies that can be applied to several different dystonias. That both patients with DRD and the DRD mice are rare cases where dystonia is L-DOPA-responsive can mislead investigators into concluding that neither is very useful for predictive studies that have broad application. Instead, investigators can use this L-DOPA response as a lead toward treatment strategies more applicable to broader patient groups. Correcting a specific deficit, like the blunted D2DAR signaling, may be more effective than applying an indirect agonist like L-DOPA, especially in dystonia cases where DA synthesis is unaffected. Indeed, there are case reports for direct DA receptor agonism being effective for L-DOPA-nonresponsive dystonia cases (Zuddas et al., 1996). Work clarifying the role for dysfunctional DA receptor signaling could better guide how direct DA receptor agonism should be used for dystonia.

For example, the contribution of blunted D2DAR signaling to the phenotype of DRD mice could be elucidated using transgenetic techniques. To test the hypothesis that the dystonic movement arises from blunted D2DAR signaling, the DRD mice could be crossed with mice designed to overexpress D2DAR, generated by Kellendonk and collegues (Kellendonk et al., 2006). If the dystonic phenotype was blunted in these double mutants, then one could reasonably conclude that blunted D2DAR signaling plays a major role in the dystonic phenotype of DRD mice. The next phase of this effort would be to determine which cell-types were necessary for this effect. To assess this, one could use viral vectors to overexpress D2DAR in specific striatal cell-types. For example, if the hypothesis was

that blunted D2DAR signaling in D2DAR-expressing MSNs is necessary for the expression of the dystonic movement, one could generate a virus containing D2DAR driven by a promoter found only in MSNs, like the promotor for the A2A adenosine receptor (Urs et al., 2012). If MSN-specific D2DAR overexpression were sufficient in reducing the dystonic movements of DRD mice, then future focus could be placed on intracellular signaling specific to MSNs. Using emerging knowledge on biased D2DAR signaling in MSNs (Brust et al., 2015, Peterson et al., 2015), one could screen D2DAR agonists with bias toward Gαi-mediated signaling or β-arrestin2-mediated signaling. Results from these experiments could be combined with *ex vivo* biochemistry that characterizes whether these signaling pathways are perturbed in DRD mice. All of this work would hopefully illustrate a specific, correctable signaling deficit that could guide the use of specific D2DAR agonists for several different dystonias.

That is not to say the sole focus with DRD mice going forward should be on dopaminergic and basal ganglia mechanisms. Our data showing THP efficacy in the DRD mice support future studies on muscarinic systems in the mice. Further, it is important to not rule out other brain regions in the design of future studies. Contributions of the whole motor network to the phenotype of the DRD mice needs to be considered. Though the data here clearly implicate striatal DA loss as an essential instigator of the dystonic movement of DRD mice, they do not rule out more global motor network dysfunction in the mice (Prudente et al., 2014). Restoration of normal DA signaling may merely be masking abnormal communication between several brain regions essential for normal movement. Thus, the challenge going forward will be to integrate DRD mice into several lines of both basic science and clinical research. They will hopefully serve a vital role for both understanding the phenomenology of this fascinating disorder as well as in developing treatments to stop it.

References

The Gene Expression Nervous System Atlas (GENSAT) Project, NINDS Contracts N01NS02331 & HHSN271200723701C to The Rockefeller University (New York, NY).

Albanese A, Bhatia K, Bressman SB, Delong MR, Fahn S, Fung VS, Hallett M, Jankovic J, Jinnah HA, Klein C, Lang AE, Mink JW, Teller JK. Phenomenology and classification of dystonia: a consensus update. Mov Disord 2013; 28:863-873.

Albin RL, Young AB, Penney JB. The functional anatomy of basal ganglia disorders. Trends Neurosci 1989; 12:366-375.

Alexander GE, DeLong MR, Strick PL. Parallel organization of functionally segregated circuits linking basal ganglia and cortex. Annu Rev Neurosci 1986; 9:357-381.

Allen GI, Tsukahara N. Cerebrocerebellar communication systems. Physiol Rev 1974; 54:957-1006.

Andersen OA, Flatmark T, Hough E. Crystal structure of the ternary complex of the catalytic domain of human phenylalanine hydroxylase with tetrahydrobiopterin and 3-(2-thienyl)-L-alanine, and its implications for the mechanism of catalysis and substrate activation. J Mol Bio 2002; 320:1095-1108.

Andersson M, Hilbertson A, Cenci MA. Striatal fosB expression is causally linked with l-DOPA-induced abnormal involuntary movements and the associated upregulation of striatal prodynorphin mRNA in a rat model of Parkinson's disease. Neurobiol Dis 1999; 6:461-474.

Anzalone A, Lizardi-Ortiz JE, Ramos M, De Mei C, Hopf FW, Iaccarino C, Halbout B, Jacobsen J, Kinoshita C, Welter M, Caron MG, Bonci A, Sulzer D, Borrelli E. Dual Control of Dopamine Synthesis and Release by Presynaptic and Postsynaptic Dopamine D2 Receptors. J Neurosci 2012; 32:9023-9034.

Aperia AC. Intrarenal dopamine: a key signal in the interactive regulation of sodium metabolism. Ann Rev Phys 2000; 62:621-647.

Arnt J, Hyttel J, Sanchez C. Partial and full dopamine D1 receptor agonists in mice and rats: relation between behavioural effects and stimulation of adenylate cyclase activity in vitro. Eur J Pharmacol 1992; 213:259-267.

Asanuma K, Ma Y, Okulski J, Dhawan V, Chaly T, Carbon M, Bressman SB, Eidelberg D. Decreased striatal D2 receptor binding in non-manifesting carriers of the DYT1 dystonia mutation. Neurology 2005; 64:347-349.

Bademci G, Edwards TL, Torres AL, Scott WK, Zuchner S, Martin ER, Vance JM, Wang L. A rare novel deletion of the tyrosine hydroxylase gene in Parkinson disease. Hum Mutat 2010; 31:E1767-1771.

Baik JH, Picetti R, Saiardi A, Thiriet G, Dierich A, Depaulis A, Le Meur M, Borrelli E. Parkinsonian-like locomotor impairment in mice lacking dopamine D2 receptors. Nature 1995; 377:424-428.

Bamford NS, Zhang H, Schmitz Y, Wu NP, Cepeda C, Levine MS, Schmauss C, Zakharenko SS, Zablow L, Sulzer D. Heterosynaptic dopamine neurotransmission selects sets of corticostriatal terminals. Neuron 2004; 42:653-663.

Bandmann O, Wood NW. Dopa-responsive dystonia -- the story so far. Neuropediatrics 2002; 33:1-5.

Bara-Jimenez W, Bibbiani F, Morris MJ, Dimitrova T, Sherzai A, Mouradian MM, Chase TN. Effects of serotonin 5-HT1A agonist in advanced Parkinson's disease. Mov Disord 2005; 20:932-936.

Berger TW, Kaul S, Stricker EM, Zigmond MJ. Hyperinnervation of the striatum by dorsal raphe afferents after dopamine-depleting brain lesions in neonatal rats. Brain Res 1985; 336:354-358.

Berlanga ML, Price DL, Phung BS, Giuly R, Terada M, Yamada N, Cyr M, Caron MG, Laakso A, Martone ME, Ellisman MH. Multiscale imaging characterization of dopamine transporter knockout mice reveals regional alterations in spine density of medium spiny neurons. Brain Res 2011; 1390:41-49.

Berman BD, Hallett M, Herscovitch P, Simonyan K. Striatal dopaminergic dysfunction at rest and during task performance in writer's cramp. Brain 2013; 136:3645-3658.

Bernard V, Le Moine C, Bloch B. Striatal neurons express increased level of dopamine D2 receptor mRNA in response to haloperidol treatment: a quantitative in situ hybridization study. Neuroscience 1991; 45:117-126.

Bernheimer H, Birkmayer W, Hornykiewicz O, Jellinger K, Seitelberger F. Brain dopamine and the syndromes of Parkinson and Huntington. Clinical, morphological and neurochemical correlations. J Neural Sci 1973; 20:415-455.

Bhatia KP, Marsden CD. The behavioural and motor consequences of focal lesions of the basal ganglia in man. Brain 1994; 117 (Pt 4):859-876.

Biglan KM, Holloway RG. A review of pramipexole and its clinical utility in Parkinson's disease. Expt Opin Pharm 2002; 3:197-210.

Bishop C, Krolewski DM, Eskow KL, Barnum CJ, Dupre KB, Deak T, Walker PD. Contribution of the striatum to the effects of 5-HT1A receptor stimulation in L-DOPA-treated hemiparkinsonian rats. J Neurosci Res 2009; 87:1645-1658.

Bishop C, Tessmer JL, Ullrich T, Rice KC, Walker PD. Serotonin 5-HT2A receptors underlie increased motor behaviors induced in dopamine-depleted rats by intrastriatal 5-HT2A/2C agonism. J Pharmacol Exp Ther 2004; 310:687-694.

Bjorklund A, Dunnett SB. Dopamine neuron systems in the brain: an update. Trends Neurosci 2007; 30:194-202.

Bohn LM, Gainetdinov RR, Caron MG. G protein-coupled receptor kinase/beta-arrestin systems and drugs of abuse: psychostimulant and opiate studies in knockout mice. Neuromol Med 2004; 5:41-50.

Bohn LM, Gainetdinov RR, Sotnikova TD, Medvedev IO, Lefkowitz RJ, Dykstra LA, Caron MG. Enhanced rewarding properties of morphine, but not cocaine, in beta(arrestin)-2 knock-out mice. J Neurosci 2003; 23:10265-10273.

Bolam JP, Hanley JJ, Booth PA, Bevan MD. Synaptic organisation of the basal ganglia. J Anat 2000; 196 (Pt 4):527-542.

Bostan AC, Dum RP, Strick PL. The basal ganglia communicate with the cerebellum. Proc Natl Acad Sci U S A 2010; 107:8452-8456.

Bragg DC, Armata IA, Nery FC, Breakefield XO, Sharma N. Molecular pathways in dystonia. Neurobiol Dis 2011; 42:136-147.

Bravi D, Mouradian MM, Roberts JW, Davis TL, Chase TN. End-of-dose dystonia in Parkinson's disease. Neurology 1993; 43:2130-2131.

Breese GR, Baumeister AA, McCown TJ, Emerick SG, Frye GD, Crotty K, Mueller RA. Behavioral differences between neonatal and adult 6-hydroxydopamine-treated rats to dopamine agonists: relevance to neurological symptoms in clinical

syndromes with reduced brain dopamine. J Pharmacol Exp Ther 1984a; 231:343-354.

Breese GR, Baumeister AA, McCown TJ, Emerick SG, Frye GD, Mueller RA. Neonatal-6-hydroxydopamine treatment: model of susceptibility for self-mutilation in the Lesch-Nyhan syndrome. Pharm Biochem Behav 1984b; 21:459-461.

Breese GR, Napier TC, Mueller RA. Dopamine agonist-induced locomotor activity in rats treated with 6-hydroxydopamine at different ages - functional supersensitivity of D-1 dopamine recpetors in neonatally lesioned rats. J Pharmacol Exp Ther 1985; 234:447-455.

Breese GR, Traylor TD. Developmental characteristics of brain catecholamines and tyrosine hydroxylase in the rat: effects of 6-hydroxydopamine. Br J Pharmacol 1972; 44:210-222.

Brun L, Ngu LH, Keng WT, Ch'ng GS, Choy YS, Hwu WL, Lee WT, Willemsen M, Verbeek MM, Wassenberg T, Regal L, Orcesi S, Tonduti D, Accorsi P, Testard H, Abdenur JE, Tay S, Allen GF, Heales S, Kern I, Kato M, Burlina A, Manegold C, Hoffmann GF, Blau N. Clinical and biochemical features of aromatic L-amino acid decarboxylase deficiency. Neurology 2010; 75:64-71.

Brust TF, Hayes MP, Roman DL, Burris KD, Watts VJ. Bias analyses of preclinical and clinical D2 dopamine ligands: studies with immediate and complex signaling pathways. J Pharmacol Exp Ther 2015; 352:480-493.

Cahill AL, Ehret CF. Circadian variations in the activity of tyrosine hydroxylase, tyrosine aminotransferase, and tryptophan hydroxylase: relationship to catecholamine metabolism. J Neurochem 1981; 37:1109-1115.

Calabresi P, Centonze D, Gubellini P, Pisani A, Bernardi G. Blockade of M2-like muscarinic receptors enhances long-term potentiation at corticostriatal synapses. Eur J Neurosci 1998; 10:3020-3023.

Calabresi P, Centonze D, Gubellini P, Pisani A, Bernardi G. Acetylcholine-mediated modulation of striatal function. Trends Neurosci 2000; 23:120-126.

Calabresi P, Mercuri NB, Sancesario G, Bernardi G. Electrophysiology of dopamine-denervated striatal neurons. Implications for Parkinson's disease. Brain 1993; 116 (Pt 2):433-452.

Calderon DP, Fremont R, Kraenzlin F, Khodakhah K. The neural substrates of rapid-onset Dystonia-Parkinsonism. Nat Neurosci 2011; 14:357-365.

Calvo AC, Scherer T, Pey AL, Ying M, Winge I, McKinney J, Haavik J, Thony B, Martinez A. Effect of pharmacological chaperones on brain tyrosine hydroxylase and tryptophan hydroxylase 2. J Neurochem 2010; 114:853-863.

Campbell DB, Hess EJ. Cerebellar circuitry is activated during convulsive episodes in the tottering (tg/tg) mutant mouse. Neuroscience 1998; 85:773-783.

Campbell DB, North JB, Hess EJ. Tottering mouse motor dysfunction is abolished on the Purkinje cell degeneration (pcd) mutant background. Exp Neurol 1999; 160:268-278.

Campbell DG, Hardie DG, Vulliet PR. Identification of four phosphorylation sites in the N-terminal region of tyrosine hydroxylase. J Biol Chem 1986; 261:10489-10492.

Carbon M, Kingsley PB, Su S, Smith GS, Spetsieris P, Bressman S, Eidelberg D. Microstructural white matter changes in carriers of the DYT1 gene mutation. Ann Neurol 2004a; 56:283-286.

Carbon M, Su S, Dhawan V, Raymond D, Bressman S, Eidelberg D. Regional metabolism in primary torsion dystonia: effects of penetrance and genotype. Neurology 2004b; 62:1384-1390.

Carlsson A, Atack CV, Lindqvis.M, Kehr W, Davis JN. Simultaneous measurement of tyrosine and tyrptophan hydroxylase activities in brain in-vivo using an an inhibitor of aromatic amino-acid decarboxylase. Naunyn Schmied Arch Pharmacol 1972; 275:153-168.

Carlsson A, Lindqvist M, Magnusson T. 3,4-Dihydroxyphenylalanine and 5-hydroxytryptophan as reserpine antagonists. Nature 1957; 180:1200.

Carlsson A, Lindqvist M, Magnusson T, Waldeck B. On the presence of 3-hydroxytyramine in brain. Science 1958; 127:471.

Casey PJ, Gilman AG. G protein involvement in receptor-effector coupling. J Biol Chem 1988; 263:2577-2580.

Caudle WM, Richardson JR, Wang MZ, Taylor TN, Guillot TS, McCormack AL, Colebrooke RE, Di Monte DA, Emson PC, Miller GW. Reduced vesicular storage

of dopamine causes progressive nigrostriatal neurodegeneration. J Neurosci 2007; 27:8138-8148.

Chen CH, Fremont R, Arteaga-Bracho EE, Khodakhah K. Short latency cerebellar modulation of the basal ganglia. Nat Neurosci 2014; 17:1767-1775.

Chen J, Rusnak M, Luedtke RR, Sidhu A. D1 dopamine receptor mediates dopamine-induced cytotoxicity via the ERK signal cascade. J Biol Chem 2004; 279:39317-39330.

Chu HY, Atherton JF, Wokosin D, Surmeier DJ, Bevan MD. Heterosynaptic regulation of external globus pallidus inputs to the subthalamic nucleus by the motor cortex. Neuron 2015; 85:364-376.

Claing A, Laporte SA, Caron MG, Lefkowitz RJ. Endocytosis of G protein-coupled receptors: roles of G protein-coupled receptor kinases and beta-arrestin proteins. Prog Neurobiol 2002; 66:61-79.

Cleary DR, Raslan AM, Rubin JE, Bahgat D, Viswanathan A, Heinricher MM, Burchiel KJ. Deep brain stimulation entrains local neuronal firing in human globus pallidus internus. J Neurophysiol 2013; 109:978-987.

Clot F, Grabli D, Cazeneuve C, Roze E, Castelnau P, Chabrol B, Landrieu P, Nguyen K, Ponsot G, Abada M, Doummar D, Damier P, Gil R, Thobois S, Ward AJ, Hutchinson M, Toutain A, Picard F, Camuzat A, Fedirko E, San C, Bouteiller D, LeGuern E, Durr A, Vidailhet M, Brice A, Network FD. Exhaustive analysis of BH4 and dopamine biosynthesis genes in patients with Dopa-responsive dystonia. Brain 2009; 132:1753-1763.

Cloud LJ, Jinnah HA. Treatment strategies for dystonia. Exp Opin Pharmacother 2010; 11:5-15.

Cooper IS. 20-year followup study of the neurosurgical treatment of dystonia musculorum deformans. Adv Neurol 1976; 14:423-452.

Corbett D, Wise RA. Intracranial self-stimulation in relation to the ascending dopaminergic systems of the midbrain: a moveable electrode mapping study. Brain Res 1980; 185:1-15.

Correll CU, Schenk EM. Tardive dyskinesia and new antipsychotics. Curr Opin Psych 2008; 21:151-156.

Corvol JC, Muriel MP, Valjent E, Feger J, Hanoun N, Girault JA, Hirsch EC, Herve D. Persistent increase in olfactory type G-protein alpha subunit levels may underlie D1 receptor functional hypersensitivity in Parkinson disease. J Neurosci 2004; 24:7007-7014.

Costa RM, Lin SC, Sotnikova TD, Cyr M, Gainetdinov RR, Caron MG, Nicolelis MA. Rapid alterations in corticostriatal ensemble coordination during acute dopamine-dependent motor dysfunction. Neuron 2006; 52:359-369.

Cotzias GC, Van Woert MH, Schiffer LM. Aromatic amino acids and modification of parkinsonism. New Eng Journ Med 1967; 276:374-379.

Creese I, Iversen SD. Amphetamine response in rat after dopamine neurone destruction. Nat New Biol 1972; 238:247-248.

Criswell H, Mueller RA, Breese GR. Priming of D1-dopamine receptor responses: long-lasting behavioral supersensitivity to a D1-dopamine agonist following repeated administration to neonatal 6-OHDA-lesioned rats. J Neurosci 1989; 9:125-133.

Criswell HE, Mueller RA, Breese GR. Long-term D1-dopamine receptor sensitization in neonatal 6-OHDA-lesioned rats is blocked by an NMDA antagonist. Brain Res 1990; 512:284-290.

Crittenden JR, Graybiel AM. Basal Ganglia disorders associated with imbalances in the striatal striosome and matrix compartments. Front Neuroanat 2011; 5:59.

Cui G, Jun SB, Jin X, Pham MD, Vogel SS, Lovinger DM, Costa RM. Concurrent activation of striatal direct and indirect pathways during action initiation. Nature 2013; 494:238-242.

Cuny E, Ghorayeb I, Guehl D, Escola L, Bioulac B, Burbaud P. Sensory motor mismatch within the supplementary motor area in the dystonic monkey. Neurobiol Dis 2008; 30:151-161.

Dahlstroem A, Fuxe K. Evidence for the Existence of Monoamine-Containing Neurons in the Central Nervous System. I. Demonstration of Monoamines in the Cell Bodies of Brain Stem Neurons. Acta physiologica Scandinavica Supplementum 1964; SUPPL 232:231-255.

Damier P, Thobois S, Witjas T, Cuny E, Derost P, Raoul S, Mertens P, Peragut JC, Lemaire JJ, Burbaud P, Nguyen JM, Llorca PM, Rascol O, French Stimulation for

Tardive Dyskinesia Study G. Bilateral deep brain stimulation of the globus pallidus to treat tardive dyskinesia. Arch Gen Psychiatry 2007; 64:170-176.

Dang MT, Yokoi F, McNaught KS, Jengelley TA, Jackson T, Li J, Li Y. Generation and characterization of Dyt1 DeltaGAG knock-in mouse as a model for early-onset dystonia. Exp Neurol 2005; 196:452-463.

Dang MT, Yokoi F, Pence MA, Li Y. Motor deficits and hyperactivity in Dyt1 knockdown mice. Neurosci Res 2006; 56:470-474.

Davis R. Cerebellar stimulation for cerebral palsy spasticity, function, and seizures. Arch Med Res 2000; 31:290-299.

Day M, Wang Z, Ding J, An X, Ingham CA, Shering AF, Wokosin D, Ilijic E, Sun Z, Sampson AR, Mugnaini E, Deutch AY, Sesack SR, Arbuthnott GW, Surmeier DJ. Selective elimination of glutamatergic synapses on striatopallidal neurons in Parkinson disease models. Nat Neurosci 2006; 9:251-259.

de Carvalho Aguiar P, Sweadner KJ, Penniston JT, Zaremba J, Liu L, Caton M, Linazasoro G, Borg M, Tijssen MA, Bressman SB, Dobyns WB, Brashear A, Ozelius LJ. Mutations in the Na+/K+ -ATPase alpha3 gene ATP1A3 are associated with rapid-onset dystonia parkinsonism. Neuron 2004; 43:169-175.

de la Fuente-Fernandez R. Drug-induced motor complications in dopa-responsive dystonia: Implications for the pathogenesis of dyskinesias and motor fluctuations. Clin Neuropharm 1999; 22:216-219.

Defazio G, Conte A, Gigante AF, Fabbrini G, Berardelli A. Is tremor in dystonia a phenotypic feature of dystonia? Neurology 2015; 84:1053-1059.

DeLong M, Wichmann T. Update on models of basal ganglia function and dysfunction. Parkinsonism Relat Disord 2009; 15 Suppl 3:S237-240.

DeLong MR. Primate models of movement disorders of basal ganglia origin. Trends Neurosci 1990; 13:281-285.

DeLong MR, Wichmann T. Deep brain stimulation for Parkinson's disease. Ann Neurol 2001; 49:142-143.

DeLong MR, Wichmann T. Circuits and circuit disorders of the basal ganglia. Arch Neurol 2007; 64:20-24.

Devanagondi R, Egami K, LeDoux MS, Hess EJ, Jinnah HA. Neuroanatomical substrates for paroxysmal dyskinesia in lethargic mice. Neurobiol Dis 2007; 27:249-257.

Ehringer H, Hornykiewicz O. [Distribution of noradrenaline and dopamine (3-hydroxytyramine) in the human brain and their behavior in diseases of the extrapyramidal system]. Klinische Wochenschrift 1960; 38:1236-1239.

Elzaouk L, Leimbacher W, Turri M, Ledermann B, Burki K, Blau N, Thony B. Dwarfism and low insulin-like growth factor-1 due to dopamine depletion in Pts-/- mice rescued by feeding neurotransmitter precursors and H4-biopterin. J Biol Chem 2003; 278:28303-28311.

Eskow KL, Gupta V, Alam S, Park JY, Bishop C. The partial 5-HT(1A) agonist buspirone reduces the expression and development of l-DOPA-induced dyskinesia in rats and improves l-DOPA efficacy. Pharmacol Biochem Behav 2007; 87:306-314.

Fahn S. The spectrum of levodopa-induced dyskinesias. Ann Neurol 2000; 47:S2-9; discussion S9-11.

Fallon JH, Moore RY. Catecholamine innervation of basal forebrain .4. topography of dopamine projection to basal forbrain and neostriatum J Comp Neurol 1978; 180:545-&.

Fan XL, Xu M, Hess EJ. D2 dopamine receptor subtype-mediated hyperactivity and amphetamine responses in a model of ADHD. Neurobiol of Dis 2010; 37:228-236.

Fasano C, Bourque MJ, Lapointe G, Leo D, Thibault D, Haber M, Kortleven C, Desgroseillers L, Murai KK, Trudeau LE. Dopamine facilitates dendritic spine formation by cultured striatal medium spiny neurons through both D1 and D2 dopamine receptors. Neuropharm 2013; 67:432-443.

Ferguson SS, Downey WE, 3rd, Colapietro AM, Barak LS, Menard L, Caron MG. Role of beta-arrestin in mediating agonist-promoted G protein-coupled receptor internalization. Science 1996; 271:363-366.

Fernagut PO, Diguet E, Stefanova N, Biran M, Wenning GK, Canioni P, Bioulac B, Tison F. Subacute systemic 3-nitropropionic acid intoxication induces a distinct motor disorder in adult C57Bl/6 mice: behavioural and histopathological characterisation. Neuroscience 2002; 114:1005-1017.

Ferris MJ, Espana RA, Locke JL, Konstantopoulos JK, Rose JH, Chen R, Jones SR. Dopamine transporters govern diurnal variation in extracellular dopamine tone. Proc Natl Acad Sci U S A 2014; 111:E2751-2759.

Fitzpatrick PF. The aromatic amino acid hydroxylases. Advances in enzymology and related areas of molecular biology 2000; 74:235-294.

Ford CP. The role of D2-autoreceptors in regulating dopamine neuron activity and transmission. Neuroscience 2014; 282C:13-22.

Fossbakk A, Kleppe R, Knappskog PM, Martinez A, Haavik J. Functional Studies of Tyrosine Hydroxylase Missense Variants Reveal Distinct Patterns of Molecular Defects in DOPA Responsive Dystonia. Hum Mutat 2014.

Fuchs T, Saunders-Pullman R, Masuho I, Luciano MS, Raymond D, Factor S, Lang AE, Liang TW, Trosch RM, White S, Ainehsazan E, Herve D, Sharma N, Ehrlich ME, Martemyanov KA, Bressman SB, Ozelius LJ. Mutations in GNAL cause primary torsion dystonia. Nat Genet 2013; 45:88-92.

Furukawa Y, Lang AE, Trugman JM, Bird TD, Hunter A, Sadeh M, Tagawa T, St George-Hyslop PH, Guttman M, Morris LW, Hornykiewicz O, Shimadzu M, Kish SJ. Gender-related penetrance and de novo GTP-cyclohydrolase I gene mutations in dopa-responsive dystonia. Neurology 1998; 50:1015-1020.

Furukawa Y, Mizuno Y, Narabayashi H (1996) Early-onset parkinsonism with dystonia - Clinical and biochemical differences from hereditary progressive dystonia or DOPA-responsive dystonia. In: Parkinson's disease, vol. 69 (Battistin, L. et al., eds), pp 327-337 Philadelphia: Lippincott-Raven Publ.

Furukawa Y, Nygaard TG, Gutlich M, Rajput AH, Pifl C, DiStefano L, Chang LJ, Price K, Shimadzu M, Hornykiewicz O, Haycock JW, Kish SJ. Striatal biopterin and tyrosine hydroxylase protein reduction in dopa-responsive dystonia. Neurology 1999; 53:1032-1041.

Galardi G, Perani D, Grassi F, Bressi S, Amadio S, Antoni M, Comi GC, Canal N, Fazio F. Basal ganglia and thalamo-cortical hypermetabolism in patients with spasmodic torticollis. Acta neurologica Scandinavica 1996; 94:172-176.

Gerfen CR, Engber TM, Mahan LC, Susel Z, Chase TN, Monsma FJ, Sibley DR. D1 and D2 dopamine receptor regulated gene expression of striatonigral and striatopalidal neurons. Science 1990; 250:1429-1432.

Girault JA, Valjent E, Caboche J, Herve D. ERK2: a logical AND gate critical for drug-induced plasticity? Curr Opin in Pharmacol 2007; 7:77-85.

Giros B, Jaber M, Jones SR, Wightman RM, Caron MG. Hyperlocomotion and indifference to cocaine and amphetamine in mice lacking the dopamine transporter. Nature 1996; 379:606-612.

Goodchild RE, Dauer WT. Mislocalization to the nuclear envelope: an effect of the dystonia-causing torsinA mutation. Proc Natl Acad Sci U S A 2004; 101:847-852.

Goodchild RE, Kim CE, Dauer WT. Loss of the dystonia-associated protein torsinA selectively disrupts the neuronal nuclear envelope. Neuron 2005; 48:923-932.

Gorke W, Bartholome K. Biochemical and neurophysiological investigations in two forms of Segawa's disease. Neuropediatrics 1990; 21:3-8.

Graybiel AM, Aosaki T, Flaherty AW, Kimura M. The basal ganglia and adaptive motor control. Science 1994; 265:1826-1831.

Greene P, Shale H, Fahn S. Analysis of open-label trials in torsion dystonia using high dosages of anticholinergics and other drugs. Mov Disord 1988; 3:46-60.

Greengard P. The neurobiology of dopamine signaling. Biosci Rep 2001; 21:247-269.

Grundmann K, Reischmann B, Vanhoutte G, Hubener J, Teismann P, Hauser TK, Bonin M, Wilbertz J, Horn S, Nguyen HP, Kuhn M, Chanarat S, Wolburg H, Van der Linden A, Riess O. Overexpression of human wildtype torsinA and human DeltaGAG torsinA in a transgenic mouse model causes phenotypic abnormalities. Neurobiol Dis 2007; 27:190-206.

Ha AD, Jankovic J. An introduction to dyskinesia--the clinical spectrum. International review of neurobiology 2011; 98:1-29.

Haavik J, Martinez A, Flatmark T. pH-dependent release of catecholamines from tyrosine hydroxylase and the effect of phosphorylation of Ser-40. FEBS Lett 1990; 262:363-365.

Hanihara T, Inoue K, Kawanishi C, Sugiyama N, Miyakawa T, Onishi H, Yamada Y, Osaka H, Kosaka K, Iwabuchi K, Owada M. 6-pyruvoyl-tetrahydropterin synthase deficiency with generalized dystonia and diurnal fluctuation of symptoms: A clinical and molecular study. Mov Disord 1997; 12:408-411.

He F, Zhang S, Qian F, Zhang C. Delayed dystonia with striatal CT lucencies induced by a mycotoxin (3-nitropropionic acid). Neurology 1995; 45:2178-2183.

Hendrix CM, Vitek JL. Toward a network model of dystonia. Ann N Y Acad Sci 2012; 1265:46-55.

Hierholzer J, Cordes M, Schelosky L, Richter W, Keske U, Venz S, Semmler W, Poewe W, Felix R. Dopamine D2 receptor imaging with iodine-123-iodobenzamide SPECT in idiopathic rotational torticollis. J Nucl Med 1994; 35:1921-1927.

Hitchcock E. Dentate lesions for involuntary movement. Proceedings of the Royal Society of Medicine 1973; 66:877-879.

Hnasko TS, Sotak BN, Palmiter RD. Cocaine-conditioned place preference by dopamine-deficient mice is mediated by serotonin. J Neurosci 2007; 27:12484-12488.

Homma D, Sumi-Ichinose C, Tokuoka H, Ikemoto K, Nomura T, Kondo K, Katoh S, Ichinose H. Partial biopterin deficiency disturbs postnatal development of the dopaminergic system in the brain. J Biol Chem 2011; 286:1445-1452.

Horie C, Suzuki Y, Kiyosawa M, Mochizuki M, Wakakura M, Oda K, Ishiwata K, Ishii K. Decreased dopamine D receptor binding in essential blepharospasm. Acta neurologica Scandinavica 2009; 119:49-54.

Horvath GA, Stockler-Ipsiroglu SG, Salvarinova-Zivkovic R, Lillquist YP, Connolly M, Hyland K, Blau N, Rupar T, Waters PJ. Autosomal recessive GTP cyclohydrolase I deficiency without hyperphenylalaninemia: evidence of a phenotypic continuum between dominant and recessive forms. Mol Genet Metab 2008; 94:127-131.

Hoshi E, Tremblay L, Feger J, Carras PL, Strick PL. The cerebellum communicates with the basal ganglia. Nat Neurosci 2005; 8:1491-1493.

Hung SW, Hamani C, Lozano AM, Poon YY, Piboolnurak P, Miyasaki JM, Lang AE, Dostrovsky JO, Hutchison WD, Moro E. Long-term outcome of bilateral pallidal deep brain stimulation for primary cervical dystonia. Neurology 2007; 68:457-459.

Hwang WJ, Calne DB, Tsui JKC, de la Fuente-Fernandez R. The long-term response to levodopa in dopa-responsive dystonia. Parkinsonism & Related Disorders 2001; 8:1-5.

Ichinose H, Ohye T, Takahashi E, Seki N, Hori T, Segawa M, Nomura Y, Endo K, Tanaka H, Tsuji S, et al. Hereditary progressive dystonia with marked diurnal fluctuation caused by mutations in the GTP cyclohydrolase I gene. Nat Genet 1994; 8:236-242.

Ingham CA, Hood SH, Arbuthnott GW. Spine density on neostriatal neurones changes with 6-hydroxydopamine lesions and with age. Brain Res 1989; 503:334-338.

Ingham CA, Hood SH, Taggart P, Arbuthnott GW. Plasticity of synapses in the rat neostriatum after unilateral lesion of the nigrostriatal dopaminergic pathway. J Neurosci 1998; 18:4732-4743.

Jankovic J. Treatment of dystonia. Lancet Neurol 2006; 5:864-872.

Jarman PR, Bandmann O, Marsden CD, Wood NW. GTP cyclohydrolase I mutations in patients with dystonia responsive to anticholinergic drugs. J Neurol Neurosurg and Psychiatry 1997; 63:304-308.

Jinnah HA, Factor SA. Diagnosis and treatment of dystonia. Neurologic Clin 2015; 33:77-100.

Jinnah HA, Hess EJ, Ledoux MS, Sharma N, Baxter MG, Delong MR. Rodent models for dystonia research: characteristics, evaluation, and utility. Mov Disord 2005; 20:283-292.

Jinnah HA, Visser JE, Harris JC, Verdu A, Larovere L, Ceballos-Picot I, Gonzalez-Alegre P, Neychev V, Torres RJ, Dulac O, Desguerre I, Schretlen DJ, Robey KL, Barabas G, Bloem BR, Nyhan W, De Kremer R, Eddey GE, Puig JG, Reich SG, Lesch-Nyhan Disease International Study G. Delineation of the motor disorder of Lesch-Nyhan disease. Brain 2006; 129:1201-1217.

Jinnah HA, Wojcik BE, Hunt M, Narang N, Lee KY, Goldstein M, Wamsley JK, Langlais PJ, Friedmann T. Dopamine deficiency in a genetic mouse model of Lesch-Nyhan disease. J Neurosci 1994; 14:1164-1175.

Jones SR, Gainetdinov RR, Jaber M, Giros B, Wightman RM, Caron MG. Profound neuronal plasticity in response to inactivation of the dopamine transporter. Proc Natl Acad Sci U S A 1998; 95:4029-4034.

Kaneda N, Sasaoka T, Kobayashi K, Kiuchi K, Nagatsu I, Kurosawa Y, Fujita K, Yokoyama M, Nomura T, Katsuki M, et al. Tissue-specific and high-level expression of the human tyrosine hydroxylase gene in transgenic mice. Neuron 1991; 6:583-594.

Kebabian JW, Calne DB. Multiple receptors for dopamine. Nature 1979; 277:93-96.

Kellendonk C, Simpson EH, Polan HJ, Malleret G, Vronskaya S, Winiger V, Moore H, Kandel ER. Transient and selective overexpression of dopamine D2 receptors in the striatum causes persistent abnormalities in prefrontal cortex functioning. Neuron 2006; 49:603-615.

Kelly RM, Strick PL. Macro-architecture of basal ganglia loops with the cerebral cortex: use of rabies virus to reveal multisynaptic circuits. Prog Brain Res 2004; 143:449-459.

Kim DS, Froelick GJ, Palmiter RD. Dopamine-dependent desensitization of dopaminergic signaling in the developing mouse striatum. J Neurosci 2002; 22:9841-9849.

Kim DS, Szczypka MS, Palmiter RD. Dopamine-deficient mice are hypersensitive to dopamine receptor agonists. J Neurosci 2000; 20:4405-4413.

Kisilevsky AE, Mulligan SJ, Altier C, Iftinca MC, Varela D, Tai C, Chen L, Hameed S, Hamid J, Macvicar BA, Zamponi GW. D1 receptors physically interact with N-type calcium channels to regulate channel distribution and dendritic calcium entry. Neuron 2008; 58:557-570.

Klein C. Genetics in dystonia. Parkinsonism Relat Disord 2014; 20 Suppl 1:S137-142.

Knappskog PM, Flatmark T, Mallet J, Ludecke B, Bartholome K. Recessively inherited L-DOPA-responsive dystonia caused by a point mutation(Q381K) in the tyrosine-hydroxylase gene. Hum Mol Genet 1995; 4:1209-1212.

Kobayashi K, Kaneda N, Ichinose H, Kishi F, Nakazawa A, Kurosawa Y, Fujita K, Nagatsu T. Structure of the human tyrosine hydroxylase gene: alternative splicing from a single gene accounts for generation of four mRNA types. J Biochem 1988; 103:907-912.

Kobayashi K, Morita S, Sawada H, Mizuguchi T, Yamada K, Nagatsu I, Hata T, Watanabe Y, Fujita K, Nagatsu T. Targeted disruption of the Tyrosine-Hydroxylase locus results in severe catecholamine depletion and perinatal lethality in mice. J Biol Chem 1995; 270:27235-27243.

Kostrzewa RM. Dopamine-receptor supersensitivity. Neurosci Biobehav Rev 1995; 19:1-17.

Krauss JK, Mohadjer M, Braus DF, Wakhloo AK, Nobbe F, Mundinger F. Dystonia following head trauma: a report of nine patients and review of the literature. Mov Disord 1992; 7:263-272.

Kravitz AV, Freeze BS, Parker PR, Kay K, Thwin MT, Deisseroth K, Kreitzer AC. Regulation of parkinsonian motor behaviours by optogenetic control of basal ganglia circuitry. Nature 2010; 466:622-626.

Kumer SC, Vrana KE. Intricate regulation of tyrosine hydroxylase activity and gene expression. J Neurochem 1996; 67:443-462.

Kurian MA, Gissen P, Smith M, Heales S, Jr., Clayton PT. The monoamine neurotransmitter disorders: an expanding range of neurological syndromes. The Lancet Neurol 2011; 10:721-733.

Le Bourdelles B, Boularand S, Boni C, Horellou P, Dumas S, Grima B, Mallet J. Analysis of the 5' region of the human tyrosine hydroxylase gene: combinatorial patterns of exon splicing generate multiple regulated tyrosine hydroxylase isoforms. J Neurochem 1988; 50:988-991.

Ledoux MS, Dauer WT, Warner TT. Emerging common molecular pathways for primary dystonia. Mov Disord 2013; 28:968-981.

LeDoux MS, Lorden JF, Ervin JM. Cerebellectomy eliminates the motor syndrome of the genetically dystonic rat. Exp Neurol 1993; 120:302-310.

Lehericy S, Tijssen MA, Vidailhet M, Kaji R, Meunier S. The anatomical basis of dystonia: current view using neuroimaging. Mov Disord 2013; 28:944-957.

Lein ES, Hawrylycz MJ, Ao N, Ayres M, Bensinger A, Bernard A, Boe AF, Boguski MS, Brockway KS, Byrnes EJ, Chen L, Chen L, Chen TM, Chin MC, Chong J, Crook BE, Czaplinska A, Dang CN, Datta S, Dee NR, Desaki AL, Desta T, Diep E, Dolbeare TA, Donelan MJ, Dong HW, Dougherty JG, Duncan BJ, Ebbert AJ, Eichele G, Estin LK, Faber C, Facer BA, Fields R, Fischer SR, Fliss TP, Frensley C, Gates SN, Glattfelder KJ, Halverson KR, Hart MR, Hohmann JG, Howell MP, Jeung DP, Johnson RA, Karr PT, Kawal R, Kidney JM, Knapik RH, Kuan CL, Lake JH, Laramee AR, Larsen KD, Lau C, Lemon TA, Liang AJ, Liu Y, Luong LT, Michaels J, Morgan JJ, Morgan RJ, Mortrud MT, Mosqueda NF, Ng LL, Ng R, Orta GJ, Overly CC, Pak TH, Parry SE, Pathak SD, Pearson OC, Puchalski RB, Riley ZL, Rockett HR, Rowland SA, Royall JJ, Ruiz MJ, Sarno NR, Schaffnit K, Shapovalova NV, Sivisay T, Slaughterbeck CR, Smith SC, Smith KA, Smith BI, Sodt AJ, Stewart NN, Stumpf KR, Sunkin SM, Sutram M, Tam A, Teemer CD, Thaller C, Thompson CL, Varnam LR, Visel A, Whitlock RM, Wohnoutka PE, Wolkey CK, Wong VY, Wood M, Yaylaoglu MB, Young RC, Youngstrom BL, Yuan

XF, Zhang B, Zwingman TA, Jones AR. Genome-wide atlas of gene expression in the adult mouse brain. Nature 2007; 445:168-176.

Li SM, Collins GT, Paul NM, Grundt P, Newman AH, Xu M, Grandy DK, Woods JH, Katz JL. Yawning and locomotor behavior induced by dopamine receptor agonists in mice and rats. Behav Pharmacol 2010; 21:171-181.

Li ZS, Schmauss C, Cuenca A, Ratcliffe E, Gershon MD. Physiological modulation of intestinal motility by enteric dopaminergic neurons and the D2 receptor: analysis of dopamine receptor expression, location, development, and function in wild-type and knock-out mice. J Neurosci 2006; 26:2798-2807.

Linthorst AC, Van den Buuse M, De Jong W, Versteeg DH. Electrically stimulated [3H]dopamine and [14C]acetylcholine release from nucleus caudatus slices: differences between spontaneously hypertensive rats and Wistar-Kyoto rats. Brain Res 1990; 509:266-272.

Longo N. Disorders of biopterin metabolism. J Inhert Metabol Disease 2009; 32:333-342.

Louis ED, Marder K, Moskowitz C, Greene P. Arm elevation in Huntington's disease: dystonia or levitation? Mov Disord 1999; 14:1035-1038.

Ludecke B, Dworniczak B, Bartholome K. A point mutation in the tyrosine-hydroxylase gene associated with Segawa's syndrome. Human Genetics 1995; 95:123-125.

Ludecke B, Knappskog PM, Clayton PT, Surtees RA, Clelland JD, Heales SJ, Brand MP, Bartholome K, Flatmark T. Recessively inherited L-DOPA-responsive parkinsonism in infancy caused by a point mutation (L205P) in the tyrosine hydroxylase gene. Hum Mol Genet 1996; 5:1023-1028.

Magyar-Lehmann S, Antonini A, Roelcke U, Maguire RP, Missimer J, Meyer M, Leenders KL. Cerebral glucose metabolism in patients with spasmodic torticollis. Mov Disord 1997; 12:704-708.

Maltese M, Martella G, Madeo G, Fagiolo I, Tassone A, Ponterio G, Sciamanna G, Burbaud P, Conn PJ, Bonsi P, Pisani A. Anticholinergic drugs rescue synaptic plasticity in DYT1 dystonia: role of M1 muscarinic receptors. Mov Disord 2014; 29:1655-1665.

Marconi R, Lefebvre-Caparros D, Bonnet AM, Vidailhet M, Dubois B, Agid Y. Levodopa-induced dyskinesias in Parkinson's disease phenomenology and pathophysiology. Mov Disord 1994; 9:2-12.

Marsden CD, Jenner P. The pathophysiology of extrapyramidal side-effects of neuroleptic drugs. Psychol Med 1980; 10:55-72.

Marsden CD, Obeso JA, Zarranz JJ, Lang AE. The anatomical basis of symptomatic hemidystonia. Brain 1985; 108 (Pt 2):463-483.

Masri B, Salahpour A, Didriksen M, Ghisi V, Beaulieu JM, Gainetdinov RR, Caron MG. Antagonism of dopamine D2 receptor/beta-arrestin 2 interaction is a common property of clinically effective antipsychotics. Proc Natl Acad Sci U S A 2008; 105:13656-13661.

Matsuda W, Furuta T, Nakamura KC, Hioki H, Fujiyama F, Arai R, Kaneko T. Single nigrostriatal dopaminergic neurons form widely spread and highly dense axonal arborizations in the neostriatum. J Neurosci 2009; 29:444-453.

McDonald JD, Cotton RG, Jennings I, Ledley FD, Woo SL, Bode VC. Biochemical defect of the hph-1 mouse mutant is a deficiency in GTP-cyclohydrolase activity. J Neurochem 1988; 50:655-657.

Mehta SH, Morgan JC, Sethi KD. Drug-induced movement disorders. Neurologic Clinics 2015; 33:153-174.

Mergy MA, Gowrishankar R, Gresch PJ, Gantz SC, Williams J, Davis GL, Wheeler CA, Stanwood GD, Hahn MK, Blakely RD. The rare DAT coding variant Val559 perturbs DA neuron function, changes behavior, and alters in vivo responses to psychostimulants. Proc Natl Acad Sci U S A 2014; 111:E4779-4788.

Mink JW. The basal ganglia and involuntary movements - Impaired inhibition of competing motor patterns. Arch Neurol 2003; 60:1365-1368.

Missale C, Nash SR, Robinson SW, Jaber M, Caron MG. Dopamine receptors: From structure to function. Physiological Reviews 1998; 78:189-225.

Money KM, Stanwood GD. Developmental origins of brain disorders: roles for dopamine. Front Cell Neurosci 2013; 7:260.

Morelli M, Di Chiara G. Catalepsy induced by SCH 23390 in rats. Eur J Pharmacol 1985; 117:179-185.

Nagatsu T, Levitt M, S U. Tyrosine hydroxylase. The initial step in norepinephrine biosynthesis. J Biol Chem 1964; 239:2910-2917.

Nambu A, Tokuno H, Takada M. Functional significance of the cortico-subthalamo-pallidal 'hyperdirect' pathway. Neurosci Res 2002; 43:111-117.

Nardocci N. Myoclonus-dystonia syndrome. Handbook of clinical neurology 2011; 100:563-575.

Naumann M, Pirker W, Reiners K, Lange KW, Becker G, Brucke T. Imaging the pre- and postsynaptic side of striatal dopaminergic synapses in idiopathic cervical dystonia: a SPECT study using [123I] epidepride and [123I] beta-CIT. Mov Disord 1998; 13:319-323.

Neychev V, Gross R, Lehericy S, Hess E, Jinnah H. The functional neuroanatomy of dystonia. Neurobiol Dis 2011; 42:185-201.

Neychev VK, Fan XL, Mitev VI, Hess EJ, Jinnah HA. The basal ganglia and cerebellum interact in the expression of dystonic movement. Brain 2008; 131:2499-2509.

Ng J, Zhen J, Meyer E, Erreger K, Li Y, Kakar N, Ahmad J, Thiele H, Kubisch C, Rider NL, Holmes Morton D, Strauss KA, Puffenberger EG, D'Agnano D, Anikster Y, Carducci C, Hyland K, Rotstein M, Leuzzi V, Borck G, Reith ME, Kurian MA. Dopamine transporter deficiency syndrome: phenotypic spectrum from infancy to adulthood. Brain 2014; 137:1107-1119.

Niethammer M, Carbon M, Argyelan M, Eidelberg D. Hereditary dystonia as a neurodevelopmental circuit disorder: Evidence from neuroimaging. Neurobiol Dis 2011; 42:202-209.

Obeso JA, Gimenez-Roldan S. Clinicopathological correlation in symptomatic dystonia. Adv Neurol 1988; 50:113-122.

Oppenheim H. About a rare spasm disease of childhood and young age. Neurologische Centralblatt 1911; 30:1090-1107.

Ostrem J, Starr P. Treatment of dystonia with deep brain stimulation. Neurotherapeutics 2008; 5:320-330.

Ozelius LJ, Hewett JW, Page CE, Bressman SB, Kramer PL, Shalish C, de Leon D, Brin MF, Raymond D, Corey DP, Fahn S, Risch NJ, Buckler AJ, Gusella JF, Breakefield XO. The early-onset torsion dystonia gene (DYT1) encodes an ATP-binding protein. Nat Genet 1997; 17:40-48.

Papadeas ST, Blake BL, Knapp DJ, Breese GR. Sustained extracellular signal-regulated kinase 1/2 phosphorylation in neonate 6-hydroxydopamine-lesioned rats after repeated D1-dopamine receptor agonist administration: implications for NMDA receptor involvement. J Neurosci 2004; 24:5863-5876.

Paulson PE, Robinson TE. Relationship between circadiaon changes in spontaneous motor-activity and dorsal striatal dopamine neurotransmission assessed with online microdialysis. Behav Neurosci 1994; 108:624-635.

Paxinos G, Franklin K (2001) The Mouse Brain in Stereotaxic Coordinattes. San Diego: Academic Press.

Perlmutter JS, Tempel LW, Black KJ, Parkinson D, Todd RD. MPTP induces dystonia and parkinsonism - Clues to the pathophysiology of dystonia. Neurology 1997; 49:1432-1438.

Peters A, Palay S, Webster H. The fine structure of the nervous system: neurons and their supporting cells. New York: Oxford University Press 1991.

Peterson DA, Sejnowski TJ, Poizner H. Convergent evidence for abnormal striatal synaptic plasticity in dystonia. Neurobiol Dis 2010; 37:558-573.

Peterson SM, Pack TF, Wilkins AD, Urs NM, Urban DJ, Bass CE, Lichtarge O, Caron MG. Elucidation of G-protein and beta-arrestin functional selectivity at the dopamine D2 receptor. Proc Natl Acad Sci U S A 2015; 112:7097-7102.

Pettigrew LC, Jankovic J. Hemidystonia: a report of 22 patients and a review of the literature. J Neurol Neurosurg Psychiatry 1985; 48:650-657.

Picconi B, Centonze D, Hakansson K, Bernardi G, Greengard P, Fisone G, Cenci MA, Calabresi P. Loss of bidirectional striatal synaptic plasticity in L-DOPA-induced dyskinesia. Nat Neurosci 2003; 6:501-506.

Pijnenburg AJ, Honig WM, Van Rossum JM. Inhibition of d-amphetamine-induced locomotor activity by injection of haloperidol into the nucleus accumbens of the rat. Psychopharmacologia 1975; 41:87-95.

Pisani A, Bernardi G, Ding J, Surmeier DJ. Re-emergence of striatal cholinergic interneurons in movement disorders. Trends Neurosci 2007; 30:545-553.

Pisani A, Martella G, Tscherter A, Bonsi P, Sharma N, Bernardi G, Standaert DG. Altered responses to dopaminergic D2 receptor activation and N-type calcium currents in striatal cholinergic interneurons in a mouse model of DYT1 dystonia. Neurobiol Dis 2006; 24:318-325.

Pizoli C, Jinnah H, Billingsley M, Hess E. Abnormal Cerebellar Signaling Induces Dystonia in Mice. J Neurosci 2002; 22:7825-7833.

Plotkin JL, Shen W, Rafalovich I, Sebel LE, Day M, Chan CS, Surmeier DJ. Regulation of dendritic calcium release in striatal spiny projection neurons. J Neurophysiol 2013; 110:2325-2336.

Portbury AL, Chandra R, Groelle M, McMillian MK, Elias A, Herlong JR, Rios M, Roffler-Tarlov S, Chikaraishi DM. Catecholamines act via a beta-adrenergic receptor to maintain fetal heart rate and survival. Am J Physiol Heart Circul Physiol 2003; 284:H2069-H2077.

Pothos EN, Przedborski S, Davila V, Schmitz Y, Sulzer D. D2-Like dopamine autoreceptor activation reduces quantal size in PC12 cells. J Neurosci 1998; 18:5575-5585.

Prensa L, Parent A. The nigrostriatal pathway in the rat: A single-axon study of the relationship between dorsal and ventral tier nigral neurons and the striosome/matrix striatal compartments. J Neurosci 2001; 21:7247-7260.

Prieto GA, Perez-Burgos A, Fiordelisio T, Salgado H, Galarraga E, Drucker-Colin R, Bargas J. Dopamine D(2)-class receptor supersensitivity as reflected in Ca2+ current modulation in neostriatal neurons. Neuroscience 2009; 164:345-350.

Prosser ES, Pruthi R, Csernansky JG. Differences in the time course of dopaminergic supersensitivity following chronic administration of haloperidol, molindone, or sulpiride. Psychopharmacology (Berl) 1989; 99:109-116.

Prudente CN, Hess EJ, Jinnah HA. Dystonia as a network disorder: what is the role of the cerebellum? Neuroscience 2014; 260:23-35.

Prudente CN, Pardo CA, Xiao J, Hanfelt J, Hess EJ, Ledoux MS, Jinnah HA. Neuropathology of cervical dystonia. Exp Neurol 2013; 241:95-104.

Quartarone A, Pisani A. Abnormal plasticity in dystonia: Disruption of synaptic homeostasis. Neurobiol Dis 2011; 42:162-170.

Quay WB. Circadian Rhythm in Rat Pineal Serotonin and Its Modifications by Estrous Cycle and Photoperiod. Gen Comp Endocrin 1963; 3:473-479.

Raike RS, Pizoli CE, Weisz C, van den Maagdenberg A, Jinnah HA, Hess EJ. Limited regional cerebellar dysfunction induces focal dystonia in mice. Neurobiol Dis 2013; 49:200-210.

Raike RS, Pizoli CE, Weisz C, van den Maagdenberg AM, Jinnah HA, Hess EJ. Limited regional cerebellar dysfunction induces focal dystonia in mice. Neurobiol Dis 2012; 49C:200-210.

Rajput AH, Gibb WRG, Zhong XH, Shannak KS, Kish S, Chang LG, Hornykiewicz O. Dopa-responsive dystonia - pathological and biochemical observation in a case. Ann Neurol 1994; 35:396-402.

Raju DV, Ahern TH, Shah DJ, Wright TM, Standaert DG, Hall RA, Smith Y. Differential synaptic plasticity of the corticostriatal and thalamostriatal systems in an MPTP-treated monkey model of parkinsonism. Eur J Neurosci 2008; 27:1647-1658.

Ramsey AJ, Fitzpatrick PF. Effects of phosphorylation of serine 40 of tyrosine hydroxylase on binding of catecholamines: evidence for a novel regulatory mechanism. Biochemistry 1998; 37:8980-8986.

Reagan-Shaw S, Nihal M, Ahmad N. Dose translation from animal to human studies revisited. FASEB 2008; 22:659-661.

Rilstone JJ, Alkhater RA, Minassian BA. Brain dopamine-serotonin vesicular transport disease and its treatment. New Eng J Med 2013; 368:543-550.

Rios M, Habecker B, Sasaoka T, Eisenhofer G, Tian H, Landis S, Chikaraishi D, Roffler-Tarlov S. Catecholamine synthesis is mediated by tyrosinase in the absence of tyrosine hydroxylase. J Neurosci 1999; 19:3519-3526.

Ritz MC, Lamb RJ, Goldberg SR, Kuhar MJ. Cocaine receptors on dopamine transporters are related to self-administration of cocaine. Science 1987; 237:1219-1223.

Roffler-Tarlov S, Graybiel AM. The postnatal development of the dopamine-containing innervation of dorsal and ventral striatum: effects of the weaver gene. J Neurosci 1987; 7:2364-2372.

Rommelfanger KS, Edwards GL, Freeman KG, Liles LC, Miller GW, Weinshenker D. Norepinephrine loss produces more profound motor deficits than MPTP treatment in mice. Proc Natl Acad Sci U S A 2007; 104:13804-13809.

Rosales RL. X-linked dystonia parkinsonism: clinical phenotype, genetics and therapeutics. J Mov Disord 2010; 3:32-38.

Royo M, Daubner SC, Fitzpatrick PF. Effects of mutations in tyrosine hydroxylase associated with progressive dystonia on the activity and stability of the protein. Proteins-Structure Function and Bioinformatics 2005; 58:14-21.

Sanberg PR. Haloperidol-induced catalepsy is mediated by postsynaptic dopamine receptors. Nature 1980; 284:472-473.

Sanger TD, Delgado MR, Gaebler-Spira D, Hallett M, Mink JW, Task Force on Childhood Motor D. Classification and definition of disorders causing hypertonia in childhood. Pediatrics 2003; 111:e89-97.

Santini E, Valjent E, Usiello A, Carta M, Borgkvist A, Girault JA, Herve D, Greengard P, Fisone G. Critical involvement of cAMP/DARPP-32 and extracellular signal-regulated protein kinase signaling in L-DOPA-induced dyskinesia. J Neurosci 2007; 27:6995-7005.

Sato K, Sumi-Ichinose C, Kaji R, Ikemoto K, Nomura T, Nagatsu I, Ichinose H, Ito M, Sako W, Nagahiro S, Graybiel AM, Goto S. Differential involvement of striosome and matrix dopamine systems in a transgenic model of dopa-responsive dystonia. Proc Natl Acad Sci U S A 2008; 105:12551-12556.

Schambra UB, Duncan GE, Breese GR, Fornaretto MG, Caron MG, Fremeau RT, Jr. Ontogeny of D1A and D2 dopamine receptor subtypes in rat brain using in situ hybridization and receptor binding. Neuroscience 1994; 62:65-85.

Schank JR, Ventura R, Puglisi-Allegra S, Alcaro A, Cole CD, Liles LC, Seeman P, Weinshenker D. Dopamine beta-hydroxylase knockout mice have alterations in dopamine signaling and are hypersensitive to cocaine. Neuropsychopharmacol 2006; 31:2221-2230.

Schicatano EJ, Basso MA, Evinger C. Animal model explains the origins of the cranial dystonia benign essential blepharospasm. J Neurophysiol 1997; 77:2842-2846.

Schmittgen TD, Livak KJ. Analyzing real-time PCR data by the comparative C(T) method. Nat Protocol 2008; 3:1101-1108.

Sciamanna G, Tassone A, Mandolesi G, Puglisi F, Ponterio G, Martella G, Madeo G, Bernardi G, Standaert DG, Bonsi P, Pisani A. Cholinergic dysfunction alters synaptic integration between thalamostriatal and corticostriatal inputs in DYT1 dystonia. J Neurosci 2012; 32:11991-12004.

Seeman P, Lee T, Chau-Wong M, Wong K. Antipsychotic drug doses and neuroleptic/dopamine receptors. Nature 1976; 261:717-719.

Seeman P, Weinshenker D, Quirion R, Srivastava LK, Bhardwaj SK, Grandy DK, Premont RT, Sotnikova TD, Boksa P, El-Ghundi M, O'Dowd B F, George SR, Perreault ML, Mannisto PT, Robinson S, Palmiter RD, Tallerico T. Dopamine supersensitivity correlates with D2High states, implying many paths to psychosis. Proc Natl Acad Sci U S A 2005; 102:3513-3518.

Segawa M. Autosomal dominant GTP cyclohydrolase I (AD GCH 1) deficiency (Segawa disease, dystonia 5; DYT 5). Chang Gung medical journal 2009; 32:1-11.

Segawa M. Hereditary progressive dystonia with marked diurnal fluctuation. Brain & Development 2011; 33:195-201.

Segawa M, Nomura Y, Nishiyama N. Autosomal dominant guanosine triphosphate cyclohydrolase I deficiency (Segawa disease). Ann Neurol 2003; 54 Suppl 6:S32-45.

Segawa M, Ohmi K, ItoH S, Aoyama M, Hayakawa H. Childhood basal ganglia disease with remarkable response to L-DOPA. 'hereditary basal ganglia disease marked diurnal fluctuation'. Shinryo (Tokyo) 1971; 24:667-672.

Sethi KD, Hess DC, Harp RJ. Prevalence of dystonia in veterans on chronic antipsychotic therapy. Movement disorders : official journal of the Movement Disorder Society 1990; 5:319-321.

Sharma N, Baxter MG, Petravicz J, Bragg DC, Schienda A, Standaert DG, Breakefield XO. Impaired motor learning in mice expressing torsinA with the DYT1 dystonia mutation. J Neurosci 2005; 25:5351-5355.

Shaywitz BA, Yager RD, Klopper JH. Selective brain dopamine depletion in developing rats - experimental model of minimal brain dysfunction. Science 1976; 191:305-308.

Shepard KN, Liles LC, Weinshenker D, Liu RC. Norepinephrine is necessary for experience-dependent plasticity in the developing mouse auditory cortex. J Neurosci 2015; 35:2432-2437.

Shih JC, Chen K, Ridd MJ. Monoamine oxidase: from genes to behavior. Annu Rev Neurosci 1999; 22:197-217.

Shindou T, Ochi-Shindou M, Wickens JR. A Ca(2+) threshold for induction of spike-timing-dependent depression in the mouse striatum. J Neurosci 2011; 31:13015-13022.

Shirley TL, Rao LM, Hess EJ, Jinnah HA. Paroxysmal dyskinesias in mice. Mov Disord 2008; 23:259-264.

Sibley DR, Monsma FJ, Jr. Molecular biology of dopamine receptors. Trends Pharmacol Sci 1992; 13:61-69.

Simonyan K, Berman BD, Herscovitch P, Hallett M. Abnormal striatal dopaminergic neurotransmission during rest and task production in spasmodic dysphonia. J Neurosci 2013; 33:14705-14714.

Snow BJ, Nygaard TG, Takahashi H, Calne DB. Positron emission tomographic studies of dopa-responsive dystonia and early-onset idiopathic parkinsonism. Ann Neurol 1993; 34:733-738.

Snyder SH, Taylor KM, Coyle JT, Meyerhoff JL. The role of brain dopamine in behavioral regulation and the actions of psychotropic drugs. Am J Psychiatry 1970; 127:199-207.

Song CH, Bernhard D, Bolarinwa C, Hess EJ, Smith Y, Jinnah HA. Subtle microstructural changes of the striatum in a DYT1 knock-in mouse model of dystonia. Neurobiol Dis 2013; 54:362-371.

Song CH, Bernhard D, Hess EJ, Jinnah HA. Subtle microstructural changes of the cerebellum in a knock-in mouse model of DYT1 dystonia. Neurobiol Dis 2014; 62:372-380.

Song CH, Fan XL, Exeter CJ, Hess EJ, Jinnah HA. Functional analysis of dopaminergic systems in a DYT1 knock-in mouse model of dystonia. Neurobiol of Dis 2012; 48:66-78.

Sotnikova TD, Beaulieu JM, Barak LS, Wetsel WC, Caron MG, Gainetdinov RR. Dopamine-independent locomotor actions of amphetamines in a novel acute mouse model of Parkinson disease. PLoS biology 2005; 3:e271.

Sotnikova TD, Caron MG, Gainetdinov RR. DDD mice, a novel acute mouse model of Parkinson's disease. Neurology 2006; 67:S12-17.

Stamelou M, Mencacci NE, Cordivari C, Batla A, Wood NW, Houlden H, Hardy J, Bhatia KP. Myoclonus-dystonia syndrome due to tyrosine hydroxylase deficiency. Neurology 2012; 79:435-441.

Steinberger D, Korinthenberg R, Topka H, Berghauser M, Wedde R, Muller U. Dopa-responsive dystonia: mutation analysis of GCH1 and analysis of therapeutic doses of L-dopa. German Dystonia Study Group. Neurology 2000; 55:1735-1737.

Sumi-Ichinose C, Urano F, Kuroda R, Ohye T, Kojima M, Tazawa M, Shiraishi H, Hagino Y, Nagatsu T, Nomura T, Ichinose H. Catecholamines and serotonin are differently regulated by tetrahydrobiopterin. A study from 6-pyruvoyltetrahydropterin synthase knockout mice. J Biol Chem 2001; 276:41150-41160.

Sumi-Ichinose C, Urano F, Shimomura A, Sato T, Ikemoto K, Shiraishi H, Senda T, Ichinose H, Nomura T. Genetically rescued tetrahydrobiopterin-depleted mice survive with hyperphenylalaninemia and region-specific monoaminergic abnormalities. J Neurochem 2005; 95:703-714.

Sun B, Chen S, Zhan S, Le W, Krahl SE. Subthalamic nucleus stimulation for primary dystonia and tardive dystonia. Acta Neurochirurgica Suppl 2007; 97:207-214.

Surmeier DJ, Song WJ, Yan Z. Coordinated expression of dopamine receptors in neostriatal medium spiny neurons. J Neurosci 1996; 16:6579-6591.

Svenningsson P, Nishi A, Fisone G, Girault JA, Nairn AC, Greengard P. DARPP-32: an integrator of neurotransmission. Ann Rev Pharmacol Toxicol 2004; 44:269-296.

Szczypka MS, Rainey MA, Kim DS, Alaynick WA, Marck BT, Matsumoto AM, Palmiter RD. Feeding behavior in dopamine-deficient mice. Proc Natl Acad Sci U S A 1999; 96:12138-12143.

Tabbal SD, Mink JW, Antenor JAV, Carl JL, Moerlein SM, Perlmutter JS. 1-methyl-4-phenyl-1,2,3,6-tetrahydropyridine-induced acute transient dystonia in monkeys associated with low striatal dopamine. Neuroscience 2006; 141:1281-1287.

Tadic V, Kasten M, Bruggemann N, Stiller S, Hagenah J, Klein C. Dopa-Responsive Dystonia Revisited Diagnostic Delay, Residual Signs, and Nonmotor Signs. Arch Neurol 2012; 69:1558-1562.

Tan D, Zhang Y, Ye J, Han L, Qiu W, Gu X, Zhang H. [Tyrosine hydroxylase deficiency: a case of autosomal recessive dopa-responsive dystonia]. Zhonghua er ke za zhi Chin J Ped 2014; 52:616-619.

Tanabe LM, Kim CE, Alagem N, Dauer WT. Primary dystonia: molecules and mechanisms. Nat Rev Neurol 2009; 5:598-609.

Tang WJ, Gilman AG. Type-specific regulation of adenylyl cyclase by G protein beta gamma subunits. Science 1991; 254:1500-1503.

Thomas SA, Matsumoto AM, Palmiter RD. Noradrenaline is essential for mouse fetal development. Nature 1995; 374:643-646.

Thompson VB, Jinnah HA, Hess EJ. Convergent mechanisms in etiologically-diverse dystonias. Exp Opin Therap Targets 2011; 15:1387-1403.

Thony B, Blau N. Mutations in the BH4-metabolizing genes GTP cyclohydrolase I, 6-pyruvoyl-tetrahydropterin synthase, sepiapterin reductase, carbinolamine-4a-dehydratase, and dihydropteridine reductase. Human Mut 2006; 27:870-878.

Tiberi M, Jarvie KR, Silvia C, Falardeau P, Gingrich JA, Godinot N, Bertrand L, Yang-Feng TL, Fremeau RT, Jr., Caron MG. Cloning, molecular characterization, and chromosomal assignment of a gene encoding a second D1 dopamine receptor subtype: differential expression pattern in rat brain compared with the D1A receptor. Proc Natl Acad Sci U S A 1991; 88:7491-7495.

Todd RD, Perlmutter JS. Mutational and biochemical analysis of dopamine in dystonia - Evidence for decreased dopamine D-2 receptor inhibition. Mol Neurobio 1998; 16:135-147.

Tolosa E, Compta Y. Dystonia in Parkinson's disease. J Neurol 2006; 253:7-13.

Trender-Gerhard I, Sweeney MG, Schwingenschuh P, Mir P, Edwards MJ, Gerhard A, Polke JM, Hanna MG, Davis MB, Wood NW, Bhatia KP. Autosomal-dominant GTPCH1-deficient DRD: clinical characteristics and long-term outcome of 34 patients. J Neurol Neurosurg Psychiatry 2009; 80:839-845.

Ulug AM, Vo A, Argyelan M, Tanabe L, Schiffer WK, Dewey S, Dauer WT, Eidelberg D. Cerebellothalamocortical pathway abnormalities in torsinA DYT1 knock-in mice. Proc Natl Acad Sci U S A 2011; 108:6638-6643.

Ungerstedt U. Adipsia and aphagia after 6-hydroxydopamine induced degeneration of the nigro-striatal dopamine system. Acta Physiologica Scandinav Suppl 1971a; 367:95-122.

Ungerstedt U. Postsynaptic supersensitivity after 6-hydroxydopamine induced degeneration of nigro-striatal dopamine system. Acta Physiologica Scandinav Suppl 1971b; 69-93.

Urs NM, Snyder JC, Jacobsen JP, Peterson SM, Caron MG. Deletion of GSK3beta in D2R-expressing neurons reveals distinct roles for beta-arrestin signaling in antipsychotic and lithium action. Proc Natl Acad Sci U S A 2012; 109:20732-20737.

Valjent E, Aubier B, Corbille AG, Brami-Cherrier K, Caboche J, Topilko P, Girault JA, Herve D. Plasticity-associated gene Krox24/Zif268 is required for long-lasting behavioral effects of cocaine. J Neurosci 2006; 26:4956-4960.

Valjent E, Pascoli V, Svenningsson P, Paul S, Enslen H, Corvol JC, Stipanovich A, Caboche J, Lombroso PJ, Nairn AC, Greengard P, Herve D, Girault JA. Regulation of a protein phosphatase cascade allows convergent dopamine and glutamate signals to activate ERK in the striatum. Proc Natl Acad Sci U S A 2005; 102:491-496.

Vallone D, Picetti R, Borrelli E. Structure and function of dopamine receptors. Neurosci Biobehav Rev 2000; 24:125-132.

van den Heuvel L, Luiten B, Smeitink JAM, Rijk-van Andel JF, Hyland K, Steenbergen-Spanjers GCH, Janssen RJT, Wevers RA. A common point mutation in the tyrosine hydroxylase gene in autosomal recessive L-DOPA-responsive dystonia in the Dutch population. Hum Gene 1998; 102:644-646.

van Harten PN, Matroos GE, Hoek HW, Kahn RS. The prevalence of tardive dystonia, tardive dyskinesia, parkinsonism and akathisia The Curacao Extrapyramidal Syndromes Study: I. Schizophrenia Res 1996; 19:195-203.

van Harten PN, Tenback DE. Tardive dyskinesia: clinical presentation and treatment. Internat Rev Neurobiol 2011; 98:187-210.

Van Hartesveldt C, Meyer ME, Potter TJ. Ontogeny of biphasic locomotor effects of quinpirole. Pharmacol Biochem Behav 1994; 48:781-786.

Vemula SR, Puschmann A, Xiao J, Zhao Y, Rudzinska M, Frei KP, Truong DD, Wszolek ZK, LeDoux MS. Role of Galpha(olf) in familial and sporadic adult-onset primary dystonia. Hum Mol Genet 2013; 22:2510-2519.

Verney C, Berger B, Adrien J, Vigny A, Gay M. Development of the dopaminergic innervation of the rat cerebral cortex. A light microscopic immunocytochemical study using anti-tyrosine hydroxylase antibodies. Brain Res 1982; 281:41-52.

Villalba RM, Lee H, Smith Y. Dopaminergic denervation and spine loss in the striatum of MPTP-treated monkeys. Exp Neurol 2009; 215:220-227.

Villalba RM, Smith Y. Differential striatal spine pathology in Parkinson's disease and cocaine addiction: a key role of dopamine? Neuroscience 2013; 251:2-20.

Visser JE, Bar PR, Jinnah HA. Lesch-Nyhan disease and the basal ganglia. Brain Res Rev 2000; 32:449-475.

Visser JE, Schretlen DJ, Bloem BR, Jinnah HA. Levodopa is Not a Useful Treatment for Lesch-Nyhan Disease. Mov Disord 2011; 26:746-749.

Voon V, Fernagut PO, Wickens J, Baunez C, Rodriguez M, Pavon N, Juncos JL, Obeso JA, Bezard E. Chronic dopaminergic stimulation in Parkinson's disease: from dyskinesias to impulse control disorders. Lancet Neurol 2009; 8:1140-1149.

Vrana KE, Walker SJ, Rucker P, Liu X. A carboxyl terminal leucine zipper is required for tyrosine hydroxylase tetramer formation. J Neurochem 1994; 63:2014-2020.

Vrana SL, Vrana KE, Koves TR, Smith JE, Dworkin SI. Chronic cocaine administration increases CNS tyrosine hydroxylase enzyme activity and mRNA levels and tryptophan hydroxylase enzyme activity levels. J Neurochem 1993; 61:2262-2268.

Wadia PM, Lim SY, Lozano AM, Adams JR, Poon YY, Torres Diaz CV, Moro E. Bilateral pallidal stimulation for x-linked dystonia parkinsonism. Arch Neurol 2010; 67:1012-1015.

Wahnschaffe U, Fredow G, Heintz P, Loscher W. Neuropathological studies in a mutant hamster model of paroxysmal dystonia. Mov Disord 1990; 5:286-293.

Wallace LJ, Traeger JS. Dopac distribution and regulation in striatal dopaminergic varicosities and extracellular space. Synapse 2012; 66:160-173.

Weber M, Lauterburg T, Tobler I, Burgunder JM. Circadian patterns of neurotransmitter related gene expression in motor regions of the rat brain. Neurosci Lett 2004; 358:17-20.

Weiss-Wunder LT, Chesselet MF. Acute and repeated administration of fluphenazine-N-mustard alters levels of tyrosine hydroxylase mRNA in subsets of mesencephalic dopaminergic neurons. Neuroscience 1992; 49:297-305.

Westerink BH. Sequence and significance of dopamine metabolism in the rat brain. Neurochem Int 1985; 7:221-227.

Westin JE, Vercammen L, Strome EM, Konradi C, Cenci MA. Spatiotemporal pattern of striatal ERK1/2 phosphorylation in a rat model of L-DOPA-induced dyskinesia and the role of dopamine D1 receptors. Biol Psychiatry 2007; 62:800-810.

Wichmann T. Commentary: Dopaminergic dysfunction in DYT1 dystonia. Exp Neurol 2008; 212:242-246.

Wickremaratchi MM, Knipe MD, Sastry BS, Morgan E, Jones A, Salmon R, Weiser R, Moran M, Davies D, Ebenezer L, Raha S, Robertson NP, Butler CC, Ben-Shlomo Y, Morris HR. The motor phenotype of Parkinson's disease in relation to age at onset. Mov Disord 2011; 26:457-463.

Wijemanne S, Jankovic J. Dopa-responsive dystonia-clinical and genetic heterogeneity. Nat Rev Neurol 2015.

Willemsen MA, Verbeek MM, Kamsteeg EJ, de Rijk-van Andel JF, Aeby A, Blau N, Burlina A, Donati MA, Geurtz B, Grattan-Smith PJ, Haeussler M, Hoffmann GF, Jung H, de Klerk JB, van der Knaap MS, Kok F, Leuzzi V, de Lonlay P, Megarbane A, Monaghan H, Renier WO, Rondot P, Ryan MM, Seeger J, Smeitink JA, Steenbergen-Spanjers GC, Wassmer E, Weschke B, Wijburg FA, Wilcken B, Zafeiriou DI, Wevers RA. Tyrosine hydroxylase deficiency: a treatable disorder of brain catecholamine biosynthesis. Brain 2010; 133:1810-1822.

Williams SM, Goldman-Rakic PS. Widespread origin of the primate mesofrontal dopamine system. Cereb Ctx 1998; 8:321-345.

Wilson BK, Hess EJ. Animal models for dystonia. Mov Disord 2013; 28:982-989.

Wood PL, Altar CA. Dopamine release in vivo from nigrostriatal, mesolimbic, and mesocortical neurons: utility of 3-methoxytyramine measurements. Pharmacological Rev 1988; 40:163-187.

Zafeiriou DI, Willemsen MA, Verbeek MM, Vargiami E, Ververi A, Wevers R. Tyrosine hydroxylase deficiency with severe clinical course. Mol Gene Metabol 2009; 97:18-20.

Zeng BY, Heales SJR, Canevari L, Rose S, Jenner P. Alterations in expression of dopamine receptors and neuropeptides in the striatum of GTP cyclohydrolase-deficient mice. Exp Neurol 2004; 190:515-524.

Zetler G. Haloperidol catalepsy in grouped and isolated mice. Pharmacology 1975; 13:526-532.

Zhang L, Yokoi F, Jin YH, DeAndrade MP, Hashimoto K, Standaert DG, Li Y. Altered dendritic morphology of Purkinje cells in Dyt1 DeltaGAG knock-in and purkinje cell-specific Dyt1 conditional knockout mice. PLoS One 2011; 6:e18357.

Zhang L, Yokoi F, Parsons DS, Standaert DG, Li Y. Alteration of striatal dopaminergic neurotransmission in a mouse model of DYT11 myoclonus-dystonia. PLoS One 2012; 7:e33669.

Zhao Y, DeCuypere M, LeDoux MS. Abnormal motor function and dopamine neurotransmission in DYT1 DeltaGAG transgenic mice. Exp Neurol 2008; 210:719-730.

Zhou FC, Bledsoe S, Murphy J. Serotonergic sprouting is induced by dopamine lesion in substantia nigra of adult rat brain. Brain Res 1991; 556:108-116.

Zhou QY, Palmiter RD. Dopamine-Deficient Mice are Severly Hypoactive, Adipsic, and Aphagic. Cell 1995; 83:1197-1209.

Zhou QY, Quaife CJ, Palmiter RD. Targeted disruption of the tyrosin-hydroxylase gene reveals that catecholamines are required for mouse fetal development. Nature 1995; 374:640-643.

Zhuang X, Belluscio L, Hen R. G(olf)alpha mediates dopamine D1 receptor signaling. J Neurosci 2000; 20:RC91.

Zigmond RE, Schwarzschild MA, Rittenhouse AR. Acute regulation of tyrosine hydroxylase by nerve activity and by neurotransmitters via phosphorylation. Annu Rev Neurosci 1989; 12:415-461.

Zoons E, Tijssen MA. Pathologic changes in the brain in cervical dystonia pre- and post-mortem - a commentary with a special focus on the cerebellum. Exp Neurol 2013; 247:130-133.

Zuddas A, Pintor M, DeMontis N, Giovanna Marrosu M, Cianchetti C. Continuous infusion of apomorphine improves torsion dystonia in a boy unresponsive to other dopaminergic drugs. J Child Neurol 1996; 11:343-345.